Fall 12-1-2014

Development of a Methodology for Evaluating Quality Characteristics of Fused Deposition Modeling

Dominique Winston Sealy
Indiana State University

DEVELOPMENT OF A METHODOLOGY FOR EVALUATING QUALITY CHARACTERISTICS OF FUSED DEPOSITION MODELING

A Dissertation

Presented to

The College of Graduate and Professional Studies

Department of Technology

Indiana State University

Terre Haute, Indiana

In Partial Fulfillment

of the Requirements for the Degree

Doctor of Philosophy

---

by

Dominique Winston Sealy

December 2014

Keywords: Parametric Modeling, Fused Deposition Modeling, Technology Management, Manufacturing, Investment Casting

VITAE

Dominique Winston Sealy

EDUCATION

Ph.D.	Indiana State University, Terre Haute, Indiana, 2014 Major: Technology Management, Manufacturing Systems
M.S.	University of St. Thomas, St Paul, Minnesota, 2004 Major: Technology Management, Systems Engineering
B.S.	Minnesota State University, Mankato, Minnesota, 1994 Major: Electronic Engineering Technology

PROFESSIONAL EXPERIENCE

Assistant Professor
Minnesota State University, Mankato, Minnesota, 2013 - Present

Pre-Doctoral Fellow
Minnesota State University, Mankato, Minnesota, 2011 - 2013

Chair, School of Drafting & Design
ITT Technical Institute, Eden Prairie, Minnesota, 2005 - 2010

Assistant Professor
Brown College, Mendota Heights, Minnesota, 2004 - 2005

Product Manager
Orbotech Inc., Eden Prairie, Minnesota, 2002 - 2003

AOI Technical Project Manager
Orbotech Inc., Eden Prairie, Minnesota, 1997 - 2002

Development Engineer
Management Graphics Inc., Minneapolis, Minnesota, 1995 - 1997

COMMITTEE MEMBERS

Committee Chair: Marion Schafer, PhD

Professor and Coordinator, Department of Applied Engineering and Technology Management

Indiana State University

Committee Member: A. Mehran Shahhosseini, D.Eng

Associate Professor, Department of Applied Engineering and Technology Management

Indiana State University

Committee Member: W. Tad Foster, Ed.D

Professor, Department of Human Resource Development and Performance Technologies

Indiana State University

ABSTRACT

Additive Manufacturing rapid reproductive systems are gaining popularity within the manufacturing industry. One of the many benefits of such systems has been the exploration of building practical sacrificial patterns for investment casted metals. Methods such as, Castform and Quickcast, has been developed for selective laser sintering and Stereolithography apparatus technologies respectively. Research has demonstrated significant cost savings when Additive manufacturing rapid reproductive systems are utilized for customized or small batch production of sacrificial patterns.

The purpose of this study was to develop a methodology for evaluating quality characteristics of Fused Deposition Modeling. Since Fused Deposition Modeling have been demonstrated by a number of experimental studies as a viable alternative to wax sacrificial patterns, this study explored the effects of wall thickness and raster resolution on quality characteristics such as, diametric accuracy, cylindricity, and concentricity. The results of the study indicated raster resolution had no effect on the measured quality characteristics, however, the ANOVA and Kruskal-Wallis tests showed statistical significance (α=0.05) for wall thickness of cylindricity of a small diameter (0.5”) and concentricity of two cylindrical features of diameters 0.5” and 1”.

Moreover, the main contributions of this study involved the development of an accurate and robust design of experiment methodology. In addition, implications and recommendations for practice were also discussed.

ACKNOWLEDGMENTS

Many people have been instrumental, both directly and indirectly, in the realization of this research. For this, I would like to say a heartfelt thank you for all your support. Thank you to Craig Walker, Sales Manager at InvestCast Inc., Minneapolis, Minnesota for welcoming me into your facilities. A special thanks to John Hausladen, Quality Engineer, and Drew Sahlstrom, Design Engineer at Dotson Iron Castings, Mankato, Minnesota, for your much appreciated assistance in qualifying my design specimens. Without which, this research would have been a lot more challenging to complete.

Thank you to Dr. Bruce Jones and Dr. Kuldeep Agarwal at Minnesota State University for your support, encouragement, and guidance throughout this process. Thanks to my committee, Dr. Marion Schafer, chair, Dr. Mehran Shahhosseini and Dr. Tad Foster for your patience, guidance and sincere feedback.

Finally, I would like to thank my family for being patient and supportive throughout this process. A deep thank you to my wife, Juanita, for keeping me level headed, my daughter, Brittley, for all the hugs and my son Dominique, for the pats on the back. I love you all!

TABLE OF CONTENTS

LIST OF TABLES

LIST OF FIGURES

CHAPTER 1

INTRODUCTION

Manufacturers are constantly searching for methods of improving efficiencies, which reduces overall costs and frees up much needed resources. This allows manufacturers to be more competitive by sharing those savings throughout the entire supply chain. Moreover, more efficient methods reduce time to product realization. In addition, resources tied up in less efficient methods can become available for more efficient production processes. Presently, one of many methods of processing metals prevalent in the manufacturing and jewelry industries is investment casting or the lost wax process. Investment casting is one of the oldest metal processing methods still being used. Cast objects over 4000 years old have been found from ancient Assyrian, and Chinese cultures (Bruce et al., 2010). The process is fundamentally unchanged. A wax sacrificial pattern is coated with a thick layer of refractory material. The wax is melted then molten metal is poured into the cavity to create the form.

Although the methods are unchanged, many studies indicate inefficiencies in traditional investment casting processes especially for customized or small batch productions. A significant percentage of the investment casting cost occurs during the tooling of the patterns. Cheah et at. (2005) proposed that the tooling stage typically can range from 6 to 14 weeks. Further, specialized, highly skilled machinist are required for tool fabrication that can generate estimated costs as high as $30,000 per tool (Winker, 2010). Tooling, therefore, is economical for large batch productions as cost reductions can be realized through economies of scale. That way, costs could be recouped from repetitive use of a single tool. Customized or small batch production, on the other hand, becomes challenging to some manufacturers utilizing traditional methods of expensive tooling for investment casting. Without a doubt, the costs of inflexibility and expensive tooling are directly transfered to the customer and end user.

With the advent of additive manufacturing rapid reproductive systems, expensive tooling can be eliminated altogether and replaced by less expensive 3D printed sacrificial patterns. The patterns can be printed directly from computer-aided design (CAD) files, totally eliminating the tooling stage. Granting the cost savings from repetitive use of a single tool, the true benefits of additive manufacturing rapid reproductive systems become evident when customization or small batch productions are needed. Dickens and Hopkinson (2003), in their experimental study comparing three additive manufacturing technologies to injection molded wax sacrifitial patterns concluded that additive manufacturing rapid reproductive systems were more economical than traditional investment casting techniques of tooling for production volumes in the thousands. The study compared cost savings of production of a small part (less than 2” X 2” X 2”) that resulted in volumes of less than 14,000 as more economical for additive manufacturing technologies when compared to injection molding sacrificial patterns for investment casting. The study noted a cost saving of approximately half for production volumes of 6000, with further reductions of approximately 10 fold for production volumes of 2000. Grimm (2003) in an experimental evaluation study of additive manufacturing rapid reproductive systems for investment casting applications noted that additive manufacturing has provided the advantage to manufacturers of cost effective short runs with economic order quantities as low as one. In the experimental study, Grimm (2003) compared the dimensional accuracy and surface finishes of three Fused

Deposition Modeling (FDM) systems. The Maxum, Titan, and Prodigy Plus were compared for dimensional accuracy of dimensions ranging from 0.25” to 4”. Of the three systems, the Prodigy Plus resulted in the largest percent deviation of 0.6% when compared to the Maxum and Titan systems of 0.37% and 0.47% respectively. Grimm further adds that additive manufacturing rapid reproductive systems are suitable for investment casting applications with little modifications to the standard foundry process. Since additive manufacturing rapid reproductive systems can be used as an alternative to tooling and injection molding, little change is required to the existing investment casting process. Sacrificial patterns can be created from additive manufacturing rapid reproductive systems during the front end stages of investment casting, and then integrated into the process easily and with few modifications.

A survey of the literature regarding the application of additive manufacturing rapid reproductive systems for investment casting favors the economic benefits associated with customized or small batch production. Additive manufacturing rapid reproductive systems replace costly tooling with patterns built directly from CAD files. The process is more efficient, eliminates wastes and facilitates rapid product realization. Although, traditional investment casting practices utilize wax for sacrificial pattern designs, the majority of additive manufacturing rapid reproductive systems utilize a non-wax material for building parts. Chhabra and Singh (2011) established that any material that can be flashed fired without damaging the ceramic shell, can be suitable for use as an investment casting sacrificial pattern (Chhabra and Singh, 2011). FDM technology deposits an acrylonitrile butadiene styrene (ABS) filament that is heated and extruded to create the part. After the layer hardens, a new layer is deposited. This process is repeated until the part is done. According to Sealy (2011), some of the advantages of FDM include minimal wastage, ease of support removal and ease of material change. The main disadvantages of FDM include limited accuracy due to filament size, slow processes and unpredictable shrinkages caused by the heating and rapid cooling of the extrude head.

Despite the fact that non-wax patterns are stronger, more durable, and can better withstand finishing operations compared to wax patterns, issues such as shell cracking, incomplete burnout and residual ash remains a problem (Cheah et al. 2005). Non-wax patterns experience a greater rate of expansion than the surrounding ceramic shell leading to shell fractures. Jacobs (1993), and Yao and Leu (1999) studied this phenomenon, and both concluded the design of thin walled sacrificial pattern geometries eliminated the effects of shell fractures as a result of solid geometry expansions. Jacobs (1993) focused his study primarily on Stereolithography Apparatus (SLA) and developed a QuickCast technique of replacing solids with triangular geometric patterns. Yao and Leu (1999) demonstrated that triangular geometric designs of sacrificial patterns eliminated induced thermal stresses. Their study demonstrated that a triangular geometrically designed sacrificial pattern exerted no thermal stresses on the surrounding ceramic shell due to the pattern melting and collapsing inwards during the burnout stage.

Strengths and Weaknesses of Additive Manufacturing Systems

Sealy (2011) notes that most manufacturers hesitate using additive manufacturing rapid reproductive systems as a viable manufacturing process due to the repeatability and accuracy inconsistencies of manufactured parts. Manufacturers are skeptical of the structural integrity of the finished products, especially in comparison to conventional subtractive manufacturing processes. Repeatability of subtractive manufacturing processes for the most part requires and utilizes a closed-loop system for dynamic feedback during part creation. Unlike subtractive manufacturing systems, additive manufacturing rapid reproductive systems do not utilize a closed-loop system for immediate feedback. As a result, additive manufacturing rapid reproductive systems involves processes that are more challenging to control.

Even with the challenges of process control in additive manufacturing rapid reproductive systems, certain unique capabilities make additive manufacturing rapid reproductive systems superior to other conventional manufacturing systems (Bourell, *et al*., 2009). Additive manufacturing rapid reproductive systems can build virtually any shape. The layering process allows for the construction of complex cellular structures involving the optimization of material distribution. Material and property tailoring can be achieved by customizing layers or points. In addition, additive manufacturing rapid reproductive systems allow for component integration during the build process. Various hardware, such as, sensors, actuators, and conductive materials can be embedded into parts. As such, fully functional assemblies can be manufactured.

Another critical advantage that Additive Manufacturing has over conventional manufacturing processes is from a design perspective. Most designers today designing for conventional manufacturing processes must not only be aware of the manufacturing processes, but must also take into account the skillset of the workers. Designs that cannot be manufactured are merely conceptual and will never be realized as a working tangible product. Designers must be aware of the process capabilities. They must take into account machine limitations and worker skillset in designing products. On the one hand, knowledge of the process is beneficial to the organization if manufacturing is done in house. However, if any part of manufacturing is outsourced, the required knowledge for manufacturing becomes more challenging to manage. Most organizations are protective of their processes mainly due to the competitive nature of business. This lack of manufacturing process capability knowledge discourages the designer from more intricate, complex designs. Additive manufacturing rapid reproductive systems are immune to part design limitations, and can build more intricate and complex parts.

Problem Statement

Additive manufacturing rapid reproductive systems allow most manufacturers the ability to visualize and quickly investigate the form, fit and function of their designs. Additive manufacturing rapid reproductive systems, therefore, can serve as a functional tool for creating sacrificial patterns. Extensive costs associated with tooling can therefore be reduced or eliminated. Moreover, customized and small batch production can become economically feasible through the use of additive manufacturing rapid reproductive techniques for developing sacrificial patterns in investment casting. As a result, the cost of investment casting can be significantly reduced with the elimination of associated tooling. Even so, additive manufacturing rapid reproductive systems utilizing non-wax materials still face the inherent problem of ceramic shell failures due to thermal expansion of dissimilar materials.

The problem of this study is the lack of understanding on the effects of wall thickness and raster resolution on quality characteristics, such as, diametric accuracy, cylindricity, and concentricity of fused deposition modeled sacrificial patterns. Diametric accuracy, cylindricity, and concentricity are critical quality characteristics used in determining process capabilities of the investment casting process. Dickens and Hague (2001) experimental study of non-wax sacrificial patterns consisting of a Finite Element Analysis (FEA) and qualified by an experimental design, observed that the thermal expansion approximately doubled (from 88 X 10^{-6} to 181 X 10^{-6}) around the glass transition temperature of the material. In the study, three 50mm cubes were constructed and coated with a ceramic shell. One solid and two hollow (5mm and 2.5mm wall thickness) cubes were simulated using FEA software. The FEA results were further qualified by an experimental design consisting of ceramic coated cubes fitted with strain gauges and thermocouples. The ceramic shell fractured at 60°C as a result of expansion. Harun et. al. (2008) conducted an experimental study to evaluate dimensional accuracy, surface roughness and distortion of six solid and six hollow specimens. The specimens were produced using FDM technology then coated with a ceramic shell. Burnout temperatures for each of the six specimens were set at 300°C, 400°C, 450°C, 500°C, 550°C and 600°C. The hollow specimens showed no ceramic shell cracking during burnout. The solid specimens, on the other hand, showed visible signs of ceramic shell cracking at temperatures of 300°C, 400°C, 450°C, and 500°C. Based on the results of the experimental studies, ceramic shell fractures occur due to the differences in thermal expansion coefficients between the sacrificial pattern and ceramic shell materials. During the burnout stage non-wax sacrificial patterns exhibit a greater expansion than that of the surrounding ceramic shell. As a result, thermal stresses are induced on the ceramic shell causing fractures that lead to failure during the metal pouring stage.

Statement of the Purpose

The purpose of this study was to investigate the effects of wall thickness and raster resolution on diametric accuracy, cylindricity and concentricity of fused deposition modeled sacrificial patterns. A full factorial design of experiment was used for the study. Each factor consisted of two levels, namely, wall thickness dimensions of 0.060” and 0.120”, and raster resolution values of normal (0.020”) and fine (0.012”). A 2 X 2 randomized complete block design of experiment was investigated and analyzed through hypothesis testing. The randomized complete block design technique was employed primarily to diminish the effects of nuisance variables such as time, temperature fluctuations or material variability.

Research Questions and Hypotheses

The method was guided by the design of experiment principles in addressing the following questions:

Research Question 1

Will the diametric accuracy of fused deposition modeling of the Prodigy Plus™ utilizing ABS material be affected by wall thickness or raster resolution?

Research Question 2

Will fillet radius of fused deposition modeling of the Prodigy Plus™ utilizing ABS material be affected by wall thickness or raster resolution”?

Research Question 3

Will the cylindricity of fused deposition modeling of the Prodigy Plus™ utilizing ABS material be affected by wall thickness or raster resolution?

Research Question 4

Will the concentricity of fused deposition modeling of the Prodigy Plus™ utilizing ABS material be affected by wall thickness or raster resolution?

Research Question 5

Will there be any interaction of fused deposition modeling of the Prodigy Plus™ utilizing ABS material between wall thickness and raster resolution for diametric accuracy, cylindricity, and concentricity?

The research questions were statistically qualified through hypothesis testing to determine the statistical significance of the effects of wall thickness and raster resolution along with any interactions on the diametric variability of fused deposition modeling. The following hypotheses will provide the basis for the study.

Hypothesis 1

There is no significant difference between the average diameters of fused deposition modeling for wall thicknesses of 0.060”, and 0.120”.

$$H_{01} : \mu_{0\ (0.060")} = \mu_{1\ (0.120")}$$

There is significant difference between the average diameters of fused deposition modeling of wall thicknesses of 0.060”, and 0.120”.

$$H_{11} : \mu_{0\ (0.060")} \neq \mu_{1\ (0.120")}$$

Hypothesis 2

There is no significant difference between the average diameters of fused deposition modeling for normal or fine raster resolution.

$$H_{02} : \mu_{0\ (\text{normal})} = \mu_{1\ (\text{fine})}$$

There is significant difference between the average diameters of fused deposition modeling of normal or fine raster resolution.

$$H_{12} : \mu_{0\ (\text{normal})} \neq \mu_{1\ (\text{fine})}$$

Hypothesis 3

There is no significant difference between the 0.3” radius fillets of fused deposition modeling for wall thicknesses of 0.060”, and 0.120”.

$$H_{03} : \mu_{0\ (0.060")} = \mu_{1\ (0.120")}$$

There is significant difference between the 0.3” radius fillets of fused deposition modeling for wall thicknesses of 0.060”, and 0.120”.

$$H_{13} : \mu_{0\ (0.060")} \neq \mu_{1\ (0.120")}$$

Hypothesis 4

There is no significant difference between the 0.3" radius fillets of fused deposition modeling for normal or fine raster resolution.

$$H_{04} : \mu_{0\ (\text{normal})} = \mu_{1\ (\text{fine})}$$

There is significant difference between the 0.3" radius fillets of fused deposition modeling for normal or fine raster resolution.

$$H_{14} : \mu_{0\ (\text{normal})} \neq \mu_{1\ (\text{fine})}$$

Hypothesis 5

There is no significant difference between the average cylindricity of fused deposition modeling for wall thicknesses of 0.060", and 0.120".

$$H_{05} : \mu_{0\ (0.060")} = \mu_{1\ (0.120")}$$

There is significant difference between the average cylindricity of fused deposition modeling of wall thicknesses of 0.060", and 0.120".

$$H_{15} : \mu_{0\ (0.060")} \neq \mu_{1\ (0.120")}$$

Hypothesis 6

There is no significant difference between the average cylindricity of fused deposition modeling for normal or fine raster resolution.

$$H_{06} : \mu_{0\ (\text{normal})} = \mu_{1\ (\text{fine})}$$

There is significant difference between the average cylindricity of fused deposition modeling for normal or fine raster resolution.

$$H_{16} : \mu_{0\ (\text{normal})} \neq \mu_{1\ (\text{fine})}$$

Hypothesis 7

There is no significant difference between the average concentricity of fused deposition modeling for wall thicknesses of 0.060”, and 0.120”.

$$H_{07} : \mu_{0\ (0.060")} = \mu_{1\ (0.120")}$$

There is significant difference between the average concentricity of fused deposition modeling of wall thicknesses of 0.060”, and 0.120”.

$$H_{17} : \mu_{0\ (0.060")} \neq \mu_{1\ (0.120")}$$

Hypothesis 8

There is no significant difference between the average concentricity of fused deposition modeling for normal or fine raster resolution.

$$H_{08} : \mu_{0\ (\text{normal})} = \mu_{1\ (\text{fine})}$$

There is significant difference between the average concentricity of fused deposition modeling for normal or fine raster resolution.

$$H_{18} : \mu_{0\ (\text{normal})} \neq \mu_{1\ (\text{fine})}$$

Hypothesis 9

There is no significant difference between the diameter, cylindricity, and concentricity of fused deposition modeling for interaction between wall thicknesses (0.060”, and 0.120”), and normal or fine raster resolutions.

There is significant difference between at least one of the diameter, cylindricity, or concentricity of fused deposition modeling for interaction between wall thicknesses (0.060”, and 0.120”), and normal or fine raster resolutions.

Statement of Assumptions

The following assumptions were applied to the study:

- The FDM default shrinkage compensation value was optimized and did not affect the accuracy of average diameter due to variations caused by shrinkage.
- The findings of the study can be translated with minor revisions to any non-wax thin walled sacrificial pattern design.

Statement of Limitations

The entire system employed in the study presented constraints and limitations. A delimitation of this study was the use of a specific 3D printer technology, Prodigy Plus™ FDM. Although other 3D printer technologies may be available to manufacturers, this study does not address or compare those technologies. The Prodigy Plus™ has a build envelope of 8” W X 8 D” X 12” H. Although larger sized specimens can be built as multiple sections, the accuracy and integrity of the specimens can be severely diminished by the process of stitching and gluing individual components. As a result, the build envelope was defined as a limitation for the study. The model and support materials were also defined as a limitation. Single cartridges of model and support materials were used. Therefore, variations amongst materials were not explored. It is impossible to design every possible geometric pattern variation. Therefore, this study is limited to a benchmark test panel. The design of the benchmark parts does not apply to all possible design options. A small scale benchmark specimen was design for exploration of the effects of wall thickness and raster resolution on certain quality characteristics. The geometric features and dimensional constraints of the benchmark design further served as a limitation for the study. The benchmark design consisted of three axisymmetric features of diameters 0.5”, 1” and radius of 0.3”. Good form geometric properties were limited to a build wall thickness of 0.06”. Although smaller wall thicknesses can be achieved based on a preliminary experimental study, good form consistencies were not achieved. The build process was set to and limited by a layer thickness of 0.010. The study was also limited by the measuring equipment used to acquire the statistics. Parts were qualified utilizing a Fowler digital caliper of 0.0010 inch accuracy (see appendix A) and a Zeiss Contura G2 Coordinate Measuring Machine (CMM). The caliper readout was limited to ten-thousandths of an inch. The CMM was capable of measuring accuracies of 0.02 thousandth of an inch. Environmental conditions were also critical factors that influenced the results of the study. Although temperature and humidity were controlled to some extent, precise control was not possible. Therefore, environmental conditions such as temperature and humidity were monitored and documented as a limitation range for the study. Although extreme care was exercised during the handling, measuring, and interpretation of the specimens, and data, observations and measurements were limited due to the possibility of human error by the researcher.

Preliminary Experimental Study

The purpose of the preliminary experimental study was to determine the smallest wall thickness dimension of good form capability of the Prodigy Plus™ FDM and establish that both setup and operating parameters were optimized for the study. The smallest wall thickness geometry is a direct function of the extruded model material diameter. The resultant average diameter was calculated at 0.015”.

The minimum extruded diameter was used as a guideline for determining the experimental wall thicknesses. A benchmark specimen was designed and a pilot part built. The pilot test consisted of printing four specimens consisting of a 2^2 factorial combination. Two factors of wall thicknesses at levels of 0.030” (2x minimum) and 0.060” (4x minimum) wall thickness and raster resolution of levels normal and fine were printed.

The results of the pilot test indicated abnormalities in the 0.030” wall thickness specimens. It was observed that the layers separated during part build. This was more pronounced during the construction of the fillet geometric feature. During the building process, layers are allowed to solidify as the extrusion head is returned to its home position. As such, small wall thickness bonding becomes weakened, leading to layer separation. As a result of this phenomenon, the benchmark test specimens were redesigned to incorporate wall thicknesses of 0.060” (4x minimum) and 0.120” (8x minimum). The redesigned benchmark specimen consisted of three axisymmetric geometric features of good form and also allowing for the addition of the effects of wall thickness and raster resolution on concentricity.

Two factors each of two levels were used for the design of experiment and analysis. Wall thickness (independent factor) of levels 0.06” (4x minimum) and 0.12” (8x minimum) along with raster resolution (independent factor) of levels normal and fine were investigated for their effects on diametric variability of 0.5” and 1”, fillet radius of 0.3”, average cylindricity, and concentricity of the 0.5” diameter feature to the base (1”) diameter geometric feature.

Statement of Methodology

All benchmark test specimens were printed on a Stratasys Prodigy Plus™ printer utilizing FDM technology. The equipment used during the study consisted of Pro-Engineer (Wildfire Ver. 5) CAD software for benchmark specimens design and tessellation, Insight software for slicing and toolpath generation, Stratasys Prodigy Plus™ printer, Fowler 6" Digital Caliper (model # 54-101-150-2) and Zeiss Contura G2 coordinate measuring machine. Parametric models of the specimens were translated into Stereolithography (STL) files, and then printed on a Prodigy Plus™ printer utilizing the fused deposition process.

Two benchmark test specimens were designed using Pro-Engineer (Wildfire Ver. 5). Chua et al. (2004) asserts that the implementation of a benchmark test part is an essential practice in most evaluation studies conducted on any manufacturing system or process. Each benchmark test specimen consisted of three axisymmetric geometric features. The features consisted of two cylinders of diameters 0.5” and 1” and a fillet of radius 0.3”. Wall thicknesses of 0.060” and 0.120” were used for each one of the specimen.

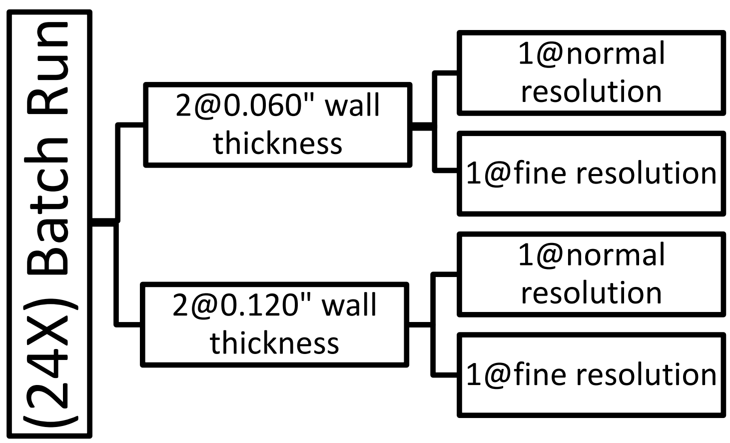

Figure 1: Design of Experiment Factor Combination

The process involved building four benchmark specimens using FDM technology. Two specimens at wall thickness 0.06” and two at 0.12” were constructed. During the setup of the build process, one of the two wall thickness was coded as normal and the other as fine raster resolution. The design of experiment consisted of building four specimens of two factors. Each specimen was randomly positioned and replicated 24 times (figure 1). Due to the building process of the Prodigy Plus™ printer, each build session consisted of a 16 specimen build plate.

The 16 specimen build plates were replicated 6 times (blocked) for a total of 96 individual specimens.

Six build plates of 16 specimens each were printed on a Stratasys Prodigy Plus™. The printer has a build volume of 10” (L) x 10” (W) x 12” (H) with a layer thickness of 0.01” and 0.013” (Statasys, 2012). For the study, a layer thickness of 0.01” was selected.

Data acquisition was conducted using a digital caliper (see appendix A) and Zeiss Contura G2 CMM (appendix F). The data were analyzed using IBM SPSS statistical software (Ver. 12). The analysis and interpretations were guided by the design of experiment principles. Statistical significance was determined through hypotheses testing utilizing the Analysis of Variance (ANOVA) technique. Interactions amongst the factors were also be explored for statistical significance.

Statement of Terminology

3D Printer: A printer that creates three dimensional parts by building one layer at a time (Hiemenz, 2010).

Additive Manufacturing Rapid Reproductive System: Any system capable of creating three dimensional parts layer by layer. A broad term used to describe several related processes that create physical models directly from a CAD database. Prototyping systems use a variety of techniques, including stereolithography and fused deposition modeling (Bertoline and Wiebe, 2003).

Benchmark Test Panel: A valuable tool for evaluating strengths and weaknesses of the system tested (Chua, et. al., 2003).

Concentricity: A condition in which all cross sectional elements of a cylinder, cone, or sphere are common to a datum axis (Bertoline and Wiebe, 2003).

Cylindricity: A condition where all points on a surface should be equidistant from a common axis (Bertoline and Wiebe, 2003).

Design of Experiment: Testing in which purposeful changes are made to input variables of a process to observe changes in the output (Montgomery, 2010).

Fused Deposition Modeling (FDM): A process of extruding heated thermoplastic filaments to create a 3D part (Stratasys, 2012).

Mold: A shaped cavity used in casting to form parts from molten materials (Bruce et. al., 2010).

Parametric Model: A feature based CAD model consisting of design intent and history (Qing-Hui et al., 2010).

Raster Resolution: The intent of this feature is to improve part appearance while allowing for a coarser, faster fill. Normal raster has no change from prior behavior. Fine raster fills exposed horizontal surface regions with minimum width rasters. (Stratasys, 2012)

Sacrificial Pattern: Investment casting tooling representing the shape of the part to be made (Bruce et. al., 2010).

STereoLithography (STL): A meshed CAD file consisting of tiny triangles used to approximate geometries for 3D printed parts (Chang et al., 1998).

Chapter 2

REVIEW OF LITERATURE

This chapter presents a throughall review of a scheme of physical, virtual and personal references and observations in defining the problem and significance of this study. The investment casting process is delineated highlighing its limitations. Additive manufacturing is reviewed to showcase the variety of technologies and applications in investment casting. The FDM process is reviewed as it relates to investment casting of non-wax materials. The detailed literature review resulted in no duplication of the study to investigate the effects of wall thickness and raster resolution on diametric variability of fused deposition modeling on a Prodigy Plus™.

Investment Casting

Traditional investment casting processes consists of tooling used to create the wax sacrificial patterns. The tooling stage is tedious, time consuming, and on average demands 4 – 6 weeks of precise machining. Although overall costs varies, Winker (2010) estimates costs can range from $3,000 to $30, 000 per tool. In addition, Cheah et at. (2005) proposes the tooling stage typically ranges from 6 to 14 weeks. Tooling, therefore, is economical for large batch sizes as costs reductions are realized through economies of scale. As a result, costs could be recouped from multiple use of tools. Small batch production, on the other hand, become challenging to some manufacturers utilizing traditional investment casting methods. The costs of inflexibility and expensive tooling are usually transfered directly to the customer or end user. In a study conducted by Dickens and Hopkinson (2003), the results of comparing three Additive Manufacturing technologies as alternatives to traditional investment casting tooling reccommended additive manufacturing to be more economical than traditional investment casting tooling for production quantities in the thousands. In the study, a small lever (~1.4 inch) and a medium sized cover (~ 8 inch) were casted using a wax injection molding tool and compared to Stereolithography Aparatus(SLA), Fused Deposition Modelling (FDM) and Selective Laser Sintering (SLS) technologies. For the lever with volumes greater than 14000, traditional methods were cited as more economical. Likewise, the study favored the traditional method of tooling for the midium sized cover part for volumes greater than 700 units. However, small parts of unit volumes less than 14000 and medium parts less than 700 units resulted in substantial cost savings when additive manufacturing techniques were employed. According to the researchers, significant cost reductions of up to 6 folds were realized.

Moreover, Chhabra and Singh (2011) have identified the following limitations to traditional investment casting tooling:

- Production of metal tooling for sacrificial patterns can lead to cost justification problems regarding prototyping, pre-series, customized and single, small and medium quantity production.
- Metal tooling consumes a substantial portion of the lead time.
- Costs and lead time increases due to tool design iterations.

Figure 2 provides a graphical illustration comparing traditional investments casting processes to investment casting utilizing additive manufacturing techniques. As illustrated, additive manufacturing techniques eliminates costly and time consuming tooling resulting in a significant reduction of the pre-shell stage. More importantly, the use of additive manufacturing techniques in investment casting allows for greater flexibilities, especially for small or customized production.

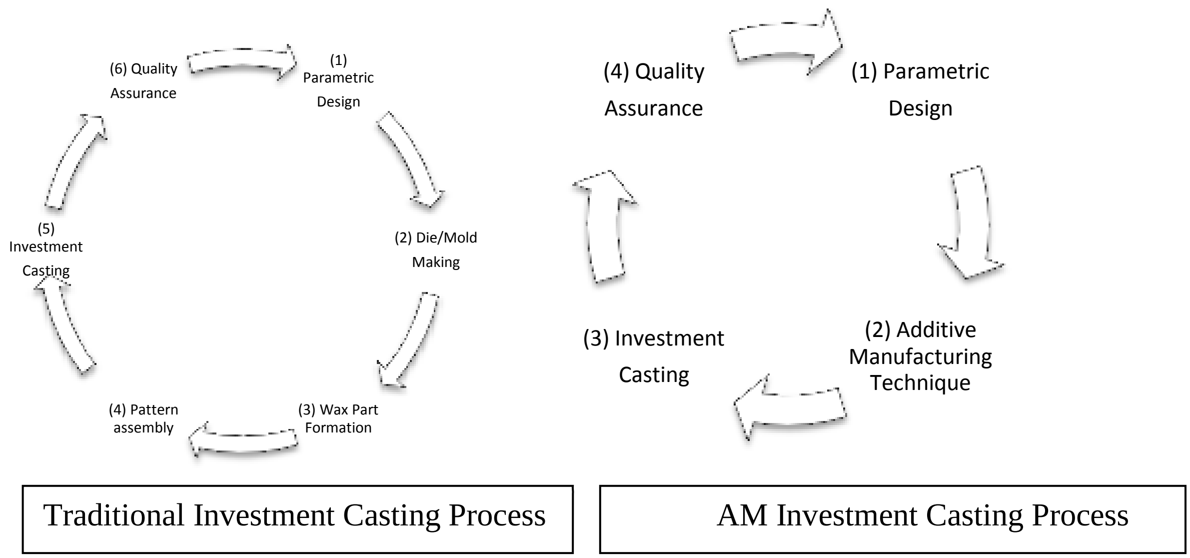

Figure 2: A Comparison of the AM Techniques to Traditional Investment Casting

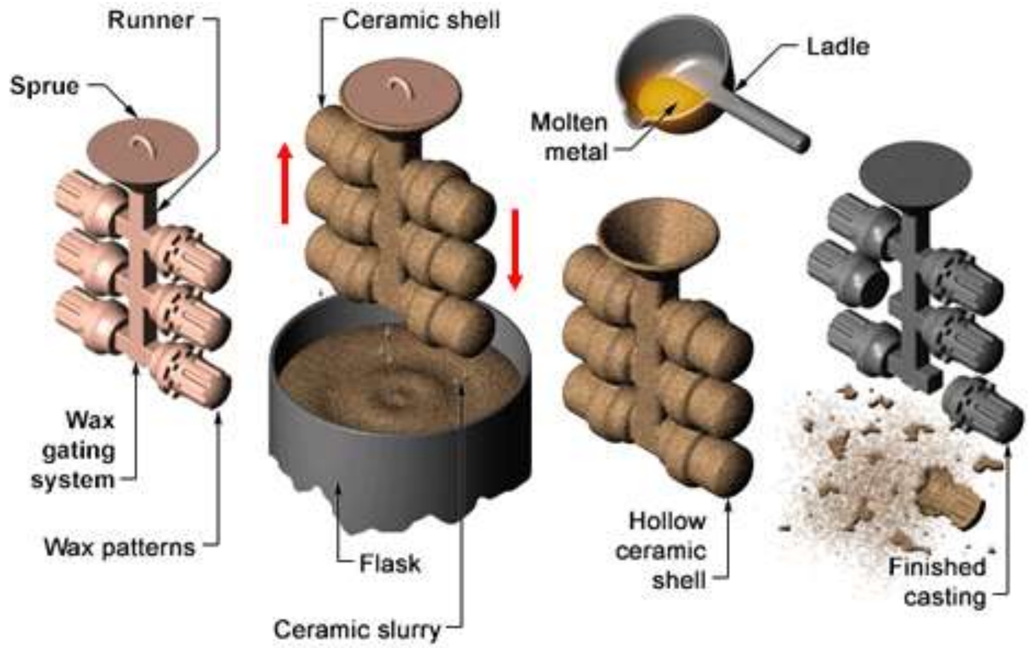

Figure 3: Investment Casting Process. (Extracted from: http://www.ddgrinding.com/wpcontent/uploads/2011/06/investment-casting.png)

Figure 4: Aluminum Mold

An overview of the history and process of traditional investment casting is reviewed (figure 3). Investment casting is one of the oldest casting processes. Early civilizations used beeswax and clay molds to form various metals. Today, investment casting is common in the jewelry and dentistry industries. After World War II, the process was adopted by the industrialized world to form metals for product development.

The Investment casting process begins with the design and manufacture of a mold or die (figure 4). The mold is an outer cavity form of the part. Molds are commonly made by a machining specialist out of aluminum. Molten wax poured into the mold solidifies to the shape. For increased efficiencies, wax patterns are attached to a runner and sprue assembly (Figure 5). A ceramic shell is grown by dipping the assembly into a combination of ceramic slurry and fine sand. The ceramic thickness is achieved by the number of layers applied (figure 6). After the slurry is fully formed and dried, the wax is melted and the assembly fully cured. Molten metal is then poured into the cavity and allowed to solidify. The application of porous slurry material allows gasses to be dissipated during metal solidification. This eliminates the buildup of hotspots caused by gases. The ceramic shell is removed through a combination of vibrations and chiseling. The final steps involve separating the parts by sawing and then applying finishing procedures.

Figure 5: Technician Assembling Parts on

Figure 6: Shell Drying Process

Design of Experiment

According to Montgomery (2010), the three basic principles of experimental design are randomization, replication and blocking. In addition, Chua et al. (2004) asserts benchmark test panels are essential for most evaluation studies conducted on any manufacturing system or process. The design of experiment involves building benckmark test panel on a Prodigy Plus™ FDM system. Replication as defined by Montgomery (2010) is the independent repeat of each factor combination. Each factor combination will be replicated six times. As such, four repeated measures and six replications of two factors, each at two levels will be randomized by a computer algorithm. Research Randomizer is a pseudo random number generator that generates random numbers through a complex algorithm (Urbaniak and Plous, 2013). Blocking is used to eliminate the effects of nuisance variables which can be caused by either material and or minor temperature variations (Montgomery, 2010). Since, each experimental run will be printed at different times where variances in temperature or material may exist, replications will be treated as blocks. Therefore, the design of experiment will consist of six blocks.

Related Research

A review of the literature showcased a number of successful studies employing non-wax sacrificial patterns for investment casting applications. Dotchev and Soe (2006) investigated CastForm using SLS technologies, Yao (1998) studied SLA technology during his doctoral research, and Qingbin et al. (2004) developed a novel technology investigating rapid freeze prototyping. FDM technology has also been heavily researched by Blake and Gouldsen (1998), Grimm (2003), Cheah et al. (2005), Harun et al. (2009), and Singh et al. (2012). Although many detailed studies have been conducted on various additive manufacturing technologies, such as SLA, SLS, and Laminated Object Manufacturing (LOM), FDM technology has been documented as one of the cleanest technologies. Burnout of Acrylonitrile Butadiene Styrene (ABS) material produced no toxicity especially when compared to materials such as epoxy and polycarbonate. The literature highlighted some significant research of FDM applications in investment casting.

While additive manufacturing rapid repoductive systems provide significant bennefits for investment casting applications, non-wax materials still poses the challenge of shell cracking, incomplete burnout and residual ash. A mismatch of the coefficient of thermal expansion between the non-wax sacrificial pattern and ceramic shell leads to inconsistent expansion of the two materials. In turn, thermal stresses are induced on the ceramic shell that creates fractures. Granting their effects can be minimized through various techniques in design and processing, the risk still exist.

Wax patterns are sensitive to environmental conditions and are not ideal for thin wall castings. As a result, any additive manufacturing generated component that can be flashed fired without damaging the ceramic shell can be used as a substitute of wax investment casting pattern (Chhabra and Singh, 2011). Although many studies have shown that in selecting non-wax patterns, problems such as, shell cracking, incomplete burnout and residual ash, should be avoided, non-wax patterns allows finishing operations that can drastically improve surface quality of finished products. Non-wax patterns have two significant advantages over wax patterns (Cheah et al. 2005). Firstly, the durability and strength allow for thinner walls and more intricate design options. Secondly, finishing operations can be easily applied to improve surface quality and finish.

Despite the fact that a number of additive manufacturing technologies can be used for either mold or sacrificial patterns in investment casting, this study only investigates FDM additive manufacturing techniques for the creation of thin walled sacrificial patterns. In addition, additive manufacturing techniques such as FDM provides the benefits of small and complex parts due to the independence of geometry (Bak, 2003; Bourell et al., 2009; Ramos et al., 2003; Wang et al., 1999). According to the literature, it is established by a number of studies that shell failure is an inherent problem when using non-wax sacrificial patterns. The problem occurs due to thermal expansion of the sacrificial pattern during burnout. Jacobs (1993) suggests using the QuickCast technique developed by 3D Systems as a possible workaround. QuickCast replaces solid geometries with triangular shells. As a result, the hollow sacrificial pattern melts and collapses inwards eliminating thermal stresses due to expansion (Yao and Leu, 1999).

One direct application of additive manufacturing systems in investment casting involves systems that utilize wax materials. 3D system’s Thermojet, for example, is capable of building direct wax sacrificial patterns. Since the wax material is similar to traditional investment casting wax, little change is required to the process.

3D printing and SLS technologies utilize an infiltration process for investment casting. A starch-based material used in 3D printing is infiltrated with wax then assembled on a runner and sprue for shelling. Similarly, SLS builds with a polystyrene material that is also infiltrated with wax prior to assembly. CastForm, developed by 3D Systems, builds polystyrene parts through laser sintering. For casting, the green polystyrene part is treated in a wax infiltration process. Many studies have been conducted on the CastForm process. Dotchev and Soe (2006), for example, concluded that the weakest link of the CastForm process involved the infiltration of wax into the green part. Since the green part is so fragile, cleaning and movement should be limited and performed with extreme care. The main principle is not to move or touch the green part during wax infiltration when the material strength is minimal (Dotchev and Soe, 2006).

Current practices of wax infiltration involve manual processes, where, the green part is submerged into a vat of wax or the wax in poured over the part. Consequently, the wax infiltration process can produce inconsistencies that are difficult to control. For the most part, the cooling rate of wax must be controlled, as inconsistent or rapid cooling can damage the green part, particularly thin walled features.

Yao (1998) in his dissertation research investigated SLA technology for building sacrificial investment casted patterns. Since non-wax materials induces thermal stresses capable of shell cracking during the burnout process, Yao's experimental study, investigated conditions that were attributable to shell failure. In the study a Finite Element Analysis (FEA) was conducted to determine induced shell stresses which were further verified experimentally. The study explored three patterns of the QuickCast technique. Hexagonal, triangular and square web structures were investigated and compared. The hexagonal structure performed best compared to the triangular and square structures with reduced stresses of 32% and 22% respectively (Yao, 1998).

Table 1 summarizes the accuracy, transferability and toxicity of some common additive manufacturing technologies. Thermoplastics and casting wax were classified as non-toxic in FDM and SPI technologies. Although SLA technologies exhibited excellent accuracies, the epoxy material measured toxicity during burnout. Yao (1998) demonstrated casting wax and low melting thermoplastics produced no toxicity of both FDM and SPI technologies.

Table 1: Compatibility of RP processes with investment casting (Yao, 1998)

RP Process	Material	Accuracy	Transferability	Material Toxicity
SLA	Epoxy	Excellent	Thermal expansion	yes
SLS	Casting wax, polycarbonate	Poor	Material shrinkage	yes
FDM	Casting wax	Good	Similar to “Lost wax”	No
SPI, MODEL MAKER	Low melting Thermoplastic	Excellent	Negligible Thermal expansion	No
DSPC	Casting ceramic	Poor	Material shrinkage	Yes
LOM	Sheet paper	Fair	Residual ash	Yes

Qingbin et al. (2004) investigated a rapid freeze prototyping system for manufacturing investment casted parts utilizing water. Two experiments were conducted to demonstrate the viability of the process. The first experiment examined two critical factors of additive manufacturing, namely, surface finish and dimensional accuracy. The second experiment reviewed and compared ice sacrificial patterns to traditional wax patterns.

The rapid freeze prototyping system builds 3D ice parts directly from CAD (figure 7). The water in the feeding pipe is ejected drop by drop in a drop-on-demand mode. The build environment is kept at a temperature below water’s freezing point. Pure water or colorized water is ejected from the nozzle and deposited onto the substrate or the previously solidified ice surface. In the process, water droplets do not solidify immediately. Instead, they spread and unite together to become part of a continuous water line. The newly deposited water is cooled by the low temperature environment through convection and by the previously formed ice layer through conduction. After a layer is finished, the nozzle is elevated upwards the height of one layer thickness. After a predetermined delay, for solidification, the next layer begins. This procedure continues until the designed ice part has been fabricated.

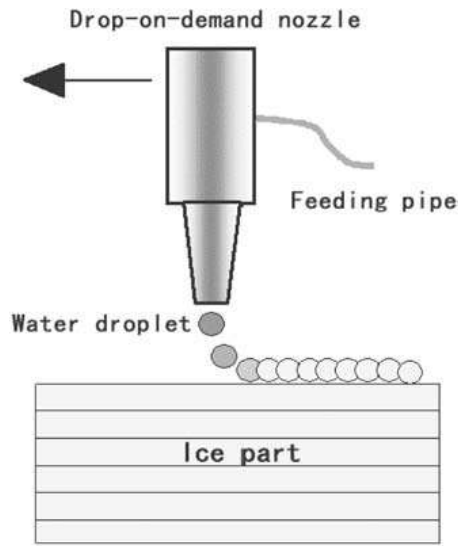

Figure 7: Rapid Freeze Principle (Qingbin et al. 2004)

Advantages of rapid freeze prototyping include:

- Cheap and clean process
- Decreased likelihood of investment shell cracking as compared to wax patterns
- Makes ice patterns directly from CAD models in a short time, without the high cost and other issues of mold making of metal castings

Dimensional accuracy and surface finish were measured for 12 casted cylinders of diameter 7.62 mm (0.3") and height 8.128mm (0.32"). The results of the measurements of the ice build compared to the nominal values are shown in table 2. The casted dimensional measurements and surface finishes for ice prints and wax are compared in tables 3 and 4, respectively.

Table 2: Ice Dimensions (Qingbin et al., 2004)

No.	Measured OD (mm)	OD deviation (mm)	Measured height (mm)	Height deviation (mm)
1	7.518	−0.102	8.233	0.105
2	7.544	−0.076	8.084	−0.044
3	7.658	0.038	8.487	0.359
4	7.634	0.014	8.013	−0.115
5	7.601	−0.019	7.912	−0.216
6	7.633	0.013	7.971	−0.157
7	7.633	0.013	8.451	0.323
8	7.645	0.025	8.458	0.330
9	7.626	0.006	8.426	0.298
10	7.629	0.009	8.509	0.381
11	7.629	0.009	8.352	0.224
12	7.638	0.018	8.261	0.133
Average	7.616	0.028	8.263	0.224

Table 3: Casted Ice Measurements (Qingbin et al., 2004)

No.	Measured OD (mm)	OD deviation (mm)	Measured height (mm)	Height deviation (mm)	Ra (μm)
1	7.633	0.013	8.100	−0.028	3.55
2	7.565	−0.055	8.091	−0.037	4.77
3	7.763	0.143	8.673	0.544	4.92
4	7.695	0.075	7.817	−0.312	3.81
5	7.835	0.215	7.929	−0.199	4.90
6	7.805	0.185	8.145	0.017	3.51
7	7.783	0.163	8.355	0.227	3.44
8	7.795	0.175	8.575	0.447	3.72
9	7.713	0.093	8.440	0.312	4.50
10	7.795	0.175	8.388	0.259	4.16
11	7.683	0.063	8.249	0.121	4.03
12	7.645	0.025	8.310	0.182	5.00
Average	7.726	0.115	8.256	0.224	4.19

Table 4: Casted Wax Measurements (Qingbin et al., 2004)

No.	Measured OD (mm)	OD deviation (mm)	Measured height (mm)	Height deviation (mm)	Ra (μm)
1	7.66	0.04	8.00	−0.13	5.25
2	7.70	0.08	8.00	−0.13	4.77
3	7.66	0.04	8.02	−0.11	4.44
4	7.58	−0.04	8.05	−0.08	5.99
5	7.65	0.03	8.02	−0.11	5.37
6	7.64	0.02	8.11	−0.02	5.25
7	7.67	0.05	8.07	−0.06	6.50
8	7.67	0.05	8.07	−0.06	5.81
9	7.66	0.04	7.93	−0.20	4.37
10	7.59	−0.03	8.02	−0.11	6.65
11	7.70	0.08	8.04	−0.09	6.21
12	7.64	0.02	8.02	−0.11	6.36
Average	7.65	0.04	8.03	0.10	5.58

The results of the study indicated that the dimensional accuracy of wax investment casted parts had better accuracy than ice patterns, however, castings from ice patterns displayed better surface finish. The poor dimensional accuracy was attributed to the interface agent used to seal the ice prior to shelling, along with the effects of firing.

A Review of Applications of FDM in Investment Casting

Blake and Gouldsen (1998) concluded that FDM sacrificial patterns resulted in cleaner burn-out, more robust, and less fragile, when compared to other additive manufacturing investment casting processes. The study consisted of casted ABS FDM parts from six foundries. The test part consisted of a wedge design as illustrated in figure 8. The design allowed for measurements of part accuracy and determination of shrinkages. The average shrinkage result for one foundry is recorded as 0.76% (Table 5). Furthermore, the experiment demonstrated that at approximately 212°F during the burnout phase of the ABS sacrificial pattern, the average expansion was maximized at 0.35%. Thereafter, melting occurred at approximately 357°F. The report further demonstrated that hollow parts improved efficiencies with quicker builds and less mass to burn-out. Blake and Gouldsen (1998) concluded that although shrinkages varied slightly amongst foundries due to differences in methods and processes, ABS sacrificial pattern expansion of 0.35% or less did not demonstrate ceramic shell fractures.

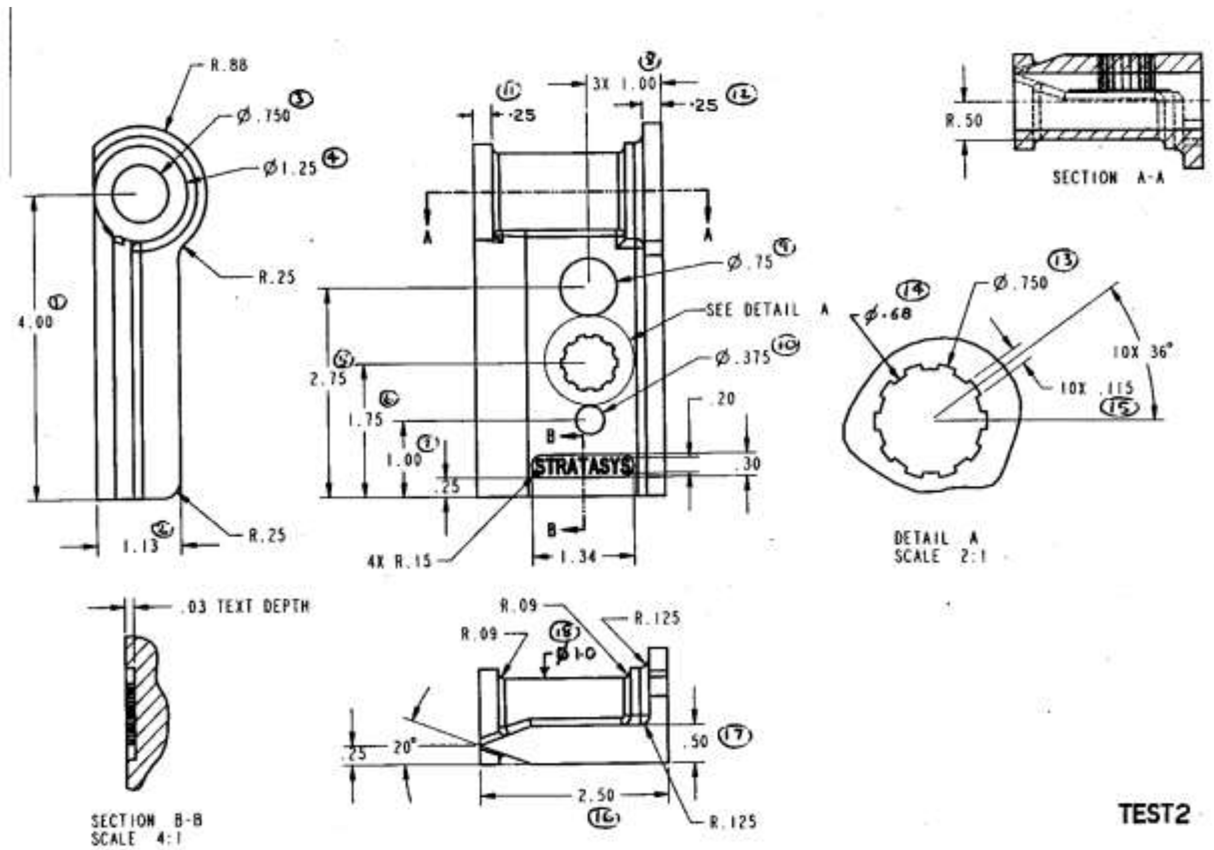

Figure 8: Wedge Part Design (Blake and Gouldsen, 1998)

Rapid Prototyping has provided the advantage to manufacturers of cost effective short runs with economic order quantities as low as one (Grimm, 2003). In an experimental evaluation study of three FDM, one SLS and SLA systems, Grimm (2003) concluded that although surface finish is a limitation for FDM when compared to other additive manufacturing technologies, such as SLS and SLA, FDM patterns are more suitable for investment casting applications, with little modification to the standard foundry process. In the experimental study, twelve linear dimensions were measured and compared to nominal values. The dimensions ranging from 2.54

mm (0.1”) to 152.4 mm (6”) measured an average deviation of 0.6% from nominal. The largest deviation was measured along the z-axis (2.05%). Surface finishes were best on the side walls (parallel to z-axis), with an average value of 437.5 µin. The bottom surface measured the worst due to contact with the base material. Bottom and top surface finishes measured 562.5 µin and 512.5 µin respectively. Even with the limitation of surface finish, Grimm (2003) demonstrated that ABS material can be finished to achieve significant improvements of approximately 83% surface improvement. One key advantage of FDM over SLA is that of dimensional stability. According to the study, time and environmental exposure alters the dimensions on parts built with an SLA process. Even after SLA parts are allowed to settle at room temperature the size of features can change. Unlike SLA, FDM dimension remains fixed and on average more robust to time and minor environmental changes.

Through collaborative research between the Universiti Teknologi Malaysia and Universiti Malaysia, Pahang, Harun, Idris and Sharif (2008) summarized the following:

- Surface roughness is consistent for both hollow and solid pattern construction
- Hollow patterns had better dimensional accuracies compared to solid patterns
- Hollow patterns exhibited greater distortion (33.11%) than solid patterns
- Hollow patterns did not cause shell cracking during all investigated burning temperatures as compared to solid patterns (Singh et al., 2012)

Table 5: Average Shrinkage Measurements (Blake and Gouldsen, 1998)

Dimension ID	Drawing dimension	Average RP dimension (ABS)	Average casting dimension (alu)	Deviation	% shrink
1	4	3.999	3.990	0.009	0.23
2	1.13	1.123	1.103	0.020	1.76
3	0.75	0.731	0.743	-0.012	-1.62
4	1.25	1.242	1.228	0.014	1.11
5	2.75	2.747	2.739	0.008	0.30
6	1.75	1.748	1.742	0.006	0.34
7	1	1.000	0.993	0.007	0.70
8	1	0.997	1.014	-0.017	-1.71
9	0.75	0.745	0.742	0.004	0.50
10	0.375	0.372	0.369	0.003	0.87
11	0.25	0.249	0.241	0.009	3.41
12	0.25	0.247	0.239	0.008	3.34
13	0.75	0.746	0.737	0.009	1.24
14	0.68	0.678	0.674	0.004	0.55
15	0.115	0.114	0.113	0.001	1.09
16	2.5	2.498	2.470	0.028	1.12
17	0.5	0.510	0.505	0.005	0.93
18	1	0.994	0.991	0.003	0.30
			Average	0.005	0.76

The research consisted of designing and printing four solid and four hollow patterns using FDM technology. The patterns were evaluated and compared for dimensional accuracy, surface finish and distortion. Following printing, the patterns were shelled then burned at temperatures ranging from 300°C to 600°C. Twenty-six dimensions were measured to an accuracy of 1µm. During the burnout process, a digital weighing machine was used to measure the weight loss of the pattern as the temperature increased from 300°C to 600°C. For each temperature increment, the patterns were baked for 1 hour then left to cool for 12 hours. Although no cracking was observed on the hollow shell throughout the experiment, at temperatures ranging from 300°C to 500°C there were visible signs of cracking on the solid shell. The study also demonstrated that there was no shell cracking of the solid pattern for temperatures of 550°C to 600°C (Harun et al., 2008). “In the range of 200°C to 300°C it gets softened and become paste…above 570°C ABS turns into ash” (Singh et at., 2012). The researchers attributed cracking of the solid shell to thermal expansion stresses exerted on the ceramic shell.

Table 6 summarizes the accuracy results of research conducted by Cooper and Wells (2000) in evaluating rapid prototyping applications for investment casting at the Marshall Space Flight Center. In an experimental study of casting six fuel pump models, a range of additive manufacturing technologies were utilized to determine dimensional accuracy. In addition, surface finishes for SLS, FDM, LOM, and Z-Corp were measured at 200 µin, 60 µin, 60 µin, and 300 µin, respectively.

Table 6: SLS, FDM, LOM, Z-CORP Dimensional Results (Cooper and Wells, 2000)

FDM-ABS	*x* Accuracy	*y* Accuracy	*z* Accuracy	*x* Per Inch	*y* Per Inch	*z* Per Inch
CAD-RP	0.0068	0.0003	0.0035	0.0015	0.0000	0.0008
RP-Casting	0.0055	0.0125	−0.0116	0.0012	0.0020	−0.0027
CAD-Casting	0.0132	0.0128	−0.0081	0.0028	0.0021	−0.0019

LOM	*x* Accuracy	*y* Accuracy	*z* Accuracy	*x* Per Inch	*y* Per Inch	*z* Per Inch
CAD-RP	0.0130	−0.0113	−0.0293	0.0028	−0.0018	−0.0069
RP-Casting	0.0003	0.0300	0.0286	0.0001	0.0049	0.0067
CAD-Casting	0.0132	0.0187	−0.0006	0.0028	0.0031	−0.0001

Z-Corp	*x* Accuracy	*y* Accuracy	*z* Accuracy	*x* Per Inch	*y* Per Inch	*z* Per Inch
CAD-RP	0.0065	−0.0085	0.0142	0.0014	−0.0014	0.0033
RP-Casting	0.0142	0.0349	0.0400	0.0030	0.0057	0.0094
CAD-Casting	0.0207	0.0264	0.0543	0.0044	0.0043	0.0127

SLS-Polycarb	*x* Accuracy	*y* Accuracy	*z* Accuracy	*x* Per Inch	*y* Per Inch	*z* Per Inch
CAD-RP	−0.0105	−0.0090	0.0032	−0.0022	−0.0015	0.0008
RP-Casting	0.0439	0.0301	0.0496	0.0094	0.0049	0.0116
CAD-Casting	0.0334	0.0211	0.0529	0.0071	0.0034	0.0124

In a survey of applications for investment casting using additive manufacturing rapid reproductive systems, Cheah et al. (2005) reviewed both mold and direct pattern fabrication. The survey summarized that dimensional accuracy, surface quality and part durability must be further investigated and improved. Shrinkage compensation factors, post machining allowances and foundry requirements are critical pre-requisites that also must be considered for improving quality. Even with the variety of additive manufacturing technologies used for investment casting applications, there is no clear evidence as to which technology is most beneficial.

Validation of FDM ABS sacrificial Patterns

A number of experimental studies involving both academia and industry supports and have successfully demonstrated the use of non-wax materials, such as ABS, for sacrificial patterns in investment casting applications. According to Blake and Gouldsen's (1998) comprehensive study involving six foundries, the maximum thermal expansion of fused deposition ABS sacrificial patterns was .35%. The study consisted of building ABS patterns utilizing FDM technology for mechanical and thermal property testing. Thin walled test parts of thicknesses .025", .035", .04", .05", .07", and .1" were supplied to six different foundries for casting. The burnout sequences for three foundries are recorded in table 7.

Table 7: Burn-out sequences from three foundries (Blake and Gouldsen, 1998)

Foundry	Pre-heat & load	Ramp to:	Hold	Cooling
A	1600 °F (871 °C)	1950 °F (1066°C)	1.5 - 2 hr.	Natural over night
B	1600 °F (871 °C) for 10 minutes	2050 °F (1120 °C)	50 mins.	1600 °F (871°C) remove to cool
C	Ambient	1800 °F (982 °C)	3 hr.	Natural over night

Thermal expansion and decomposition were measured using a dilatometer and thermo gravimetric analysis respectively. The dilatometer recorded a maximum of .35% linear expansion at 356°F with an average of .24% linear expansion at a temperature of 352°F. It was also noted that ABS reached a softening point where expansion declined between 221°F and

352°F. At temperatures between 572 and 752°F, 95% burnout of a 4oz sample was achieved. The study further notes that the remaining material burned off at 1067°F. The experimental study demonstrated that FDM sacrificial patterns that are built from ABS material are suitable for investment casting applications. Each foundry was capable of producing acceptable investment castings. All in all, ABS sacrificial patterns produced clean burn-out and robustness for better handling.

Singh et. al. (2012) in an experimental study comparing sacrificial patterns of FDM and SLS technologies, agreed with Blake and Gouldsen (1998) thermal expansion of .35%. In their experimental study, 12mm ABS cubes were measured for thermal expansion using a dilatometer. The results of the test were identical to Blake and Gouldsen (1998) ABS thermal expansion of .35%. The study also involved the worthiness of ABS as a sacrificial pattern, behavior of ABS during burnout and castability. ABS started softening above 302°F and burned between 572°F and 842°F. Similar to Blake and Gouldsen (1998), total burnout was achieved at approximately 1058°F. Furthermore, recent studies conducted at Missouri University of Science and Technology and Virginia Tech supports and demonstrate the successful application of ABS sacrificial patterns for investment casting.

Chapter 3

METHODOLOGY

The purpose of this study was to investigate the effects of wall thickness and raster resolution on diametric variability, cylindricity, and concentricity of fused deposition modeled sacrificial patterns. The study was conducted in two stages. The pre-experimental stage involved validating the extrusion diameter of ABS400 model material. This average measured diameter was used as a guideline to selecting wall thicknesses for the study. As delineated in the preliminary experimental study, the benchmark test specimens were redesigned to achieve optimal build conditions on the Prodigy Plus™ FDM printer. Based on the results of the preliminary experimental study, a pilot test run was conducted to verify both setup and process were properly defined. The second stage of the study involved of a design of experiment to investigate the effects of wall thickness and raster resolution on diametric variability, cylindricity, and concentricity. The prodigy Plus was calibrated and loaded with new model and support materials. Both materials were purged to eliminate any residual materials in the liquefied head. Environmental conditions, such as, temperature, and humidity were monitored throughout the study.

Two wall geometries and two raster resolution settings were examined and analyzed for statistical significance through hypothesis testing. Data were qualified utilizing a Zeiss Contura G2 coordinate measuring machine. The determined wall thicknesses were set to 4 and 8 times the minimum extruded material diameters as calculated in the preliminary experimental study. Two factors of independent variables, wall thickness and raster resolution, each of two levels, 0.06”, 0.12”, and normal, fine, respectively, were investigated against their effect on dependent variables of diametric dimensions, cylindricity, and concentricity.

Preliminary Experimental Study

Prior to conducting the design of experiment, a number of practical parameters first had to be established. Since experimental parameters were based on the physical limitations of the equipment utilized for the study, the smallest road width diameter capability had to be determined for the printer. The road width diameter is the diametric measurement of the extruded material (figure 9).

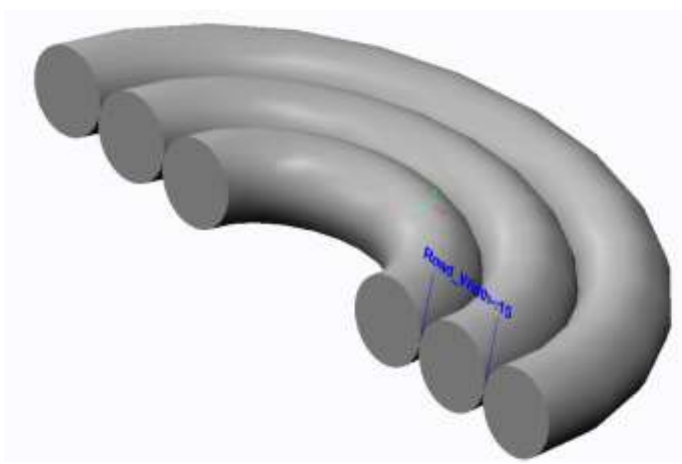

Figure 9: Road Width of FDM Toolpath

New cartridges of model and support materials were loaded and purged for 5 minutes. Appendix D consists of the certificate of conformance for the materials. Purging is the process of extruding materials through the liquefier heads. Purging allows for the removal of any residual materials leftover in the liquefier head. It also removes cartridge material that was exposed to environmental elements, especially during loading. After the initial 5 minutes of purging, a second round of purging was conducted to determine the average diameter. The extruded material was measured at 10 randomly selected points using a Fowler 6" Digital Caliper as shown in appendix A. All dimensions were measured in inches with accuracies within 10 thousandth of an inch. The average of 10 randomly selected points was calculated at 0.015”. The 10 measured diameters with calculated average were recorded in table 8. This average diameter was used as a guideline to selecting wall thicknesses for the study. Wall thicknesses were set to twice and four times the smallest extruded diameters of 0.03” and 0.06”, respectively.

Table 8: Purged FDM Model Material Diameter

Random Position	Ø1	Ø2	Ø3	Ø4	Ø5	Ø6	Ø7	Ø8	Ø9	Ø10	$Average = \frac{\sum_{i=1}^{n} x_i}{n}$
Diameter (inch)	.0151	.0151	.0149	.0150	.0149	.0150	.0150	.0150	.0150	.0150	.015

Two benchmark test specimens were designed as shown in figure 10. Utilizing Pro-Engineer (Wildfire ver. 5), benchmark test specimens were designed with a 2” square base of 0.25” high. A revolved geometric feature consisting of a 0.3” diameter cylinder and a 0.3” radius fillet were designed on the square base. Wall thickness dimensions were engraved in the lower left corner of the base as an indicator to differentiate 0.03” from .06” wall thicknesses.

The pilot test run was designed to determine the feasibility of building specimens at the predetermined wall thicknesses. In addition, the pilot test run was used to validate all setup and operation parameters for the study. Four benchmark test specimens were built. Each specimen consisted of a combination of one of two wall thickness factors of 0.03” or 0.06” and raster resolution of normal or fine. During tool path generation, part raster width was set to normal or fine.

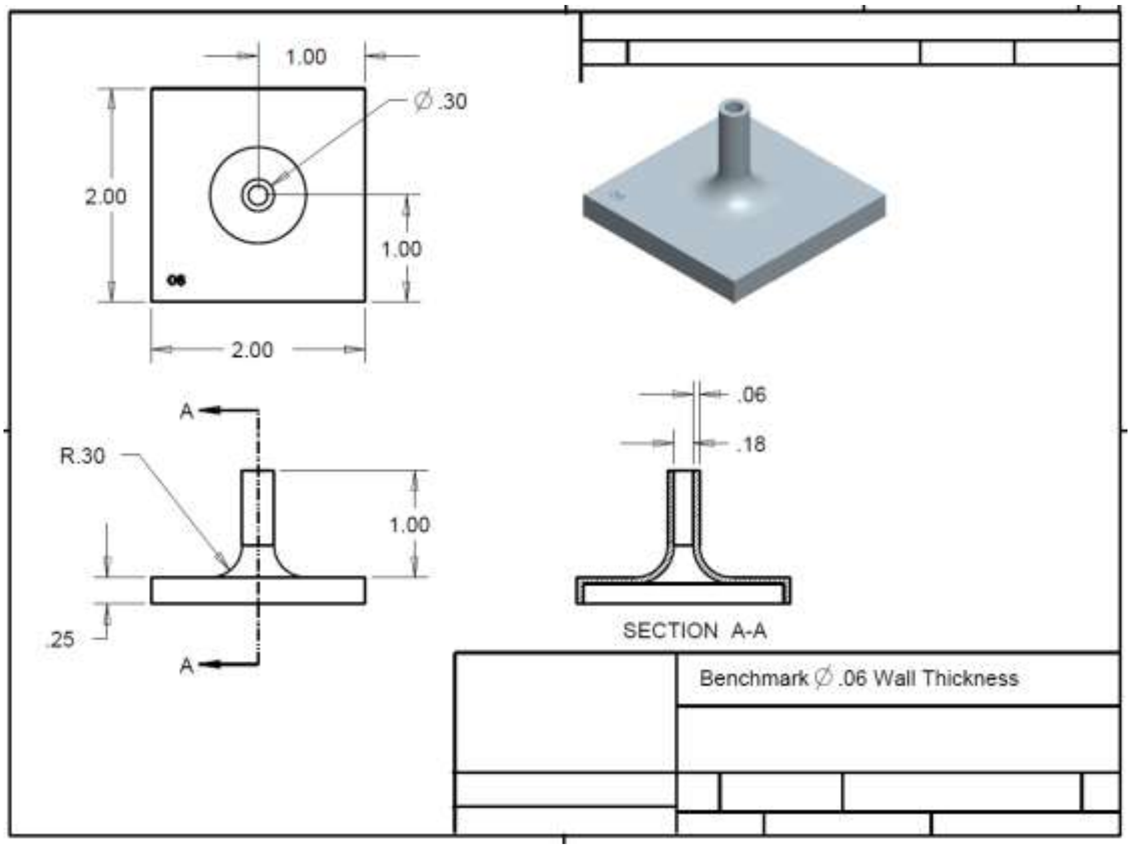

Figure 10: CAD Drawing of Benchmark Part

The results of the pilot test indicated layer separation as depicted in figure 11. Layer separation was prominent only on the 0.03” wall thickness and did not seem to be affected by raster resolution. During part build, layers are allowed to solidify as the extrusion head returns to its home position. This cooling delay created layer separation that were more pronounced on wall thicknesses of 0.03” as shown in figure 11. As a result of the layer separation at twice the minimum extruded smallest diameter, the benchmark test specimens were redesigned to incorporate good form geometries.

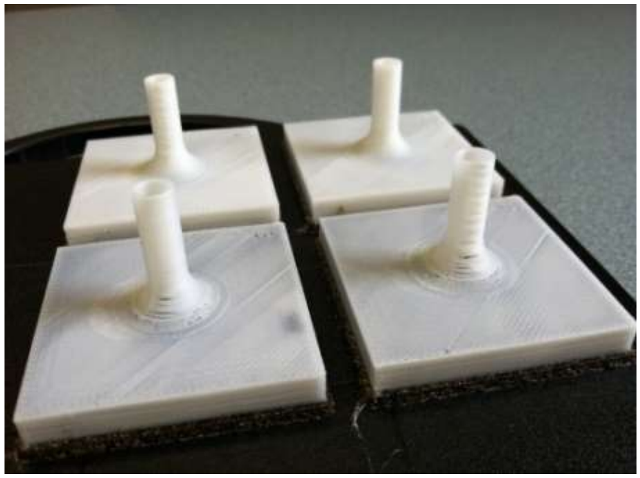

Figure 11: Layer Separation of Pilot Test Build

The redesigned benchmark specimens were built to investigate good form and time to build. For the pilot test, no notches were engraved in the fine raster resolution specimens. The results indicated good form with no layer separation. It was also observed that although the material usage for 0.06” wall thickness specimens was consistent the normal raster resolution required more time to build than the fine. Similarly, there was a marked difference in time to build for the 0.12” fine raster resolution wall thickness of 5 minutes less than normal raster resolution.

Benchmark Test Specimen Redesign

The design of experiment comprised four individual benchmark test specimens. The decision to use four benchmark test specimens as compared to one panel consisting of four specimens was based in part to the printer’s variability. The larger the benchmark test panel, the greater the variability of cooling rates amongst the material. Therefore, part warping is an inherent artifact of the prodigy plus™ particularly on large linear dimensions. To avoid part warping, four smaller benchmark test specimens were designed versus one large test panel of four specimens.

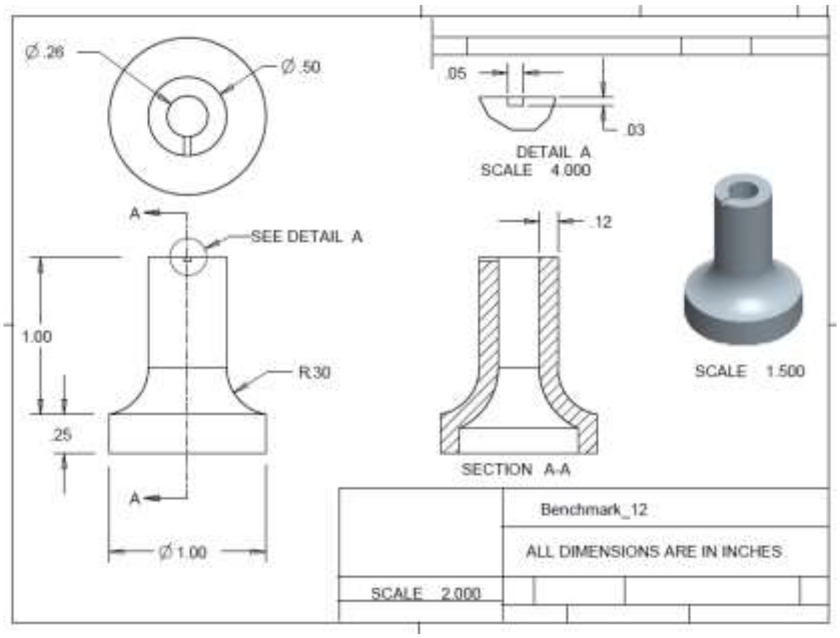

Figure 12: Sample CAD Drawing of Redesigned Benchmark Specimen

The benchmark test specimens were designed using Pro-Engineer (Wildfire Ver. 5). Figure 12 illustrates one of the two specimens. Three axisymmetric geometric features were designed. They included two cylinders of diametric dimensions of 0.5" and 1" and a fillet of radius 0.3". The specimens were designed with wall thicknesses of 4 times minimum (0.6") or 8 times minimum (0.12"). To distinguish the normal from the fine raster resolution setting, a notch of dimension 0.05" X 0.3" was designed for the fine raster resolution setting as shown in figure12, (detail A).

Design of Experiment

The full factorial 2X2 design of experiment principles was used to guide the study. A two factor, two levels set of four benchmark test specimens were built and repeated 24 times in a random order. The coding scheme and build plate position references are illustrated in figure 16. Six plates of 16 specimens were built.

Figure 13: Build Plate & Code Scheme Position

Each build plate was allocated a unique build reference number ranging from 1 to 6, located on the upper right corner (figure 13). Randomization of the build process was achieved by using Research Randomizer to generate 24 sets of 4 numbers per set. A total of 96 randomly positioned specimens were analyzed for the study. Research Randomizer, version 4.0 was utilized to create random build position references for each benchmark test specimen. Appendix B provides the input parameters and randomization results for the study.

Table 9: Randomization Coding System

Number	*Wall Thickness (1=0.06" / 2=0.12")*	*Raster Resolution (1=fine / 2=normal)*	*File Name*
1	1	1	Bench06_fine
2	1	2	Bench06
3	2	1	Bench12_fine
4	2	2	Bench12

Using the coding scheme depicted in table 9, each specimen was randomly placed on the build plate. To achieve maximum spacing, the pack was set to "un-restricted" in the preference menu. This allowed for tighter spacing of specimens. This in turn allowed more specimens per build plate, reducing the overall time to build.

Repetition and blocking for the study was achieved during part build. Each factor combination was repeated 4 times during a single plate build. A total of 16 specimens per plate were constructed. Six plates of 16 specimens each were built. Each plate build created a block. The study consisted of six blocks of 16 specimens, randomly placed for a total of 96 specimens (table 10). In this study, blocking was used to improve precision by eliminating nuisance variability in material and temperature. Since error within was significantly less than error between, each plate was classified as a block.

Table 10: Independent Factor Combination

Plate/Block	Wall Thickness (0.06"/0.12")	Raster Resolution (normal / fine)	Interaction (Wall thickness & raster resolution)
1	8 @ 0.06", 8 @ 0.12"	8 @ normal, 8 @ fine	4 of 0.06" & 4 of 0.12" @ normal and @ fine
2	8 @ 0.06", 8 @ 0.12"	8 @ normal, 8 @ fine	4 of 0.06" & 4 of 0.12" @ normal and @ fine
3	8 @ 0.06", 8 @ 0.12"	8 @ normal, 8 @ fine	4 of 0.06" & 4 of 0.12" @ normal and @ fine
4	8 @ 0.6", 8 @ 0.12"	8 @ normal, 8 @ fine	4 of 0.06" & 4 of 0.12" @ normal and @ fine
5	8 @ 0.06", 8 @ 0.12"	8 @ normal, 8 @ fine	4 of 0.06" & 4 of 0.12" @ normal and @ fine
6	8 @ 0.06", 8 @ 0.12"	8 @ normal, 8 @ fine	4 of 0.06" & 4 of 0.12" @ normal and @ fine

Figure 14: Prodigy Plus™ FDM Printer

The 2^2 factorial design of experiment was use to guide the study. Four benchmark test specimens were designed utilizing Pro-Engineer (ver. 5) and built utilizing a prodigy plus™ (figure 14). The benchmark test specimens were constructed of a thermoplastic ABS400 polymer material (see Appendix C for material properties). Preparation and setup for printing was done using Insight software.

Preparation for Printing

Insight software was utilized for preparing the model for printing. Prior to printing, the Pro-Engineer CAD file was converted to an STL format. The process involved saving the CAD model as an STL format with Chord Height and Angle Control set to 0 and 1 respectively. The smallest Chord Height was calculated based on the CAD geometry. The 0.12" benchmark test model, for example, resulted in a chord height of 0.0001" (figure 15).

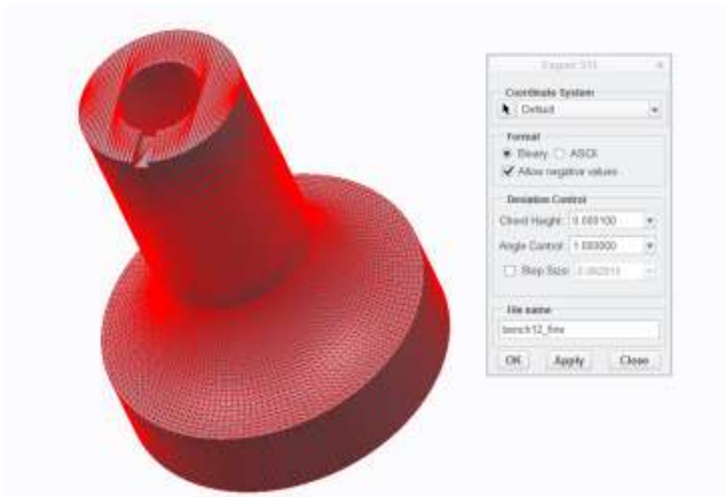

Figure 15: STL file Generation in Pro-E

The tessellated approximation of geometry was treated using Insight software. Three basic processes were requiring prior to printing. Slicing, support material definition and tool path generation were defined and configured for printing.

Slicing of Benchmark Test Panel

The FDM build process construct parts one layer at a time. Layers were generated through a process of slicing the CAD stl. model. After loading the model into Insight, an

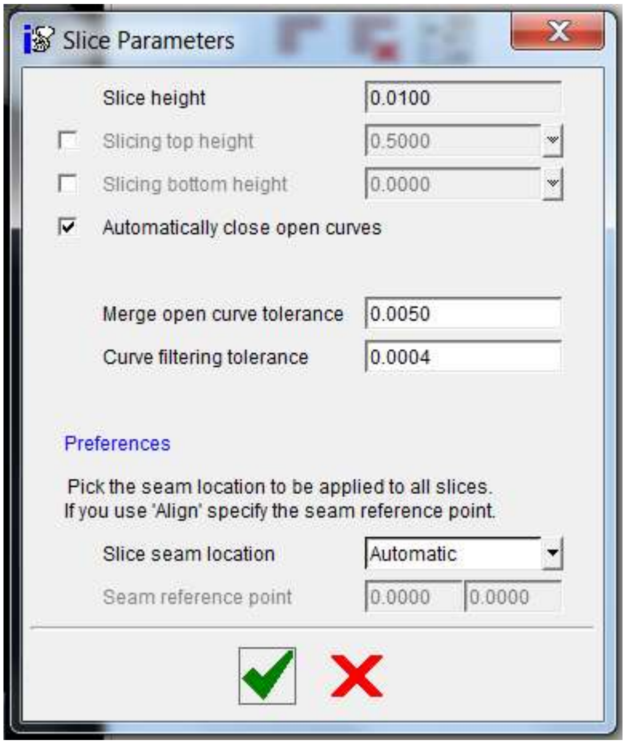

Figure 16: Slice Setup and

appropriate orientation was determined based on efficiency of material use and build time. For the study, the benchmark test models were oriented with the vertical cylinders upright. This orientation provided the least amount of build time. In addition to build time, a vertical orientation provided the most optimal use of support material. Any other orientation would require additional support material for construction of the axisymmetric geometric features. The slice height was set to 0.010” and all other parameters were set to default as shown in figure 16.

Support Material Definition

Figure 17 illustrates the setup parameters and configuration for generating support material. Support material is required for any free standing geometry, such as, overhangs. In addition, support material was used as a transition material between the build plate and the model ABS material. This technique allows for easier removal of the specimens while drastically reducing damage to the specimens. Such a practice preserves geometric during part build and removal from build plate. The support material was built with a sparse style. That way, less support material was used and removal is manageable. The base transition section consisted of 10 layers of support. This base structure of support material created a solid foundation to protect and support the model build process. All other parameters were configured as defaults shown in figure 17.

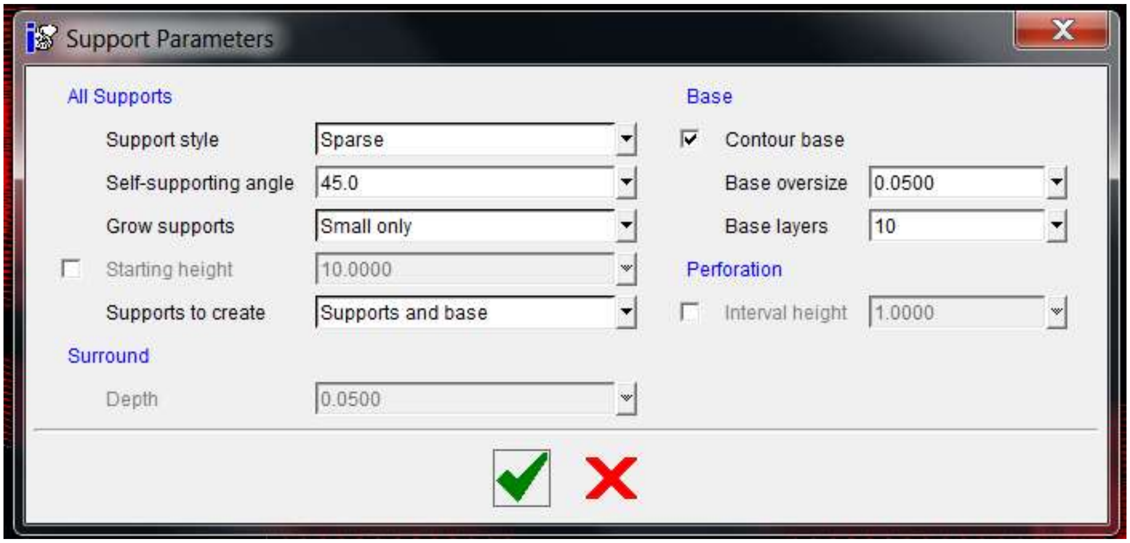

Figure 17: Support Material Setup and Configuration

Tool Path Generation

The tool path settings were configured as shown in figure 18. The visible surfaces were varied between normal and fine raster resolution for each one of the two wall thicknesses. Each one of the four specimens were processed as a combination of wall thickness and raster resolution of specimen #1 (0.06” and fine), specimen #2 (0.06” and normal), specimen #3 (0.012” and fine), and specimen #4 (0.012” and normal). All other parameter settings were configured to the standard default setting as shown in figure 18.

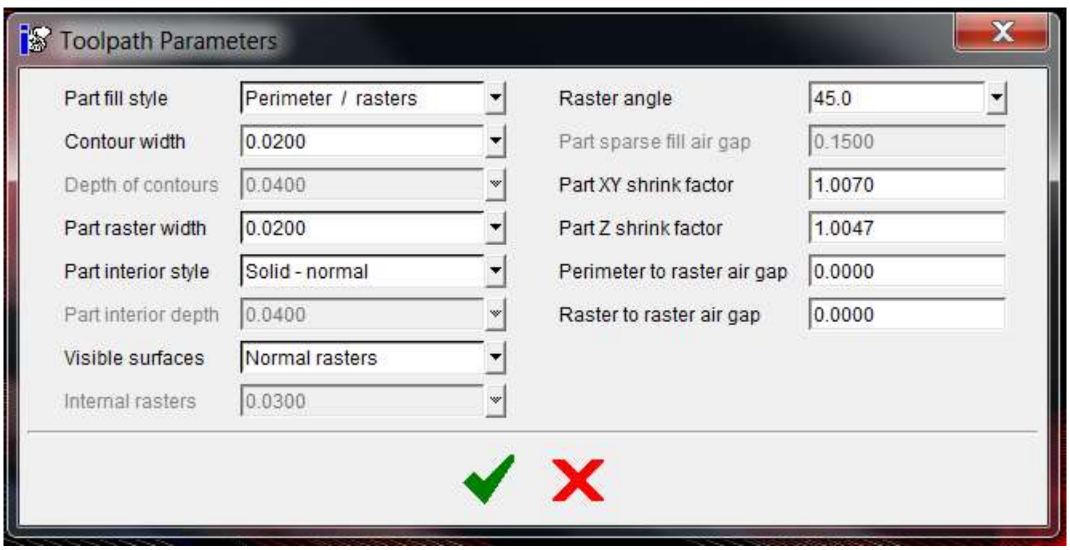

Figure 18: Tool Path Setup and Configuration

Sample Size

Four benchmark test specimens consisting each of three axisymmetric features, two cylinders and a fillet, were designed and built on the Stratasys Prodigy Plus™. A fused deposition modeling process was employed in constructing the benchmark test specimens. Each one of the four specimens were processed as a combination of wall thickness and raster resolution with specimen #1 of wall thickness and raster resolution of 0.06” and fine, respectively, specimen #2 of wall thickness and raster resolution of 0.06” and normal, respectively, specimen #3 of wall thickness and raster resolution of 0.012” and fine, respectively and specimen #4 of wall thickness and raster resolution of 0.012” and normal, respectively. The overall experimental study consisted of four specimens repeated 24 times for a total of ninety-six (96) specimen sample size.

Measurement of Specimens

Two measuring systems were used to qualify geometric features. A Fowler 6" Digital Caliper (model # 54-101-150-2) and Zeiss Contura G2 coordinate measuring machine were utilized during the study. The digital caliper (appendix A) was primarily used to measure the diametric features of the purged model material during the preliminary experimental study. As mentioned previously, the results of the measurements are documented in the preliminary experimental section. The dimensional measurements acquired with the Fowler digital caliper were within an accuracy of 10 thousandth of an inch.

The Zeiss Contura G2 CMM was utilized to qualify all specimens during the study for diametric measurements, cylindricity and concentricity (see appendix F for certificate of calibration). The CMM was equipped with RDS technology allowing ease of measurement of small complex parts. The stylus probe can be arranged in smaller incremental angular positions. The probe size was selected at 1.5mm X 30mm. Prior to measurement, the probe was qualified. Details of the qualification results are listed in appendix E.

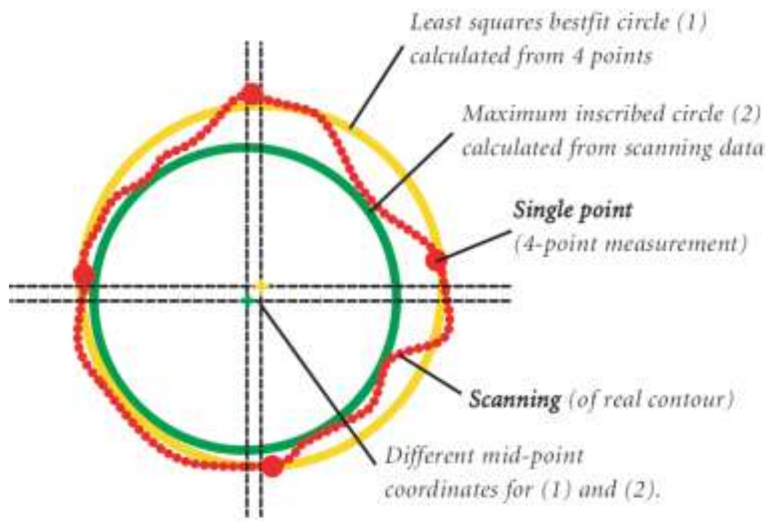

Figure 19: Scanning vs. 4 Point Least Square Fit

(Extracted from: http://www.sienkoprecision.com/specifications.pdf)

All diametric measurements, including wall thickness, cylindricity, and concentricity were measured and calculated using the least squares best fit algorithm. The least squares best fit calculated the average of points to determine geometric features. Although at least 3 points are required for diametric least squares best fit, this study utilized a scanning probe of 500 points to measure geometric features (figure 19). The scanning probe of 500 points provided better accuracy and repeatability of measured geometries at an accuracy within 0.02 thousandth of an inch.

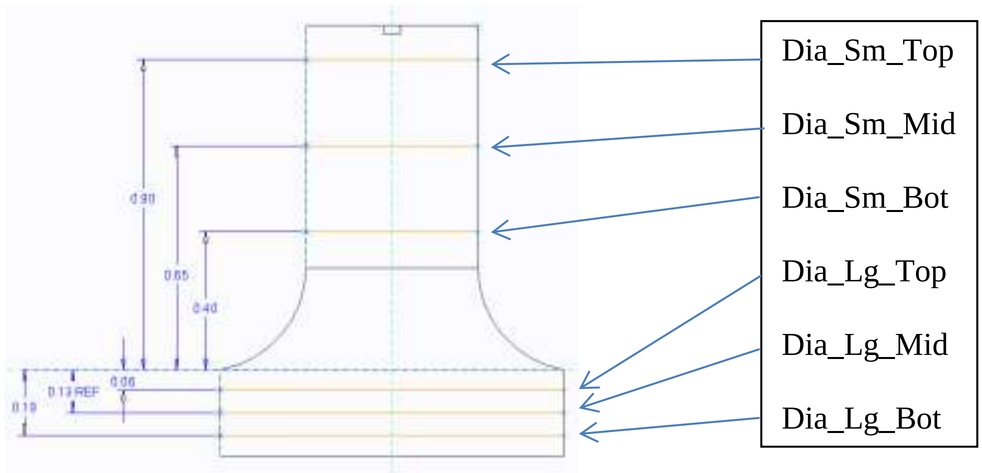

Figure 20: Measurement Planes for .5” and 1” Diameters

500 point measurement scans were taken at three planes for both diametric features (figure 20). The 500 point measurement scans were programed using Calypso software, ver. 5.2.22. The 0.5” diameter cylinder was measured at 0.4”, 0.65”, and 0.9” from the top edge of the 1” diameter cylinder. Likewise, the 1” diameter cylinder was measured at 0.06”, 0.13”, and 0.19” from the top edge of the 1” diameter cylinder. The three planes for the 0.5” diameter were labeled as Diameter Small Top (Dia_Sm_Top), Diameter Small Middle (Dia_Sm_Mid), and Diameter Small Bottom (Dia_Sm_Bot). Similarly, the three planes for the 1”diameter cylinder were labeled as Diameter Large Top (Dia_Lg_Top), Diameter Large Middle (Dia_Lg_Mid), and Diameter Large Bottom (Dia_Lg_Bot).

Environmental Data

Environmental conditions were monitored during the study. Conditions such as temperature, humidity, and pressure were sampled and recorded every 30 minutes. An Ambient weather station model WS-2080 (appendix H), was programed to monitor environmental conditions. The weather station has a temperature accuracy of ±2 °F and humidity accuracy of ±5%. The complete data set is available in appendix G.

Data Analysis

Data analyses of recorded measurements were conducted utilizing IBM SPSS version 12 software. Six batches of four repeated measures consisting of two independent variables each at two levels were recorded. A 2^2 factorial design of experiment (2 X 2 ANOVA) was used to calculate statistical significance through hypothesis testing. The following equation represents a model of the two factor experimental design (Montgomery, 2010).

$$y_{ijk} = \mu + \tau_i + \beta_j + (\tau\beta_{ij}) + \varepsilon_{ijk} \begin{cases} i = 1, 2, \dots, a \\ j = 1, 2, \dots, b \\ k = 1, 2, \dots, n \end{cases} \quad (1)$$

Where:

a = levels of factor A

b = levels of factor B

n = number of replications

μ= mean effect

τ_i = effect of ith level of factor A

β_j= effect of jth level of factor B

$\tau\beta_{ij}$ = effect of interaction between A and B

ε_{ijk} = random error

Statistical Analysis

A 2 X 2 ANOVA technique was utilized to determine statistical significance of main effect and interaction between factors. Hayden (2008) identified three key advantages of using a two way ANOVA:

- Multiple independent variables can be tested
- Type I error rate remains constant
- Interaction between independent variables can be investigated

Two factors were selected as independent variables. Factor #1 includes wall thickness of levels 0.06” and 0.12”. Factor #2 was raster resolution with levels of normal and fine. The dependent variables were the diametric measurements of the 0.5” diameter feature, 1”diameter feature, and 0.3” radius fillet. In addition to diametric measurements, the cylindricity of both cylinders, and the concentricity comparing the relationship of the 0.5” diameter cylinder to the 1” diameter cylinder were defined as dependent variables. In the ANOVA analysis, the factors were defined as categorical and the dependent variables as scale.

Type I (α) and II (β) errors are associated with hypotheses testing. A type I error occurs if the null hypothesis is rejected when it is true, and a type II error occurs if the null is not rejected when it is false. Montgomery (2010) classifies type I errors as producer’s risk and type II errors as consumer’s risk. Type I errors can be analogous to rejecting good products while type II can be viewed as failing to reject bad products.

Statistical Assumptions

The ANOVA technique is parametric, therefore, development of an accurate and robust model requires some predetermined assumptions. ANOVA requires that observations are independent random samples from normal populations with equal variances (Norusis, 2012). The design of experiment ensured independent random specimens were built. The data was analyzed for assumptions using IBM SPSS ver.12 and presented in the following chapter.

Significance Determination

Making an allowance for imperfect systems, significance levels are necessary for hypotheses testing. Due to variability amongst samples, the null hypothesis can be rejected even when it is true. Carefully selecting the level of significance can decrease the probability of a type I error. Three commonly used levels of significance are $\alpha = 0.1$, $\alpha = 0.05$, and $\alpha = 0.01$(Farber and Larson, 2003). Spiegel and Stephens (1999) agrees with Farber and Larson (2003) citing significance levels of $\alpha = 0.05$, and $\alpha = 0.01$ as customary practices. According to the literature review, confidence levels of ninety-five percent (95%) seem to be common practice in the industry. The significance level for the design of experiment study was set at $\alpha = 0.05$.

Summary

This chapter delineates the framework utilized to guide the investigative study. The design of experiment principles were employed to ensure the rigor of the scientific method. Three principles, as defined by Montgomery (2010) of randomization, repetition, and blocking set the foundation of the study. Four benchmark test specimens were designed and randomly built utilizing Prodigy Plus FDM printer. Besides, extreme care was taken in the selection, handling and presentation of all associated components of the study.

Chapter 4

RESULTS

The purpose of this study was to investigate the effects of wall thickness and raster resolution on diametric variability, cylindricity, and concentricity of fused deposition modeled sacrificial patterns. As stated earlier, the study was conducted in two stages. The first stage consisted of determining good form geometry capability of the Prodigy Plus FDM printer. This was necessary in designing and testing benchmark specimen requirements for the second stage of the study. The second stage consisted of a design of experiment where the effects of wall thickness and raster resolution were investigated for diametric variability, cylindricity, and concentricity.

The results of this experimental study were guided by the design of experiment framework in addressing the following research question:

Research Question 1 - Will the diametric accuracy of fused deposition modeling of the Prodigy Plus™ utilizing ABS material be affected by wall thickness or raster resolution?

Research Question 2 - Will fillet radius of fused deposition modeling of the Prodigy Plus™ utilizing ABS material be affected by wall thickness or raster resolution?

Research Question 3 - Will the cylindricity of fused deposition modeling of the Prodigy Plus™ utilizing ABS material be affected by wall thickness or raster resolution?

Research Question 4 - Will the concentricity of fused deposition modeling of the Prodigy Plus™ utilizing ABS material be affected by wall thickness or raster resolution?

Research Question 5 - Will there be any interaction of fused deposition modeling of the Prodigy Plus™ utilizing ABS material between wall thickness and raster resolution for diametric accuracy, cylindricity, and concentricity?

Preliminary Experimental Study Results

The purpose of the preliminary experimental study was twofold. One was to determine the smallest possible build diameter with good form and the other was to conduct a pilot test run of the study. The results of the preliminary experimental study showed that the smallest extruded diameter width was 0.015”. A factor of 2 times and 4 times the minimum diameter was used to design the benchmark test specimens for the second part of the preliminary study. The design consisted of a 0.3” diameter cylinder of wall thickness 0.03” and another of wall thickness 0.06”. A 0.3” radius fillet was also designed into the specimens. The results indicated extreme layer separation on the 0.03” diameter wall thickness specimen as observed in figure 21. The separation can be attributed to the amplification effects of layer cooling at a 0.03” diameter wall thickness.

Figure 21: Layer Separation of 0.03” Diameter Specimen

As a result of the observed phenomenon of layer separation at wall thickness of 0.03”, the specimens were redesigned to incorporate better form geometries. Wall thickness of 0.06” and 0.12” were selected to construct two cylindrical feature of a base of 1” and 0.5” with a radius fillet of 0.3”. The redesigned specimen is illustrated in figure 22.

Figure 22: Isometric View of Redesigned Specimen

The redesigned specimen allowed for the addition of another diametric test point and the concentricity form tolerance. In the second part of the preliminary study a pilot test run was conducted with the redesigned benchmark specimens. Four specimens were built with the following factor parameters, (1) wall thickness = Ø0.06” / raster resolution = normal, (2) wall thickness = Ø0.06” / raster resolution = fine, (3) wall thickness = Ø0.12” / raster resolution = normal, and (4) wall thickness = Ø0.12” / raster resolution = fine. Table 11 reflects the two factor combination of wall thicknesses (0.06” and 0.12”) and raster resolution (normal and fine).

Table 11: Specimens Time to Build and Material Usage

Parameters	*Normal_0.06*	*Fine_0.06*	*Normal_0.12*	*Fine_0.12*
Time (min)	33	32	39	34
Material Usage (in^3)	0.15	0.15	0.27	0.26

It was observed from the pilot test run that there was good form geometry. Although the material usage was relatively consistent for both wall thicknesses, with the 0.12” wall thickness having a 0.01in^3 material difference, the time to build varied slightly for the 0.06” wall thickness (1 min), but more significant for the 0.12” wall thickness (5 min). It may be assumed from the data that raster resolution may affect time to build. To keep the scope of this study manageable, time to build was not a consideration, however, future follow up studies should consider and explore the effects of raster resolution on time to build.

Environmental Results

As indicated in the methodology section, environmental conditions such as temperature and humidity can influence the results of the study. Although the temperature and humidity of the study were controlled in the laboratory to a limited extent, precise control was not possible. Therefore, temperature and humidity were defined as limitations for the study. The temperature and humidity were monitored before, during and after the experimental study. Readings were captured every 30 minutes and automatically recorded in a spreadsheet (appendix G). Environmental conditions were monitored and captured using the Weather Station WS2080 with temperature and humidity accuracies of ±2 °F and ±5% respectively (appendix H). Figure 23 present graphs of temperature and humidity observed during the study. For the study, the average temperature was calculated at 73.39 °F, and the average humidity at 60%.

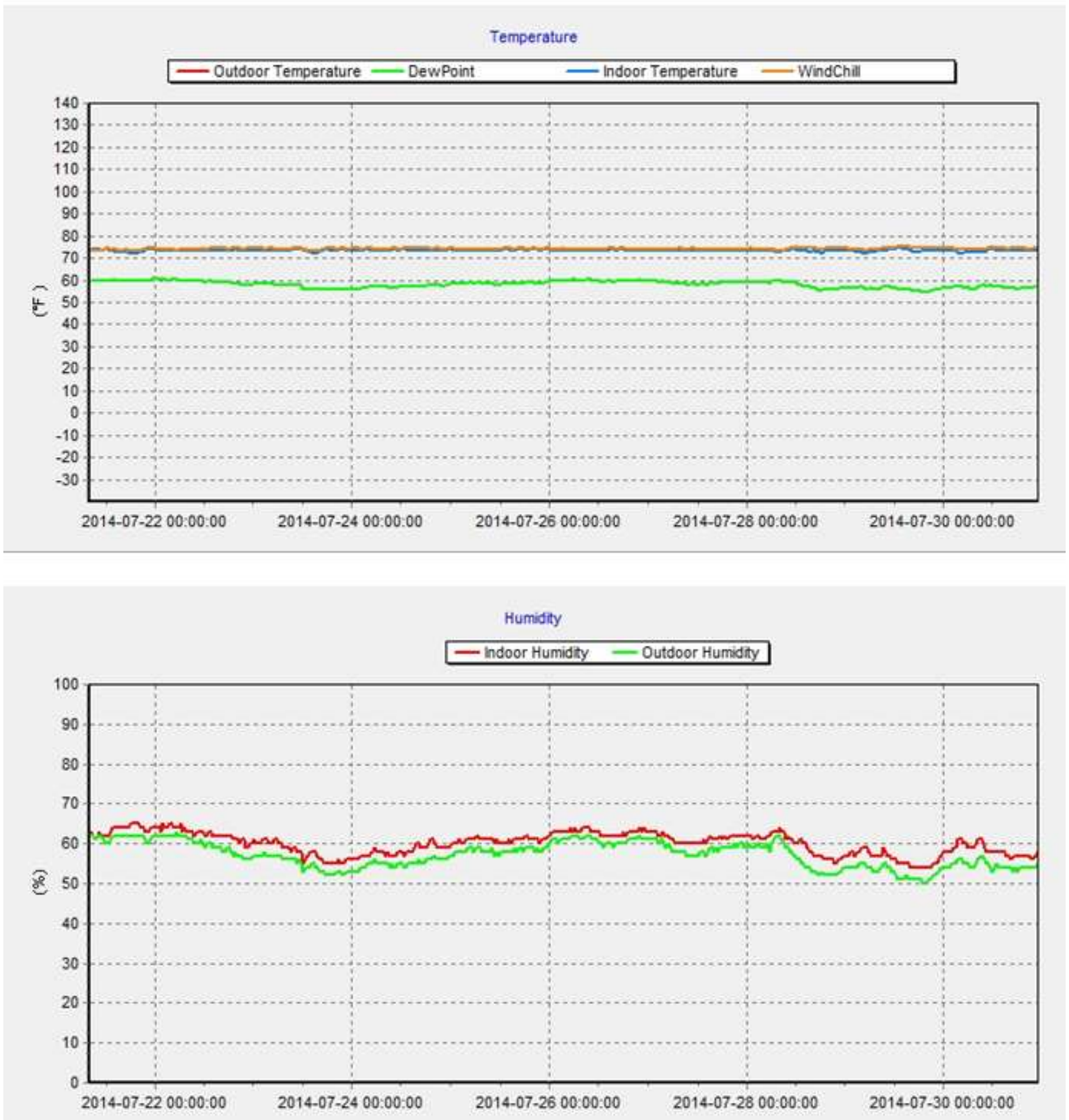

Figure 23: Temperature and Humidity Graphs of Experimental Study

Variable Coding Definition

The following table delineates the variable coding notation defined during the experimental study (table 12).

Table 12: SPSS Variable Coding Definition

SPSS Variable	Description
Dia_sm_top	Top measurement of 0.5” diameter
Dia_sm_mid	Middle measurement of 0.5”diameter
Dia_sm_bot	Bottom measurement of 0.5” diameter
Dia_sm_ave	Average measurement of 0.5” diameter
Thick_top	Wall thickness of top 0.5” measurement
Thick_mid	Wall thickness of middle 0.5” measurement
Thick_bot	Wall thickness of bottom 0.5” measurement
Cyl_sm	Cylindricity of 0.5” diameter
Fillet_rad	Radius measurement of 0.3 fillet
Cyl_lg	Cylindricity of 1” diameter
Dia_lg_top	Top measurement of 1” diameter
Dia_lg_mid	Middle measurement of 1” diameter
Dia_lg_bot	Bottom measurement of 1” diameter
Dia_lg_ave	Average measurement of 1” diameter
Concentricity	Concentricity of 0.5” diameter to 1” diameter

Experimental Results

The experimental study consisted of a full factorial randomization design of experiment. Two factors were considered for their effects on three dependent variables. Wall thickness and raster resolution were varied from 0.06” and 0.12” diameters and normal and fine resolutions respectively. Their effects were observed on diametric accuracy, cylindricity, and concentricity. A total of 96 specimens were built using fused deposition technology. The specimens were randomly positioned on build plates consisting of 16 specimens per plate. Due the method of building, each plate of 16 specimens was defined as a block in the experiment. A total of 6 plates were built.

The benchmark test specimens were designed to incorporate three axisymmetric features. The features were made up of a base cylinder of 1” diameter, a 0.5” diameter cylinder and radius fillet of 0.3”. Four individual programs were written for each factor combination. The program variations comprised of (1) wall thickness = Ø0.06” / raster resolution = normal, (2) wall thickness = Ø0.06” / raster resolution = fine, (3) wall thickness = Ø0.12” / raster resolution = normal, and (4) wall thickness = Ø0.12” / raster resolution = fine. A notch was designed into the fine raster resolution specimens in order to further differentiate raster resolution settings.

One program was created on the CMM to capture the desired data. The measurement program was written by John Hausladen, a quality engineer at Dotson Iron Casting. Dotson Iron Casting is a sand casting foundry located in Mankato, Minnesota. To achieve consistency in contact force of the CMM probe the program was written with nominal wall thicknesses of 0.09” wall thickness using Calypso software. Prior to running the program a calibration using a reference sphere was conducted.

Descriptive Statistics

ANOVA requires that observations are independent random samples from normal populations with equal variances (Norusis, 2012). Further, the design of experiment was guided by three principles, Montgomery (2010) of randomization, repetition, and blocking. The following descriptive statistics addresses normality and variances. Independent randomization was achieved through the methodology of the design of experiment as discussed earlier. Each factor combination was repeated 24 times. Blocking was achieved through the plate build process, where, six plates of 16 specimens were built.

Table 13: Descriptive Statistics

Descriptive Statistics

	N	Range	Minimum	Maximum	Mean	Std.	Skewness		Kurtosis	
	Statistic	Statistic	Statistic	Statistic	Statistic	Statistic	Statistic	Std. Error	Statistic	Std. Error
Dia_sm_top	96	.00954	.49644	.50598	.5010076	.0029758	.042	.246	-1.612	.488
Dia_sm_mid	96	.10155	.49595	.59750	.5024527	.0102400	8.572	.246	80.145	.488
Dia_sm_bot	96	.00961	.49663	.50624	.5013705	.0029548	.048	.246	-1.569	.488
Dia_sm_ave	96	.03387	.49670	.53057	.5016103	.0041775	3.485	.246	23.165	.488
Dia_lg_top	96	.02043	.99671	1.01714	1.005731	.0052346	.274	.246	-1.199	.488
Dia_lg_mid	96	.01655	.99711	1.01366	1.004680	.0042542	.201	.246	-1.273	.488
Dia_lg_bot	96	.01722	.99719	1.01441	1.005184	.0042682	.240	.246	-1.128	.488
Dia_lg_ave	96	.01565	.99824	1.01388	1.005198	.0044954	.236	.246	-1.351	.488
Fillet_rad	96	.03474	.26770	.30244	.2879941	.0051582	-.239	.246	2.314	.488
Cyl_sm	96	.00708	.00325	.01033	.0067656	.0013088	.127	.246	.444	.488
Cyl_lg	96	.00905	.00366	.01271	.0086151	.0018812	.077	.246	-.360	.488
Concentricity	96	.02195	.00028	.02223	.0098927	.0049950	.355	.246	-.413	.488
Valid N (listwise)	96									

Table 13 outlines the descriptive statistics of range, minimum and maximum values, mean, standard deviation, skewness and kurtorsis. Skewness is an indicator of how symmetrical the data distribution is, whiles, kurtorsis indicates peakedness. It appears that the data for the middle measurement of the 0.5” diameter cylinder exhibited the greatest skewness (8.572) and kurtosis (80.145).

Table 14: Levene’s Test for Homogeneity of Variance

	F	*Df1*	*Df2*	*Sig.*
Dia_sm_mid	1.965	3	92	.125
Dia_sm_ave	1.357	3	92	.261

The extreme effects of skewness and kutorsis were averaged by the data from the top and bottom measurements of the 0.5” diameter cylinder resulting in a reduced average skewness and kurtorsis of 3.485 and 23.166 respectively. Since those values were high, a follow-up test for homogeneity of variance was conducted. The Levene’s test looks at variance within the dependent variables. Based on the results of Levene’s test located in table 14, it was concluded that the variance was not statistically significant at $\alpha = 0.05$ (Dia_sm_mid : F = 1.965, p =

0.125). Likewise, Dia_sm_ave did not exhibit variance that was statistically significant at $\alpha = 0.05$ (Dia_sm_ave : $F = 1.357$, $p = 0.261$). Failure to reject the null hypothesis, therefore suggested that the data collected and calculated for the middle plane and average diameter of the 0.5” diameter cylinder were acceptable for the ANOVA test. The means and standard deviations were also recorded as follows; Dia_sm_ave (0.502, 0.004), Dia_lg_ave (1.005, 0.004), Fillet_rad (0.288, 0.005), Cyl_sm (0.007, 0.001), Cyl_lg (0.009, 0.002), and Concentricity (0.010, 0.005).

The histograms illustrated in figures Appendix M reflect normally distributed curves superimposed on the data for diametric dimensions, cylindricity, and concentricity. The histograms seem to depict a bimodal distribution. This bimodal distribute does not satisfy the normal distribution assumption required for better accuracy of the ANOVA test. The non-parametric test, Kruskal-Wallis (see appendix K for results) results was used to help validate the results of the ANOVA where the normality assumption wasn’t met. All other assumptions such as independent random samples, and homogeneity of variance were met.

Results of Hypothesis 1

In addressing the first research question, “Will the diametric accuracy of fused deposition modeling of the Prodigy Plus™ utilizing ABS material be affected by wall thickness or raster resolution?”, the following hypotheses were constructed to test statistical significance at $\alpha = 0.05$.

Table 15: ANOVA for 0.5” Diameter

Source	Type III Sum of Squares	df	Mean Square	F	Sig.
			Dia_Sm_Top		
Wall_Thick	3.725E-6	1	3.725E-6	.428	.514
Raster_Res	1.489E-5	1	1.489E-5	1.713	.194
			Dia_Sm_Mid		
Wall_Thick	.000	1	.000	1.659	.201
Raster_Res	.000	1	.000	1.609	.208
			Dia_Sm_Bot		
Wall_Thick	1.494E-5	1	1.494E-5	1.737	.191
Raster_Res	8.431E-6	1	8.431E-6	.980	.325

Table 16: ANOVA for 1” Diameter

Source	Type III Sum of Squares	df	Mean Square	F	Sig.
			Dia_Lg_Top		
Wall_Thick	1.232E-5	1	1.232E-5	.448	.505
Raster_Res	2.387E-5	1	2.387E-5	.868	.354
			Dia_Lg_Mid		
Wall_Thick	1.066E-5	1	1.066E-5	.596	.442
Raster_Res	1.387E-5	1	1.387E-5	.775	.381
			Dia_Lg_Bot		
Wall_Thick	3.519E-6	1	3.519E-6	.195	.660
Raster_Res	1.103E-5	1	1.103E-5	.611	.436

The first hypothesis as stated below addresses statistical significance of the effect of wall thickness on diametric variability of the 0.5” diameter cylindrical feature.

Null Hypothesis 1

There is no significant difference between the average diameters of fused deposition modeling for wall thicknesses of 0.060”, and 0.120”.

$$H_{01}: \mu_{0\ (0.060")} = \mu_{1\ (0.120")}$$

Alternative Hypothesis 1

There is significant difference between the average diameters of fused deposition modeling of wall thicknesses of 0.060”, and 0.120”.

$$H_{11} : \mu_{0\ (0.060”)} \neq \mu_{1\ (0.120”)}$$

Statistical Results

A 500 point scan at three axial levels was taken of the 0.5” diameter cylinder. Similarly, a 500 point scan was taken for the 1” diameter cylinder at three axial levels. 96 specimens each of 6 measurements for diameters were measured for a total of 576 diametric measurements. Raw SPSS data, ANOVA results, and Kruskal-Wallis tests are listed in appendices I, J, and K respectively. The results of the data for both 0.5” diameter cylinder and 1” diameter cylinder did not show statistical significance. The 0.5”diameter cylinder recorded the following (table 15); top measurements of $F = 0.428$, $p = 0.514$ ($X^2 = 0.323$, $p = 0.570$), middle measurements of $F = 1.659$, $p = 0.201$ ($X^2 = 2.073$, $p = 0.150$), and bottom measurements of $F = 1.737$, $p = 0.191$ ($X^2 = 2.063$, $p = 0.151$), resulting in failure to reject the null hypothesis. The results show that there was not a statistically significant difference of the 0.5” diameter measurements at three axial locations for wall thickness of 0.06”, and 0.120”. The 1”diameter cylinder recorded the following (table 16); top measurements of $F = 0.448$, $p = 0.505$ ($X^2 = 0.227$, $p = 0.634$), middle measurements of $F = 0.596$, $p = 0.442$ ($X^2 = 0.887$, $p = 0.346$) , and bottom measurements of $F = 0.195$, $p = 0.660$ ($X^2 = 0.318$, $p = 0.573$), resulting in failure to reject the null hypothesis. The results show that there was not a statistically significant difference in the 1” diameter measurements at three axial locations for wall thickness of 0.06”, and 0.120”. In summary, according to the hypothesis testing, the results indicated a failure to reject the first null hypothesis. According to the null hypothesis, there was no significant difference between the average diameters of fused deposition modeling for wall thicknesses of 0.060”, and 0.120”.

Results of Hypothesis 2

The second hypothesis addresses statistical significance of the effect of raster resolution on diametric variability of the 0.5” diameter cylindrical feature.

Null Hypothesis 2

There is no significant difference between the average diameters of fused deposition modeling for normal or fine raster resolution.

$$H_{02} : \mu_{0\ (\mathrm{normal})} = \mu_{1\ (\mathrm{fine})}$$

Alternative Hypothesis 2

There is significant difference between the average diameters of fused deposition modeling of normal or fine raster resolution.

$$H_{12} : \mu_{0\ (\mathrm{normal})} \neq \mu_{1\ (\mathrm{fine})}$$

Statistical Results

A 500 point scan at three axial levels was taken of the 0.5” diameter cylinder. Similarly, a 500 point scan was taken for the 1” diameter cylinder at three axial levels. 96 specimens each of 6 measurements for diameters were measured for a total of 576 diametric measurements. Raw SPSS data, ANOVA, and Kruskal-Wallis test results are listed in appendices I, J, and K respectively. The results of the data for both 0.5” diameter cylinder and 1” diameter cylinder did not show statistical significance. The 0.5”diameter cylinder recorded the following (table 15); top measurements of $F = 1.713$, $p = 0.194$ ($X^2 = 1.959$, $p = 0.162$), middle measurements of $F = 1.609$, $p = 0.208$ ($X^2 = 1.798$, $p = 0.180$), and bottom measurements of $F = 0.980$, $p = 0.325$ ($X^2 = 1.023$, $p = 0.312$), resulting in failure to reject the null hypothesis. The results show that there was not a statistically significant difference of the 0.5” diameter measurements at three axial locations for raster resolution of normal, and fine. The 1”diameter cylinder recorded the following (table 16); top measurements of $F = 0.868$, $p = 0.354$ ($X^2 = 1.045$, $p = 0.307$), middle measurements of $F = 0.775$, $p = 0.381$ ($X^2 = 0.668$, $p = 0.414$), and bottom measurements of $F = 0.611$, $p = 0.436$ ($X^2 = 0.210$, $p = 0.647$), resulting in failure to reject the null hypothesis. The results show that there was not a statistically significant difference in the 1” diameter measurements at three axial locations for raster resolutions of normal, and fine. In summary, according to the hypothesis testing, the results indicated a failure to reject the second null hypothesis. According to the null hypothesis, there was no significant difference between the average diameters of fused deposition modeling for raster resolutions of normal, and fine.

Results of Hypothesis 3

In addressing the second research question, “Will fillet radius of fused deposition modeling of the Prodigy Plus™ utilizing ABS material be affected by wall thickness or raster resolution?”, the following hypotheses were constructed to test statistical significance at $\alpha = 0.05$. The third hypothesis addresses statistical significance of the effect of wall thickness on diametric variability of the 0.3” radius fillet.

Table 17: ANOVA for 0.3” Radius Fillet

Source	**Type III Sum of Squares**	**df**	**Mean Square**	**F**	**Sig.**
			Fillet_Rad		
Wall_Thick	.000	1	.000	12.453	.001
Raster_Res	.000	1	.000	5.374	.023

Null Hypothesis 3

There is no significant difference between the 0.3” radius fillets of fused deposition modeling for wall thicknesses of 0.060”, and 0.120”.

$$H_{03} : \mu_{0\ (0.060”)} = \mu_{1\ (0.120”)}$$

Alternative Hypothesis 3

There is significant difference between the 0.3” radius fillets of fused deposition modeling for wall thicknesses of 0.060”, and 0.120”.

$$H_{13} : \mu_{0\ (0.060”)} \neq \mu_{1\ (0.120”)}$$

Statistical Results

Since there was statically significant interaction, F = 7.897, p = 0.006 for diametric accuracy of 0.3” radius fillet on the effects of wall thickness and raster resolution at $\alpha = 0.05$, no useful inferences were made on the individual effects of the factors. Although the data indicated rejection of null hypothesis number 3 and number 4, it is not clearly discerned which factors or at what levels affect the results. In summary, future research should be conducted to investigate the effects of shell thickness and raster resolution on multiple fillet and round geometric features.

Results of Hypothesis 4

The fourth hypothesis addresses statistical significance of the effect of raster resolution on diametric variability of the 0.3” radius fillet.

Null Hypothesis 4

There is no significant difference between the 0.3” radius fillets of fused deposition modeling for normal or fine raster resolution.

$$H_{04} : \mu_{0\ (normal)} = \mu_{1\ (fine)}$$

Alternative Hypothesis 4

There is significant difference between the 0.3” radius fillets of fused deposition modeling for normal or fine raster resolution.

$$H_{14}: \mu_{0\ (\text{normal})} \neq \mu_{1\ (\text{fine})}$$

Statistical Results

Since there was statically significant interaction, F = 7.897, p = 0.006 for diametric accuracy of 0.3” radius fillet on the effects of wall thickness and raster resolution at α = 0.05, no useful inferences were made on the individual effects of the factors. Although the data indicated rejection of null hypothesis number 3 and number 4, it is not clearly discerned which factor or at what levels affect the results.

Results of Hypothesis 5

In addressing the third research question, “Will the cylindricity of fused deposition modeling of the Prodigy Plus™ utilizing ABS material be affected by wall thickness or raster resolution?”, the following hypotheses were constructed to test statistical significance at α = 0.05. The fifth hypothesis addresses statistical significance of the effect of wall thickness on the cylindricity of the 0.5” and 1” diameter cylindrical features.

Table 18: ANOVA for 0.5” and 1” Diameter Cylindricity

Source	Type III Sum of Squares	df	Mean Square	F	Sig.
Cylindricity_Small (0.5”)					
Wall_Thick	1.729E-5	1	1.729E-5	10.977	.001
Raster_Res	1.350E-9	1	1.350E-9	.001	.977
Cylindricity_Large (1”)					
Wall_Thick	1.751E-9	1	1.751E-9	.000	.983
Raster_Res	3.688E-7	1	3.688E-7	.101	.751

Null Hypothesis 5

There is no significant difference between the average cylindricity of fused deposition modeling for wall thicknesses of 0.060”, and 0.120”.

$$H_{05} : \mu_{0\ (0.060")} = \mu_{1\ (0.120")}$$

Alternative Hypothesis 5

There is significant difference between the average cylindricity of fused deposition modeling of wall thicknesses of 0.060”, and 0.120”.

$$H_{15} : \mu_{0\ (0.060")} \neq \mu_{1\ (0.120")}$$

Statistical Results

A 500 point axial scan of the middle diameter dimensions was used for both the 0.5” and 1” diameter cylinders. The middle diameter scan for the 0.5” cylindrical feature was positioned 0.35” from the top of the specimen, while the middle diameter scan for the 1” diametric feature was at 1.125” from the top of the specimen. 96 specimens each of 2 measurements for diameters were measured for a total of 192 diametric measurements. Raw SPSS data and ANOVA results are listed in appendix I and J respectively. The results of the data for the 0.5” diameter cylinder indicated statistical significance for cylindricity of wall thicknesses 0.06” and 0.120”, while, no statistical differences were recorded for cylindricity of the 1” diameter cylinder for wall thicknesses of 0.06” and 0.120”. The 0.5”diameter cylinder recorded (table 19) a cylindricity of $F = 10.977$, $p = 0.001$ ($X^2 = 12.761$, $p = 0.000$). Since the p-value was smaller than the level of significance ($\alpha = 0.05$), the null hypothesis was rejected. The results show that there was statistically significant difference for the cylindricity of the 0.5” diameter measurements for wall thicknesses of 0.06” and 0.120”. On the other hand, the 1”diameter cylinder recorded (table 18) a cylindricity of $F = 0.000$, $p = 0.983$($X^2 = 0.001$, $p = 0.980$). Since the p-value was larger than the level of significance (α = 0.05), the results indicated a failure to reject the null hypothesis. The results show that there was not a statistically significant difference in the cylindricity of the 1” diametric cylindrical feature for shell thicknesses of 0.06” and 0.120”. In summary, according to the hypothesis testing, the results indicated a failure to reject the fifth null hypothesis only for wall thickness of 0.120”, but, rejection of the fifth null hypothesis for wall thickness of 0.06”.

Results of Hypothesis 6

The sixth hypothesis addresses statistical significance of the effect of raster resolution on the cylindricity of the 0.5” and 1” diameter cylindrical features

Null Hypothesis 6

There is no significant difference between the average cylindricity of fused deposition modeling for normal or fine raster resolution.

$$H_{06} : \mu_{0\ (\text{normal})} = \mu_{1\ (\text{fine})}$$

Alternative Hypothesis 6

There is significant difference between the average cylindricity of fused deposition modeling for normal or fine raster resolution.

$$H_{16} : \mu_{0\ (\text{normal})} \neq \mu_{1\ (\text{fine})}$$

Statistical Results

A 500 point axial scan of the middle diameter dimensions was used for both the 0.5” and 1” diameter cylinders. The middle diameter scan for the 0.5” cylindrical feature was positioned 0.35” from the top of the specimen, while the middle diameter scan for the 1” diametric feature was at 1.125” from the top of the specimen. 96 specimens each of 2 measurements for diameters were measured for a total of 192 diametric measurements. Raw SPSS data and ANOVA results are listed in appendix I and J respectively. The results of the data for the 0.5” and 1” diameter cylinders indicated that there was no statistical significance for the effects of raster resolution on cylindricity. The 0.5”diameter cylinder recorded (table 18) a cylindricity of $F = 0.001$, $p = 0.977$ ($X^2 = 0.052$, $p = 0.820$), and the 1” diameter cylinder recorded a cylindricity of $F = 0.101$, $p = 0.751$ ($X^2 = 0.256$, $p = 0.613$). Since the p-value was larger than the level of significance ($\alpha = 0.05$), the results indicated in a failure to reject the null hypothesis for the effects of raster resolution on cylindricity of both the 0.5” and 1” diameter cylinders. In summary, according to the hypothesis testing, the results indicated a failure to reject the sixth null hypothesis of there was no significant difference between the average cylindricity of fused deposition modeling for normal or fine raster resolution.

Results of Hypothesis 7

In addressing the fourth research question of, “Will the concentricity of fused deposition modeling of the Prodigy Plus™ utilizing ABS material be affected by wall thickness or raster resolution?”, the following hypotheses were constructed to test statistical significance at $\alpha = 0.05$. The seventh hypothesis addresses statistical significance of the effect of wall thickness on the concentricity of the 0.5” diameter cylindrical feature to the 1” diameter cylindrical feature.

Table 19: ANOVA for 0.5” and 1” Diameter Concentricity

Source	Type III Sum of Squares	df	Mean Square	F	Sig.
		Concentricity			
Wall_Thick	.000	1	.000	8.486	.004
Raster_Res	1.335E-7	1	1.335E-7	.006	.940

Null Hypothesis 7

There is no significant difference between the average concentricity of fused deposition modeling for wall thicknesses of 0.060”, and 0.120”.

$$H_{07}: \mu_{0\ (0.060")} = \mu_{1\ (0.120")}$$

Alternative Hypothesis 7

There is significant difference between the average concentricity of fused deposition modeling of wall thicknesses of 0.060”, and 0.120”.

$$H_{17}: \mu_{0\ (0.060")} \neq \mu_{1\ (0.120")}$$

Statistical Results

A 500 point scan at three axial levels was taken of the 0.5” diameter cylinder. Similarly, a 500 point scan was taken for the 1” diameter cylinder at three axial levels. 96 specimens each of 6 measurements for diameters were measured for a total of 576 diametric measurements. Raw SPSS data and ANOVA results are listed in appendices I and J respectively. The results of the data indicated statistical significance for concentricity of wall thicknesses 0.06” and 0.120” between the 0.5” and 1” diameter cylinders. The 0.5”diameter cylinder compared to the 1” diameter recorded (table 19) a concentricity of $F = 8.486$, $p = 0.004$ ($X^2 = 8.084$, $p = 0.004$). Since the p-value was smaller than the level of significance ($\alpha = 0.05$), the null hypothesis was rejected. The results show that there was statistical significant for the concentricity of data for shell thicknesses of 0.06” and 0.120”. In summary, according to the hypothesis testing, the results indicated a rejection the seventh null hypothesis that there was no significant difference between the average concentricity of fused deposition modeling for wall thicknesses of 0.060”, and 0.120”.

Results of Hypothesis 8

The eighth hypothesis addresses statistical significance of the effect of raster resolution on the concentricity of the 0.5” diameter cylindrical feature to the 1” diameter cylindrical feature.

Null Hypothesis 8

There is no significant difference between the average concentricity of fused deposition modeling for normal or fine raster resolution.

$$H_{08} : \mu_{0\ (normal)} = \mu_{1\ (fine)}$$

Alternative Hypothesis 8

There is significant difference between the average concentricity of fused deposition modeling for normal or fine raster resolution.

$$H_{18} : \mu_{0\ (normal)} \neq \mu_{1\ (fine)}$$

Statistical Results

A 500 point scan at three axial levels was taken of the 0.5” diameter cylinder. Similarly, a 500 point scan was taken for the 1” diameter cylinder at three axial levels. 96 specimens each of 6 measurements for diameters were measured for a total of 576 diametric measurements. Raw SPSS data and ANOVA results are listed in appendices I and J respectively. The results of the data indicated no statistical significance for concentricity of raster resolution of normal and fine between the 0.5” and 1” diameter cylinders. The 0.5”diameter cylinder compared to the 1” diameter cylinder recorded (table 19) a concentricity of $F = 0.006$, $p = 0.940$ ($X^2 = 0.015$, $p = 0.904$). Since the p-value was larger than the level of significance ($\alpha = 0.05$), the results indicated a failure to reject the null hypothesis. The results show that there was no statistical significance for the concentricity of data for raster resolution of normal or fine. In summary, according to the hypothesis testing, the results indicated a failure to reject the eighth null hypothesis that there was no significant difference between the average concentricity of fused deposition modeling for normal or fine raster resolution.

Results of Hypothesis 9

In addressing the fifth research question of, "Will there be any interaction of fused deposition modeling of the Prodigy Plus™ utilizing ABS material between wall thickness and raster resolution for diametric accuracy, cylindricity, and concentricity?", the following hypotheses were constructed to test for statistical significance at $\alpha = 0.05$. The ninth hypothesis addresses statistical significance on the interaction of wall thickness and raster resolution on the diametric variability, cylindricity, and concentricity of all geometric features.

Table 20: ANOVA Interaction between Wall Thickness and Raster Resolution

Source	Type III Sum of Squares	df	Mean Square	F	Sig.
			Dia_Sm_Top		
Wall_Thick * Raster_Res	2.282E-5	1	2.282E-5	2.625	.109
			Dia_Sm_Mid		
Wall_Thick * Raster_Res	3.271E-5	1	3.271E-5	.314	.577
			Dia_Sm_Bot		
Wall_Thick * Raster_Res	1.461E-5	1	1.461E-5	1.698	.196
			Dia_Lg_Top		
Wall_Thick * Raster_Res	3.669E-5	1	3.669E-5	1.334	.251
			Dia_Lg_Mid		
Wall_Thick * Raster_Res	4.815E-5	1	4.815E-5	2.690	.104
			Dia_Lg_Bot		
Wall_Thick * Raster_Res	5.530E-5	1	5.530E-5	3.063	.083
			Fillet_Rad		
Wall_Thick * Raster_Res	.000	1	.000	7.898	.006

			Cyl_Sm		
Wall_Thick * Raster_Res	5.340E-7	1	5.340E-7	.339	.562
			Cyl_Lg		
Wall_Thick * Raster_Res	2.410E-7	1	2.410E-7	.066	.798
			Concentricity		
Wall_Thick * Raster_Res	7.073E-7	1	7.073E-7	.030	.863

Null Hypothesis 9

There is no significant difference between the diameter, cylindricity, and concentricity of fused deposition modeling for interaction between wall thicknesses (0.060", and 0.120"), and normal or fine raster resolutions.

Alternative Hypothesis 9

There is significant difference between at least one of the diameter, cylindricity, or concentricity of fused deposition modeling for interaction between wall thicknesses (0.060", and 0.120"), and normal or fine raster resolutions.

Statistical Results

Since interaction existed between wall thickness and raster resolution for fillet radius of 0.3", no useful inferences were made regarding their individual effects. The results as stated in table 21 for interaction between the two factors of wall thickness and raster resolution, indicated $F = 7.897$, $p = 0.006$ for diametric accuracy of 0.3" radius fillet. This resulted in the rejection of the ninth hypothesis. The study showed that there was statistically significant interaction between the factors for diametric accuracy of 0.3" radius fillet at a significance level of 0.05. As a result, future work should be conducted to explore the effects of wall thickness and raster resolution on both fillets and rounds.

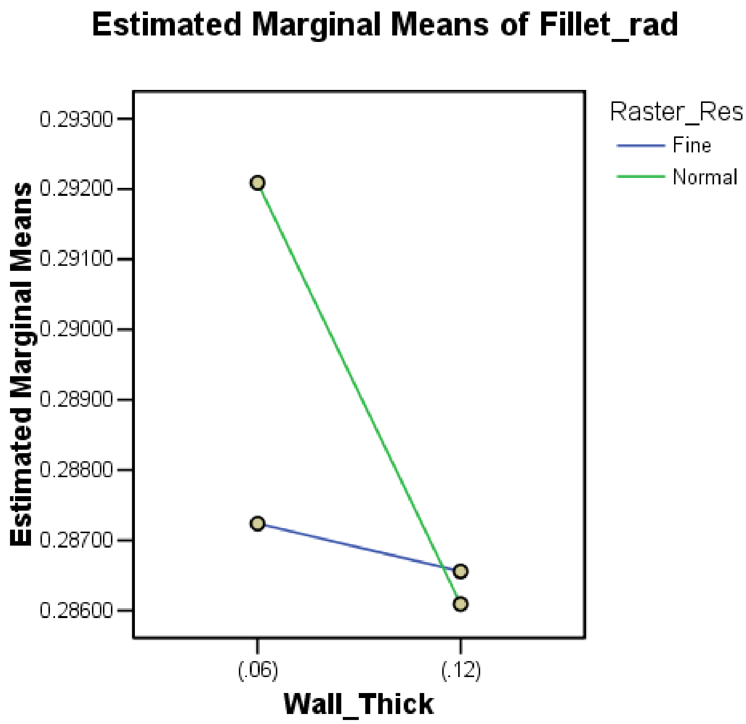

Figure 24: Fillet Estimated Marginal Means

Furthermore, a review of the estimated marginal means of fillet radius (figure 24) illustrated interaction between factors. Since the line graphs are intersecting and not parallel the graph may represent some level of interaction between levels of the two factors. A follow-up simple effects analysis was conducted to determine statistical significance of the perceived interaction. The Pairwise comparisons indicated statistical significance for fine and normal raster resolutions for interaction at a wall thickness of 0.06" (p=0.000). In appendix L, the simple effects of raster resolution for interaction was statistically significant for 0.06" wall thickness and not for 0.12", F(1,92)=13.151, p=0.000, n_{p^2} =0.125 and F(1,92)=0.121, p=0.729, n_{p^2} =0.001, respectively.

Summary of Results

According to the chapter results, a variety of responses were formulated for the effects of shell thickness and raster resolution on the diametric accuracy, cylindricity, and concentricity of fused deposition sacrificial patterns. Due to the strong interaction between factors for fillet radius, no useful inferences were made regarding their individual factor levers. However, for dependent variables that displayed no interaction of factors, such as, cylindrical diameter, cylindricity, and concentricity, level inferences were made. The results suggested that raster resolution displayed no effect on the cylindrical diametric accuracy, cylindricity, and concentricity. On the contrary, consideration must be given to concentricity and cylindricity of especially 0.5” diameter features as wall thickness can affect their results. Since the histograms for dependent variable were bimodal, Kruskal-Wallis non parametric tests were used to help validate the results from the ANOVA.

Chapter 5

CONCLUSIONS

Investment casting is one of the oldest forms of metal casting. For the most part, the process has seen little change. Tooling has proven to be a significant cost of the invesment casting process. As a result, customized or small batch production can be extremely inefficient due to exobitant tooling costs that cannot be recouped through economies of scale. A comprehensive review of the literature identified additive manufacturing processes such as Fused Deposition Modeling (FDM), Selective Laser Sintering (SLS) and Stereo Lithography Aparatus (SLA) as viable solutions to drastically reducing tooling costs associated with customized or small batch production of investment casting sacrificial patterns. Quality characteristic required for good geometic form, such as, cylindricity and concentricity, have not been explored extensively due to the relatively recent emergence of additive manufacturinf rapid reproductive systems.

The purpose of this study was to investigate the effects of wall thickness and raster resolution on diametric accuracy, cylindricity and concentricity of fused deposition modeled sacrificial patterns. The experimental study was twofold. First, a preliminary experimental study was conducted to determine the feasibility and practically of determining suitable wall thickness of good geometric form. Once achieved, a pilot test run was conducted for the benchmark test specimens used in the study. The second part of the experimental study involved a design of experiment for investigating two factors on their effects on diametric accuracy, cylindricity, and concentricity.

The study attempted to address the following research questions:

Research Question 1 - Will the diametric accuracy of fused deposition modeling of the Prodigy Plus™ utilizing ABS material be affected by wall thickness or raster resolution?

Research Question 2 - Will fillet radius of fused deposition modeling of the Prodigy Plus™ utilizing ABS material be affected by wall thickness or raster resolution?

Research Question 3 - Will the cylindricity of fused deposition modeling of the Prodigy Plus™ utilizing ABS material be affected by wall thickness or raster resolution?

Research Question 4 - Will the concentricity of fused deposition modeling of the Prodigy Plus™ utilizing ABS material be affected by wall thickness or raster resolution?

Research Question 5 - Will there be any interaction of fused deposition modeling of the Prodigy Plus™ utilizing ABS material between wall thickness and raster resolution for diametric accuracy, cylindricity, and concentricity?

Discussion of the Results

The results from the study were quantified through hypothesis testing by using the ANOVA test to determine statistical significant at a significant level of $\alpha = 0.05$. ANOVA required certain assumption to help improve the accuracy and robustness of the test. The assumption of normility was not satisfied due to the bimodal distribution of the dependent variables data. Therefore, to strengthen the overall results of the ANOVA test, the Kruskal-Wallis non-parametric test was also used to help validate the results from the ANOVA. Non-parameteric test are less sensitive to following prescribed assumptions. The ANOVA provided an F statistic and associated p-value, while the Kruskal-Wallis provided a chi-square and associated p-value.

Due to the fact that there was interaction (ressearch question #5) between factors for the fillet radius variable ($F = 7.897$, $p = 0.006$), no further inferences (research question # 2) were made at the shell thickness and raster resolution levels. The researcher reccommends further investigation of the effects of shell thickness and raster resolution on geometric features such as, fillets, rounds, and chamfers.

Research Question 1 - Will the diametric accuracy of fused deposition modeling of the Prodigy Plus™ utilizing ABS material be affected by wall thickness or raster resolution?

The response consisted of a design of two cylindrical geometric features each of three data capture points. Each cylindrical feature was measured at a prescribed top, middle, and bottom locations. The parametric ANOVA test for these measurements all agreed with a p-value greater than the defined alpha value of 0.05. Furthermore, the Kruskal-Wallis chi-square statistic test agreed with the ANOVA results of p-values greater than alpha of 0.05. Since statistical significance was not present, it was concluded that at shell thicknesses of 0.06" and 0.120", and raster resolutions of fine and normal, there were statistically the same.

Research Question 3 - Will the cylindricity of fused deposition modeling of the Prodigy Plus™ utilizing ABS material be affected by wall thickness or raster resolution?

The response consisted of a design of two cylindrical geometric features each of measurements at a prescribed middle location. The parametric ANOVA tests for these measurements were varied. Raster resolution indicated p-values greater than alpha of 0.05 for both cylindrical features, however, the 0.5" diameter cylinder recorded a p-value smaller than alpha of 0.05 for the wall thickness factor. The larger 1" diameter cylinder recorded a p-value greater than that of the alpha of 0.05. Furthermore, the Kruskal-Wallis chi-square statistic test agreed with the ANOVA results for the 0.5” diameter cylinder for shell thickness and raster resolution ($X^2 = 12.761$, $p = 0.000$ and $X^2 = 0.052$, $p = 0.820$), and the 1” diameter cylinder for shell thickness and raster resolution ($X^2 = 0.001$, $p = 0.980$ and $X^2 = 0.256$, $p = 0.613$). Since statistical significance was present for the wall thickness factor of the 0.5” diameter cylinder, it was concluded that raster resolution was statistically the same on the cylindricity of 0.5” and 1” diameter cylindrical geometric features. Also, for the wall thickness factor on cylindricity, there was no statistical significance for the 1” diameter cylindrical feature, but, statistical significance existed for the 0.5” diameter cylindrical feature.

Research Question 4 - Will the concentricity of fused deposition modeling of the Prodigy Plus™ utilizing ABS material be affected by wall thickness or raster resolution?

The response consisted of a design of two cylindrical geometric features each of measurements at a prescribed middle location. The parametric ANOVA tests for these measurements were varied. The concentricity form geometry compared the 0.5” diametric cylindrical feature to the 1” diameter cylindrical feature. The ANOVA results indicated a p-value ($F = 0.006$, $p = 0.940$) greater than an alpha of 0.05 for the raster resolution factor, but, a p-value ($F = 8.486$, $p = 0.004$) less than alpha for the shell thickness factor. Likewise, the Kruskal-Wallis test agreed with the ANOVA on the effects of raster resolution on concentricity ($X^2 = 0.015$, $p = 0.904$) and shell thickness ($X^2 = 8.084$, $p = 0.004$). It was concluded that the effects of shell thickness and raster resolution on the concentricity of 0.5” and 1” diametric cylindrical features resulted in statistical significance for wall thickness but not for raster resolution.

Implications of the Results

Additive manufacturing technologies have presented both advantages and disadvantages as dicussed in chapter 1. The ability to build virtually any shape using additive manufacturing rapid reproductive systems coupled with near net shape capabilities of investment casting, creates improved efficiencies for production of customized or small batch production.

The results of the study indicate to manufactuers who utilize fused deposition modeled sacrifical patterns for investment casting applications, that the effects of raster resolution on diametric accuracy, cylindricity, and concentricity was not statictically significant. According to the study, selecting a raster resolution of normal or fine did not effect the diametric accuracy, cylindricity, or concentricty of 0.5” and 1” cylindrical geometrc features. However, one point to note, that is recommended as future researh, was the effects of raster resolution on the time to build. As indicated earlier during the preliminary experimental study, it was noted that raster resolution seem to have an effect on time to build.

In the same way, manufactuers who utilize fused deposition modeled sacrifical patterns for investment casting applications, must consider the effects of wall thickness on quality characteristics such as diametric accuracy, cylindricity, and concentricity. According to the study, when building diametric cylidrical goemetric features, especially, with wall thicknesses of 0.06, and 0.120”, particular considerations must be given to concentricity and the cylindricity of 0.5” diameter cylinder. It was observed that wall thicknesses of 0.06” amd 0.120” exhibited statistical significance on the concentricity of the 0.5” diameter to the 1” diameter. Also, the wall thickness factor influenced the results of cylindricity of the 0.5” diametric cylindrical geometric feature. Therefore, in selecting apporpriate wall thicknesses consideration must be given to how various values can effect the overall concentricty and cylindricity of diametric features. The study did not consider wall thicknesses less than 0.60” or greater than 0.120”. Also, wall thickness between 0.06” and 0.120” is recommended for investigation.

All in all, the study adds to the existing body of knowledge. Due to the lack of understanding on the effects of shell thickness and raster resolution, especially, on quality characteristics, such as, diametric accuracy, cylindricity, and concentricity, hopefully the results of the study is welcomed. Researchers and practitioners alike, can see the benefits and added value of the study towads the application of additive manufacturing techniques in investment casting.

Recommendations for Practice

Although the work presented is limited to a foundational study using one machine and one small scale specimen design, one of the most important contributions of the study, is the development of a methodology for designing experiments. This provides a framework particularly for manufacturers wanting to evaluate their products and processes. The following recommendations for practice are geared towards seamlessly adapting the methodology to a variety of industrial practices while reducing possible errors.

Regardless of the products produced or the manufacturing processes used, evaluating the effects of certain factors for improvements can be achieved through a design of experiment. Effective design of experiments should consist of the principles of randomization, repetition and blocking (Montgomery, 2010). This study presents Research Randomizer are an effective tool for randomizing specimens. However, a number of other methods can be employer based on the product or process. Methods such as, computer algorithms for product randomization and random sampling for process randomization can be easily substituted. Furthermore, manufacturer can use historical data that were collected in an unbiased, randomized method. The key is to randomize not only the individual trials, but all other aspects of the experiment, such as material allocation.

Repetition improves the robustness of the experiment. The effects of minor anomalies in the product or process can be minimized through repetition. Manufacturers must be careful in developing true replication and not repeated measures of the factor combinations. In this study, for example, both repeated measures and replication were used. Due to the FDM building process, six plates were built consisting of 16 specimens each. Four factor combinations of four repeated measures were constructed. Each plate consisted of similar times and processes. Replication was achieved by multiple plate builds. In addition to minimizing minor variances, manufacturers can observe a more precise estimate of the sample mean used to represent the true mean. All in all, repetition improves the accuracy of the sample mean and balances uncontrollable nuisance factors.

Each plate consisted of each factor combination with four repeated measures. The study was designed with six blocks. Although the materials were from a single stock, blocking was incorporated as a safety measure of nuisance variability caused by processing time and temperatures. If selection of material is not homogenous, then blocking can be used to reduce or eliminate variability from controllable nuisance factors. In adopting the methodology, some manufacturers may be faced with nuisance factors that are uncontrollable; however, they may be measurable. On common technique would be to treat each factor as a covariance.

Another critical recommendation for practice is identifying all constraints that limits performance of the system and identify ways of reducing their effects. One such example observed in this study was the staircase effect. The staircase effect is an inherent problem with additive manufacturing rapid reproductive systems cause by the layering process. Staircase effects are more prominent along the Z-axis. Since parts are built by cross-sectional layers, true geometric features are approximated along the Z-axis based on layer thickness. Although smaller layer thicknesses reduce the effect, it still remains a challenge for the FDM process. As a result, the fillet radius for the specimen design consisted of stepped layers. Accuracy of such features can be drastically reduced or even erroneous if the measurement method used is capably of measuring the step geometries. To reduce such error, a large enough CMM probe was selected to measure along the tangent of each step.

Cosine error was also identified as a system constraint. Reducing error involves evaluating the complete system for possible variations and constraints. In addition to identifying constraints in the FDM building process, further constrains were identified with the measurement equipment. Cosine error occurs when CMM spherical probes do not make contact normal to the surface of measurement. Care should be taken to avoid cosine error wherever possible. Considerations must be given to CMM probe movement especially in relation to measurement surfaces.

Depending on the process, a number of optimization techniques can be used to improve efficiencies and reduce overall times. As such, this study was designed with unrestricted packing of specimens. The spacing between specimens was not restricted to a fixed value. This allowed more specimens to be built on each plate. The overall time to build and measure were significantly reduced.

Given the variety of manufacturing processes employed in industry, adopting this methodology will require minor alterations. The design of experiment should be accurate and robust. Principles such as randomization, repetition, and blocking are foundational to accurate and robust experimental designs. System constraints must be identified and efforts made at mitigating the direct or indirect effect of such constraints.

Recommendations for Future Research

A number of recommendations were identified for future research. Some were classified as additional controls that were not possible at the time of the study due to time constraints and scope management. Others were realized during the study and were recommended for future investigation and exploration.

The study was designed to investigate dependent variables of cylindricity and concentricity, particularly for their geometric form tolerances on cylindrical features. Although cylindrical features are common in part design and investment casting such as, flanges, and gears, other geometric forms tolerances should be considered. The effects of shell thickness and raster resolution on other quality characteristics, such as, straightness and flatness should be explored and investigated. Determining how those factors influence straightness and flatness of non-axisymmetric geometric features will greatly add to the understanding and improved accuracies of additive manufacturing and by extension the investment casting process.

Defining the scope of any project requires a delicate balance of a number of constraints. The second recommendation is to explore additional cylindrical diameters. The study focused on two diametric values (0.5” and 1”). Diametric values greater than 1”, lessor than 0.5” and in-between 0.5” and 1” should be considered for future exploration. As was noted during the study, the effect of wall thickness was statistically significant for the 0.5” diameter cylinder but not the 1” cylinder. Does this mean that based on the levels of wall thicknesses selected for the study cylindricity is only affected if the cylindrical diameter is 0.5”? Or based on the factor levels, there exist a maximum diametric value where statistical significance occurs for all values below.

The Prodigy Plus™ FDM is capable of printing using two slice height factors of 0.010" and 0.013". The study was designed with a layer slice height of 0.010". A duplication of the study at a layer slice height of 0.013" should be explored to further understand the effects of layer slice height on diametric accuracy, cylindricity, and concentricity.

In determining the concentricity of the two diametric features, the top 0.5" diameter cylinder was compared to the base 1" cylinder. The study indicated statistical significance for wall thickness factor. A couple recommendations can be considered. Firstly, calculating concentricity based on the relationship of the 1" diameter cylinder to the 0.5" diameter cylinder. Secondly, building the specimen in an inverted orientation, where the 0.5" diameter serves as the base. In doing so, considerations must be given to the additional support material needed for the 1" diameter cylinder. This would result in additional material, time, and overall increase in costs. Although the change in build orientation possesses additional constraints, exploration is necessary and to some extent specimen count can be reduced.

No inferences were concluded at the factor levels due to interaction between the factors. Therefore, it is recommended to explore and investigate designs of multiple fillets, rounds, and chamfers, as these features are common in design and investment casting.

During the preliminary experimental study, the results of time to build seem to be influenced by raster resolution. Two specimens of 0.06" wall thickness, one of normal and the other fine raster resolution and another two of 0.120" wall thickness, one of normal and the other fine raster resolutions were compared for time to build and material usage. It was noticed the for both wall thicknesses, the time to build was different as a result of the raster resolution setting. Since reductions in time can indicate reductions in costs, a recommendation to explore time to build especially pertaining to raster resolution will further expand the knowledge and help improve efficiencies of additive manufacturing FDM processes.

The final recommendation deals with material selection of the Prodigy Plus™ FDM. This study consisted of building benchmark test specimens using a polymer ABS400 material. A number of experimental studies have concluded that an inherit challenge with using non-wax materials for sacrificial patterns is the thermal expansion. Thermal expansion normally results in ceramic shell fractures. Although thermal expansion of less than 0.35% has demonstrated no ceramic shell fracturing, this recommendation considers another method of removing sacrificial patterns from ceramic shells. Traditionally, investment casting uses a burnout process for removing sacrificial pattern from ceramic shell. As an alternative to burnout, specimens can be built of water soluble support material, which can be dissolved from the ceramic shell. All of the above recommendations can be applied to the water soluble material with further investigations of the proof of concept.

REFERENCES

Bak, D. (2003). “Rapid prototyping or rapid production? 3D printing processes move industry towards the latter”, *Rapid Prototyping Journal*, *23*(4), 340-345

Bertoline, G. R., & Wiebe, E. (2003). Technical graphics communication. New York:McGraw Hill.

Blake, P., & Gouldsen, C. (1998). Investment casting using FDM/ABS rapid prototype patterns, Trade report, USA

Bourell, D., Leu, M., and Rosen, D. W. (2009), NSF Workshop - Roadmap for Additive Manufacturing: Identifying the Future of Freeform Processing, Washington, D.C.

Bruce, R. G., Dalton, W. K., Neely, J. E., & Kibbe R. R. (2010). Modern materials and manufacturing processes. New Jersey: Prentice-Hall.

Chang, T., Wysk, R., & Wang, H. (1998). Computer-aided manufacturing. Upper Saddle River: NJ.

Cheah, C. M., Chua, C. K., Feng, C., Lee C.W., Tan, L. H. (2004). Rapid investment casting: direct and indirect approaches via fused deposition modeling. *Journal of Advanced Manufacturing Technology*, *23*(1/2), 93-101.

Cheah, C. M., Chua, C. K., Lee, C. W., Feng, C. C., & Totong, K. K. (2005). Rapid prototyping and tooling techniques: a review of applications for rapid investment casting. *International Journal Of Advanced Manufacturing Technology*, *25*(3/4), 308-320.

Chhabra, M., & Singh, R. (2011). Rapid casting solutions: A review. *Rapid Prototyping Journal*, *17*(5), 328-350.

Chua, C., Leong, K., & Lim, C. (2003). *Rapid prototyping; principles and applications*. River Edge, NJ: John Wiley & Sons Inc.

Copper, K.G., Wells, D. (2000). Application of rapid prototyping to the investment casting of test hardware. Alabama.

Dickens, P., & Hague, R. (2001). Improvements in investment casting with stereolithography patterns. *Proceedings of the Institution of Mechanical Engineers, Part B: Journal of Engineering Manufacture*, *215*(1), 1-11.

Dickens, P., & Hopkinson, N. (2003). Analysis of rapid manufacturing—using layer manufacturing processes for production. *Proceedings of the Institution of Mechanical Engineers, Part C: Journal of Mechanical Engineering Science*, *217*(1), 31-39.

Dotchev, K., & Soe, S. (2006). Rapid manufacturing of patterns for investment casting: improvement of quality and success rate", *Rapid Prototyping Journal*, *12*(3), 156-164

Farber, B., Larson, R. (2003). *Elementary statistics: picturing the world*. Upper Saddle River, NJ: Prentice Hall.

Grimm, T. (2003). Fused Deposition Modelling: A Technology Evaluation. Edgewood, Kentucky: T.A. Grimm & Associates

Harun, W. S. W., Idris, M. H. & Sharif, S. (2008). Evaluation of ABS patterns produced from FDM for investment casting process. *Proceedings of the 9th Asia Pacific Industrial Engineering & Management Systems Conference*.

Hayden, M. (2008). *Multi-Factor ANOVA & Multiple Regression*. Terre Haute, IN

Hiemenz, J. (2010). 3-D Printers VS 3-D Production Systems. *Design News*, *65*(9), 50-56.

http://www.ddgrinding.com/wpcontent/uploads/2011/06/investment-casting.png

http://www.dimensionprinting.com/3d-printers/printing-productspecs1200series.aspx

Jacobs, P.F. (1993). "Stereolithography 1993: epoxy resins, improved accuracy & investment casting", *Proceedings of 4th International Conference on Rapid Prototyping, Dyton, OH, 14-17 June*, pp. 249-62

Merriam-Webster.com. Merriam-Webster. (n.d.). Retrieved from http://www.merriam-webster.com/dictionary.

Montgomery, D. (2010). *Design and Analysis of Experiments.* New Delhi, India, John Wiley and Son.

Norusis, M. J. (2010). 19.0 statistical procedures companion. Upper Saddle River, NJ: Prentice Hall.

Qingbin, L., Leu, M.C., Richards, V. L., & Schmitt, S. M. (2004). Dimensional accuracy and surface roughness of rapid freeze prototyping ice patterns and investment casting metal parts. *International Journal Of Advanced Manufacturing Technology*, *24*(7/8), 485-495.

Qing-Hui, W., Jing-Rong, L., Bao-Li, W., & Xiao-Ming, Z. (2010). Live parametric design modifications in CAD-linked virtual environment. *International Journal Of Advanced Manufacturing Technology*, *50*(9-12), 859-869. doi:10.1007/s00170-010-2575

Ramos, A.M., Relvas, C. and Simoes, J.A. (2003). "Vacuum casting with room temperature vulcanizing rubber and aluminum moulds for rapid manufacturing of quality parts: a comparative study", *Rapid Prototyping Journal*, 9(2), 111-115.

Sealy, W. (2011). Additive Manufacturing as a Disruptive Technology: How to Avoid the Pitfall. *American Journal of Engineering and Technology Research, 11*(10), 32-38.

Singh, N.K., Sivadasan, M., & Sood, A.K. (2012). Use of fused deposition modeling process in investment precision casting and risk of using selective laser sintering process. *International Journal of Applied Research In Mechanical Engineering*, 2(1).

Urbaniak, G. C., & Plous, S. (2013). Research Randomizer (Version 4.0) [Computer software]. Retrieved on September 01, 2013, from http://www.randomizer.org/

Wang, W., Conley, J.G. and Stoll, H.W. (1999). “Rapid tooling for sand casting using laminated object manufacturing process”, *Rapid Prototyping Journal*, 5(3), 134-140.

Winker, R. (2010). Investment Casting. Stratasys Inc. http://www.dimensionprinting.com/3d-printers/printing-productspecs1200series.aspx

Yao, W. (1998). *Analytical and experimental study of investment casting with laser stereolithography models.* New Jersey Institute of Technology).

Yao, W.L. and Leu, M. (1999). “Analysis of shell cracking in investment casting with laser stereolithography patterns”, *Rapid Prototyping Journal*, 5(1), 12-20.

APPENDICES

Appendix A: **Digital Caliper**

Fowler 54-101-150-2 Stainless Steel Frame Xtra-Value Cal Electronic Caliper,

6" Maximum Measurement

Extracted from

http://www.fowlercatalog.com/onlinecatalog.html?page=shop.browse&category_id=16

Appendix B: **Research Randomizer Results**

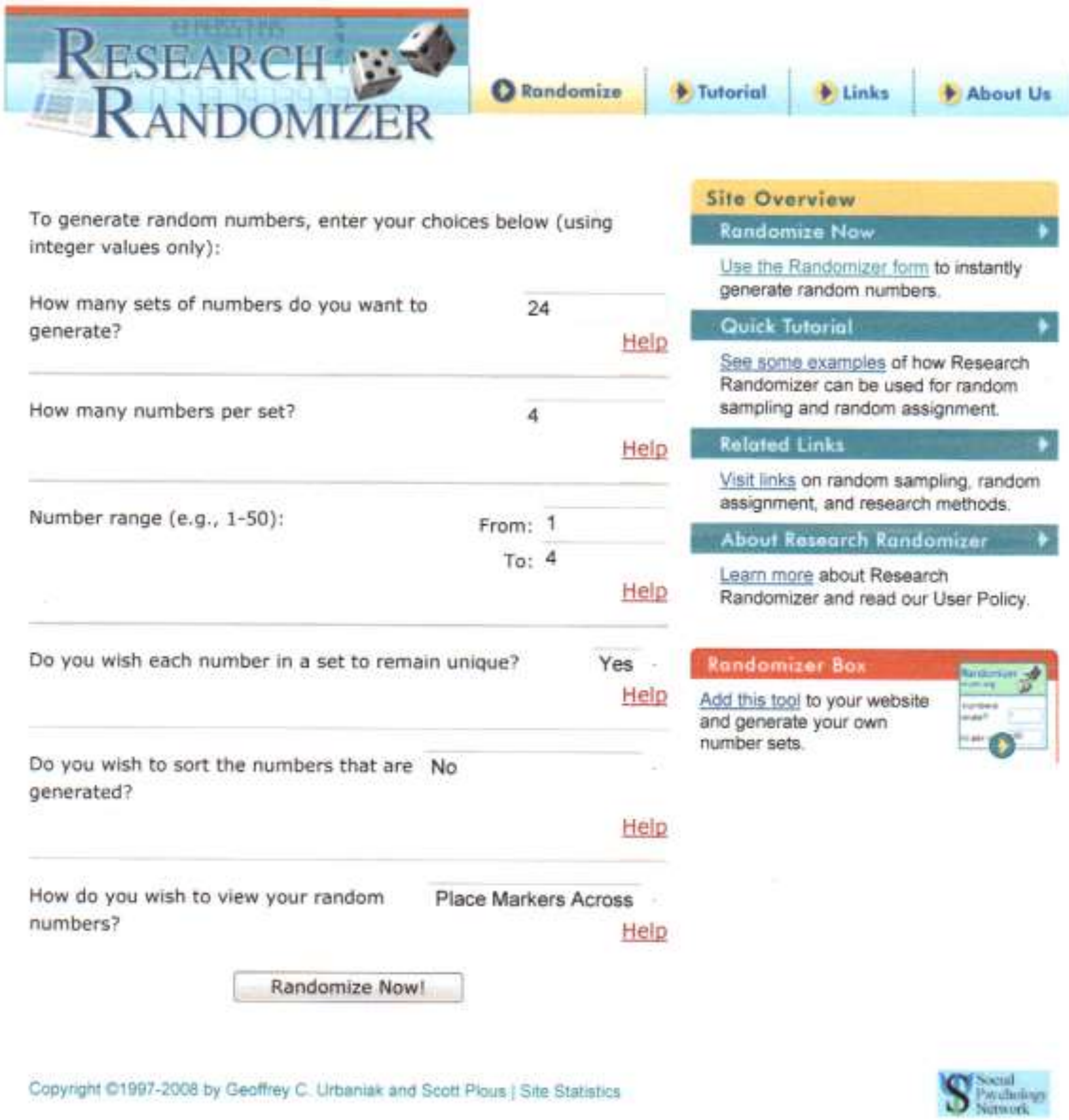
RESEARCH RANDOMIZER

Randomize | Tutorial | Links | About Us

To generate random numbers, enter your choices below (using integer values only):

How many sets of numbers do you want to generate? 24 Help

How many numbers per set? 4 Help

Number range (e.g., 1-50): From: 1 To: 4 Help

Do you wish each number in a set to remain unique? Yes Help

Do you wish to sort the numbers that are generated? No Help

How do you wish to view your random numbers? Place Markers Across Help

Randomize Now!

Site Overview

Randomize Now

Use the Randomizer form to instantly generate random numbers.

Quick Tutorial

See some examples of how Research Randomizer can be used for random sampling and random assignment.

Related Links

Visit links on random sampling, random assignment, and research methods.

About Research Randomizer

Learn more about Research Randomizer and read our User Policy.

Randomizer Box

Add this tool to your website and generate your own number sets.

Social Psychology Network

RESEARCH RANDOMIZER

Print Download in Excel Close

Research Randomizer Results

24 Sets of 4 Unique Numbers Per Set
Range: From 1 to 4 -- Unsorted

Job Status: **Finished**

Set #1:

p1=**4**, p2=**3**, p3=**2**, p4=**1**

Set #2:

p5=**2**, p6=**1**, p7=**4**, p8=**3**

Set #3:

p9=**1**, p10=**2**, p11=**4**, p12=**3**

Set #4:

p13=**3**, p14=**1**, p15=**2**, p16=**4**

Set #5:

p17=**1**, p18=**4**, p19=**3**, p20=**2**

Set #6:

p21=**3**, p22=**4**, p23=**2**, p24=**1**

Set #7:

p25=**2**, p26=**4**, p27=**3**, p28=**1**

Set #8:

p29=**1**, p30=**3**, p31=**2**, p32=**4**

Set #9:

p33=**2**, p34=**4**, p35=**1**, p36=**3**

Set #10:

p37=**2**, p38=**1**, p39=**4**, p40=**3**

Set #11:

p41=**2**, p42=**1**, p43=**3**, p44=**4**

Set #12:

p45=**4**, p46=**2**, p47=**3**, p48=**1**

Set #13:

p49=**3**, p50=**4**, p51=**1**, p52=**2**

Set #14:

p53=**4**, p54=**1**, p55=**2**, p56=**3**

Set #15:

p57=**3**, p58=**2**, p59=**1**, p60=**4**

Set #16:

p61=**3**, p62=**1**, p63=**2**, p64=**4**

Set #17:

p65=**4**, p66=**1**, p67=**2**, p68=**3**

Set #18:

p69=**1**, p70=**3**, p71=**4**, p72=**2**

Set #19:

p73=**2**, p74=**4**, p75=**1**, p76=**3**

Set #20:

p77=**4**, p78=**2**, p79=**3**, p80=**1**

Set #21:

p81=**1**, p82=**3**, p83=**4**, p84=**2**

Set #22:

p85=**4**, p86=**3**, p87=**1**, p88=**2**

Set #23:

p89=**3**, p90=**4**, p91=**2**, p92=**1**

Set #24:

p93=**1**, p94=**2**, p95=**3**, p96=**4**

Appendix C: **FDM Material Properties**

ABS
FDM Material Properties

A true industrial thermoplastic, ABS is widely used throughout industry. When combined with the Fused Deposition Modeling (FDM) systems by Stratasys, this material is ideal for the rapid production of prototypes, tooling and the direct manufacturing (tool-less) of production parts.

MECHANICAL PROPERTIES[1]

	Test Method	Imperial	Metric
Tensile Strength, Type 1, 0.125	ASTM D638	3,200 psi	22 MPa
Tensile Modulus, Type 1, 0.125	ASTM D638	236,000 psi	1,627 MPa
Tensile Elongation, Type 1, 0.125	ASTM D638	6 %	6 %
Flexural Strength	ASTM D790	6,000 psi	41 MPa
Flexural Modulus	ASTM D790	266,000 psi	1,834 MPa
IZOD Impact, un-notched	ASTM D256	4 ft-lb/in	
IZOD Impact, notched	ASTM D256	2 ft-lb/in	

THERMAL PROPERTIES

Heat Deflection (HDT)	ASTM D648	205 °F	96 °C
Glass Transition (Tg)	DMA (SSYS)	219 °F	104 °C
Melt Point		Not Applicable[2]	Not Applicable[2]

OTHER

Specific Gravity	1.05
Vertical Burning Test	HB, UL94
Coefficient of Thermal Expansion	5.60E-05 in/in/F
Rockwell Hardness	R105
Dielectric S (kV/mm)	32
Dielectric C (60Hz)	2.4

APPEARANCE

- White available on all FDM systems
- Colors available on the FDM Maxum include:
  - Black, Blue, Green, Grey (light), Grey (steel), Red and Yellow
  - Custom color program available
- Colors available on FDM Prodigy Plus
  - Black, Blue, Green, Red and Yellow
  - Custom color program available

SYSTEM AVAILABILITY

- FDM Maxum
- FDM Titan **TI**
- FDM Vantage ***SE***
- FDM Vantage ***S***
- FDM Vantage ***i*** (when configured with ABS)
- FDM Prodigy Plus

Stratasys, Inc.
14950 Martin Drive
Eden Prairie, MN USA 55344
Ph: 952.937.3000
Fax: 952.937.0070
www.stratasys.com

The information presented are typical values intended for reference and comparison purposes only. They should not be used for design specifications or quality control purposes. End-use material performance can be impacted (+/-) by, but not limited to, part design, end-use conditions, test conditions, etc. Actual values will vary with build conditions.

Product specifications are subject to change without notice.

[1] Build orientation is on side edge
[2] Due to amorphous nature, material does not display a melting point

Stratasys

FORTUS 3D PRODUCTION SYSTEMS dimension 3D PRINTERS REDEYE REDEYE ARC • XPRESS 3D

7665 Commerce Way – Eden Prairie, MN 55344; (p) 952-937-3000 – www.Stratasys.com

Product Quality Documentation

Certificate of Production Conformance

This is to certify that the FDM material(s) listed below were manufactured in accordance with the following specifications, as applicable per product type:

107988-0001 Assembly Requirements Document, Canister, Fortus (T class)

205665-0001 Assembly Requirements Document, Cartridge, 3DP

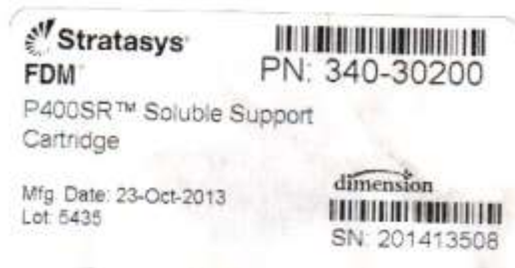

*Stratasys maintains lot specific traceability to supplier raw resin lots.

Troy Loehrs

Materials Production Manager

Jon Peterson

Supplier Quality Manager

Part Number: 109451-0001
Revision: A
Certificate of Conformance

```
================================================================================
       C A R L  Z E I S S  /  C A L Y P S O  5.2.20  Default Printout
--------------------------------------------------------------------------------
Measurement Plan              Operator          Date                     Part N
Stylus System Qualification1  Master            August 11, 2014             35
CONT_G2
--------------------------------------------------------------------------------
Names                     Description           Statistic / References      -1
Symbol / References            Actual     Nominal    Tolerance      Dev.  Histogr
================================================================================
Geometry-Requal Position #1

--------------------------------------------------------------------------------

Small Star
--------------------------------------------------------------------------------
Stylus qualification result :  Small Star

No. Stylus              Mode    X,Y,Z        R         S           Date
  2 2 Y+ A=0.0 B=0.0     R   X:  -0.01679  0.50175  0.00027  8/11/14 2:33:23 pm
                             Y:  18.94717
                             Z: -22.02152
  3 3 X+ A=0.0 B=0.0     R   X:  18.98549  0.50087  0.00043  8/11/14 2:33:53 pm
                             Y:   0.01349
                             Z: -22.03042
  4 4 Y- A=0.0 B=0.0     R   X:  -0.00445  0.50235  0.00038  8/11/14 2:34:24 pm
                             Y: -18.88635
                             Z: -22.04046
  5 5 X- A=0.0 B=0.0     R   X: -18.91970  0.50175  0.00036  8/11/14 2:34:52 pm
                             Y:  -0.01687
                             Z: -22.06884
  6 2.1 Z- A=90.0 B=     R   X: -61.97155  0.50075  0.00059  8/11/14 2:35:25 pm
                             Y: 272.70060
                             Z: 170.00020
  7 2.3 X+ A=90.0 B=     R   X: -43.05495  0.50190  0.00066  8/11/14 2:35:57 pm
                             Y: 272.68817
                             Z: 189.02685
 10 3.1 Z- A=0.0 B=9     R   X: 210.80331  0.50153  0.00020  8/11/14 2:36:32 pm
                             Y:  -0.15990
                             Z: 169.82834
 11 3.2 Y+ A=0.0 B=9     R   X: 210.77464  0.50184  0.00040  8/11/14 2:37:04 pm
                             Y:  18.79072
                             Z: 188.73314
 14 4.1 Z- A=90.0 B=     R   X: -62.04458  0.50155  0.00065  8/11/14 2:37:38 pm
                             Y:-148.89436
                             Z: 169.63192
 15 4.3 X+ A=90.0 B=     R   X: -43.08409  0.50186  0.00078  8/11/14 2:38:11 pm
                             Y:-148.88577
                             Z: 188.52554
 18 5.1 Z- A=0.0 B=-     R   X:-210.79163  0.50083  0.00023  8/11/14 2:38:44 pm
                             Y:  -0.08259
                             Z: 169.73319
 19 5.2 Y+ A=0.0 B=-     R   X:-210.79905  0.50200  0.00022  8/11/14 2:39:16 pm
                             Y:  18.82449
                             Z: 188.77015
 22 1.2 Y+ A=-15.0 B     R   X:  11.14236  0.50145  0.00018  8/11/14 2:39:48 pm
                             Y:  20.39517
                             Z: -22.01966
 23 1.4 Y- A=-15.0 B     R   X:  20.95107  0.50132  0.00056  8/11/14 2:40:16 pm
                             Y: -16.14617
                             Z: -22.03587
The following styli were not selected for CNC qualification

No. Stylus              Mode    X,Y,Z        R         S           Date
  8 2.5 X- A=90.0 B=         X: -80.92863  0.50227  0.00084  7/30/14 4:24:24 pm
                             Y: 272.69283
                             Z: 188.97544
  9 2.6 Z+ A=90.0 B=         X: -62.03164  0.50153  0.00064  7/30/14 4:24:56 pm
```

```
================================================================================
       C A R L  Z E I S S  /  C A L Y P S O  5.2.20  Default Printout
--------------------------------------------------------------------------------
Measurement Plan              Operator          Date                       Part N
Stylus System Qualification1  Master            August 11, 2014                35
CONT_G2
--------------------------------------------------------------------------------
Names                     Description           Statistic / References      -2
Symbol / References            Actual     Nominal    Tolerance      Dev.  Histogr
================================================================================
                          Y: 272.72135
                          Z: 207.91100
 12 3.4 X- A=0.0 B=9      X: 210.76295  0.50225  0.00015  7/30/14 4:25:34 pm
                          Y: -19.07233
                          Z: 188.74375
 13 3.6 Z+ A=0.0 B=9      X: 210.77611  0.50063  0.00008  7/30/14 4:26:06 pm
                          Y:  -0.14250
                          Z: 207.73743
 16 4.5 X- A=90.0 B=      X: -80.95528  0.50182  0.00058  7/30/14 4:26:40 pm
                          Y:-148.85823
                          Z: 188.55712
 17 4.6 Z+ A=90.0 B=      X: -62.01533  0.49909  0.00052  7/30/14 4:27:14 pm
                          Y:-148.89169
                          Z: 207.54171
 20 5.4 Y- A=0.0 B=-      X:-210.78630  0.50171  0.00010  7/30/14 4:27:50 pm
                          Y: -19.03782
                          Z: 188.69890
 21 5.6 Z+ A=0.0 B=-      X:-210.83495  0.50154  0.00035  7/30/14 4:28:23 pm
                          Y:  -0.15167
                          Z: 207.64496

1.5x30
--------------------------------------------------------------------------------
Stylus qualification result :  1.5x30

No. Stylus           Mode    X,Y,Z        R        S          Date
  1 1 Z- A=0.0 B=0.0  R   X:  -0.01764  0.74964  0.00047  8/11/14 2:41:13 pm
                          Y:  -0.10986
                          Z:  -1.87631
  2 2 Y+ A=90.0 B=-9  R   X: -62.09765  0.74885  0.00061  8/11/14 2:41:47 pm
                          Y: 252.53323
                          Z: 188.98714
  3 3 X+ A=0.0 B=90.  R   X: 190.61468  0.75055  0.00104  8/11/14 2:42:23 pm
                          Y:  -0.25105
                          Z: 188.72965
  4 4 Y- A=90.0 B=90  R   X: -62.12443  0.75025  0.00043  8/11/14 2:42:58 pm
                          Y:-128.72708
                          Z: 188.55536
  5 5 X- A=0.0 B=-90  R   X:-190.64324  0.74957  0.00080  8/11/14 2:43:34 pm
                          Y:  -0.21902
                          Z: 188.74155
The following styli were not selected for CNC qualification

No. Stylus           Mode    X,Y,Z        R        S          Date
  6 6 Y- A=108.0 B=7      X:-114.60218  0.74967  0.00050  7/30/14 4:29:26 pm
                          Y: -94.94332
                          Z: 139.22532
  7 7 Y- A=104.0 B=1      X:-107.67398  0.75031  0.00082  7/30/14 4:29:59 pm
                          Y: -99.92524
                          Z: 237.90692

3 x 100
--------------------------------------------------------------------------------
Stylus qualification result :  3x100

No. Stylus           Mode    X,Y,Z        R        S          Date
  1 1 Z- A=0.0 B=0.0  R   X:   0.04568  1.49979  0.00027  8/11/14 2:44:31 pm
                          Y:   0.05354
```

```
================================================================================
       C A R L  Z E I S S  /  C A L Y P S O  5.2.20  Default Printout
--------------------------------------------------------------------------------
Measurement Plan              Operator          Date                     Part No
Stylus System Qualification1  Master            August 11, 2014              355
CONT_G2
--------------------------------------------------------------------------------
Names                        Description            Statistic / References    -3-
Symbol / References               Actual     Nominal    Tolerance     Dev.  Histogr.
================================================================================
                          Z: -71.14995
  2 2 Y+ A=90.0 B=-9  R   X: -61.98385  1.49990  0.00016  8/11/14 2:45:07 pm
                          Y: 321.79891
                          Z: 188.98736
  3 3 X+ A=0.0 B=90.  R   X: 259.88257  1.49956  0.00043  8/11/14 2:45:45 pm
                          Y:  -0.14528
                          Z: 188.77709
  4 4 Y- A=90.0 B=90  R   X: -62.01847  1.49977  0.00009  8/11/14 2:46:21 pm
                          Y:-197.99462
                          Z: 188.52551
  5 5 X- A=0.0 B=-90  R   X:-259.91041  1.49988  0.00018  8/11/14 2:46:59 pm
                          Y:  -0.10558
                          Z: 188.66400
  6 6 X+ A=-60.0 B=9  R   X: 183.66793  1.49960  0.00009  8/11/14 2:47:35 pm
                          Y: 255.92674
                          Z: 188.96917
  7 7 X+ A=-22.5 B=9  R   X: 263.84010  1.49972  0.00047  8/11/14 2:48:09 pm
                          Y: 104.02906
                          Z: 188.86103
  8 8 X+ A=22.5 B=90  R   X: 216.36631  1.49979  0.00016  8/11/14 2:48:42 pm
                          Y: -94.87497
                          Z: 188.70469
  9 9 Z- A=120.0 B=-  R   X:  68.45683  1.49986  0.00037  8/11/14 2:49:18 pm
                          Y: 304.47074
                          Z: 100.12821
 10 10 Z- A=-120.0 B  R   X: -68.33428  1.49959  0.00019  8/11/14 2:49:54 pm
                          Y: 304.44739
                          Z: 100.05219
 11 11 X- A=0.0 B=-3  R   X:-149.01659  1.50022  0.00034  8/11/14 2:50:26 pm
                          Y:   0.03914
                          Z: -24.19043
 12 12 X- A=0.0 B=-6  R   X:-240.08710  1.49978  0.00041  8/11/14 2:50:58 pm
                          Y:  -0.03653
                          Z:  89.21225
 13 13 Z+ A=0.0 B=-5  R   X: -22.60257  1.50008  0.00020  8/11/14 2:51:28 pm
                          Y:   0.05036
                          Z: -70.16755
 14 14 Z+ A=45.0 B=-  R   X: -59.81444  1.50001  0.00031  8/11/14 2:51:58 pm
                          Y:  34.24524
                          Z: -70.15194

3x50
--------------------------------------------------------------------------------
Stylus qualification result :  3x50

No. Stylus           Mode    X,Y,Z        R        S           Date
  1 1 Z- A=0.0 B=0.0  R   X:   0.12473  1.50059  0.00036  8/11/14 2:52:54 pm
                          Y:  -0.04641
                          Z: -21.14036
  2 2 Y+ A=90.0 B=-9  R   X: -62.04777  1.50097  0.00048  8/11/14 2:53:29 pm
                          Y: 271.79061
                          Z: 188.86552
  3 3 X+ A=0.0 B=90.  R   X: 209.87424  1.50082  0.00062  8/11/14 2:54:06 pm
                          Y:  -0.20364
                          Z: 188.86978
  4 4 Y- A=90.0 B=90  R   X: -62.07456  1.50030  0.00022  8/11/14 2:54:41 pm
                          Y:-147.98731
                          Z: 188.67380
```

```
================================================================================
       C A R L  Z E I S S  /  C A L Y P S O  5.2.20  Default Printout
--------------------------------------------------------------------------------
Measurement Plan              Operator         Date                    Part No
Stylus System Qualification1  Master           August 11, 2014             355
CONT_G2
--------------------------------------------------------------------------------
Names                     Description             Statistic / References    -4-
Symbol / References            Actual     Nominal    Tolerance     Dev.  Histogr.
================================================================================
  5 5 X- A=0.0 B=-90  R   X:-209.90336  1.50033  0.00043  8/11/14 2:55:18 pm
                          Y:  -0.16568
                          Z: 188.59910
  6 6 Y- A=-90.0 B=-  R   X:  62.13371  1.50037  0.00035  8/11/14 2:55:51 pm
                          Y: -86.36117
                          Z:  40.22601
  7 7 Y+ A=90.0 B=-4  R   X: -62.02774  1.50106  0.00007  8/11/14 2:56:26 pm
                          Y: 210.36618
                          Z:  40.42994
  8 8 X- A=0.0 B=-45  R   X:-148.31502  1.50085  0.00050  8/11/14 2:56:59 pm
                          Y:  -0.06802
                          Z:  40.23134
  9 9 X+ A=180.0 B=-  R   X: 148.42647  1.50086  0.00080  8/11/14 2:57:32 pm
                          Y: 124.07293
                          Z:  40.42555
 10 10 X- A=22.5 B=-  R   X:-217.66784  1.50103  0.00040  8/11/14 2:58:06 pm
                          Y:  84.88156
                          Z: 188.65737
 11 11 X+ A=157.5 B=  R   X: 170.19013  1.50072  0.00036  8/11/14 2:58:41 pm
                          Y: 199.54007
                          Z: 188.88032
 12 12 X+ A=-157.5 B  R   X: 217.68189  1.50071  0.00077  8/11/14 2:59:18 pm
                          Y:  38.88518
                          Z: 188.74855
 13 13 X- A=-22.5 B=  R   X:-170.17525  1.50123  0.00029  8/11/14 2:59:52 pm
                          Y: -75.77306
                          Z: 188.54864
 14 14 X+ A=22.5 B=9  R   X: 170.14375  1.50074  0.00066  8/11/14 3:00:28 pm
                          Y: -75.78872
                          Z: 188.81387
 15 15 Y+ A=75.0 B=-  R   X:-114.25858  1.49973  0.00019  8/11/14 3:01:03 pm
                          Y: 248.57757
                          Z: 188.81869
 16 16 Y+ A=105.0 B=  R   X:  -5.60207  1.50031  0.00044  8/11/14 3:01:35 pm
                          Y: 280.70036
                          Z: 188.89387
 17 17 Y- A=105.0 B=  R   X:-114.27627  1.50066  0.00060  8/11/14 3:02:10 pm
                          Y:-124.76687
                          Z: 188.67374
 18 18 Y- A=75.0 B=9  R   X:  -5.63926  1.50000  0.00051  8/11/14 3:02:43 pm
                          Y:-156.90550
                          Z: 188.69226
 19 19 X+ A=180.0 B=  R   X: 171.94293  1.50099  0.00085  8/11/14 3:03:17 pm
                          Y: 124.04793
                          Z:  68.45047

Star Stylus
--------------------------------------------------------------------------------
Stylus qualification result :  Star Stylus

No. Stylus             Mode    X,Y,Z        R         S           Date
  1 1 Z- A=0.0 B=0.0  R   X:  -0.09743  1.50075  0.00037  8/11/14 3:04:16 pm
                          Y:  -0.02096
                          Z:-115.82326
  2 2 Y+ A=0.0 B=0.0  R   X:   0.05148  1.00051  0.00028  8/11/14 3:04:45 pm
                          Y:  35.97152
                          Z: -74.96721
  3 3 X+ A=0.0 B=0.0  R   X:  35.92484  0.99970  0.00056  8/11/14 3:05:15 pm
```

```
===============================================================================
      C A R L  Z E I S S  /  C A L Y P S O  5.2.20  Default Printout
-------------------------------------------------------------------------------
Measurement Plan              Operator          Date                     Part Nc
Stylus System Qualification1  Master            August 11, 2014              355
CONT_G2
-------------------------------------------------------------------------------
Names                    Description            Statistic / References      -5-
Symbol / References           Actual     Nominal     Tolerance      Dev.  Histogr.
===============================================================================
                          Y:  -0.34503
                          Z: -75.03820
  4 4 Y- A=0.0 B=0.0  R   X:  -0.42905  1.00068  0.00047  8/11/14 3:05:45 pm
                          Y: -36.06100
                          Z: -74.92105
  5 5 X- A=0.0 B=0.0  R   X: -36.23667  1.00045  0.00068  8/11/14 3:06:15 pm
                          Y:   0.12293
                          Z: -74.88872

5x75
-------------------------------------------------------------------------------
Stylus qualification result :  5x75

No. Stylus           Mode    X,Y,Z        R        S           Date
  1 1 Z- A=0.0 B=0.0  R   X:   0.05491  2.50101  0.00039  8/11/14 3:07:09 pm
                          Y:  -0.03023
                          Z: -44.81730
  2 2 Y+ A=90.0 B=-9  R   X: -62.04823  2.50091  0.00008  8/11/14 3:07:44 pm
                          Y: 295.47067
                          Z: 188.95094
  3 3 X+ A=0.0 B=90.  R   X: 233.55513  2.50080  0.00065  8/11/14 3:08:22 pm
                          Y:  -0.20564
                          Z: 188.79679
  4 4 Y- A=90.0 B=90  R   X: -62.07918  2.50098  0.00041  8/11/14 3:08:59 pm
                          Y:-171.66720
                          Z: 188.57442
  5 5 X- A=0.0 B= -9  R   X:-233.58333  2.50066  0.00066  8/11/14 3:09:36 pm
                          Y:  -0.16898
                          Z: 188.65835
  6 6 X+ A=0.0 B= 10  R   X: 228.01234  2.50056  0.00045  8/11/14 3:10:13 pm
                          Y:  -0.24027
                          Z: 239.35432
  7 7 X- A=-167.5 B=  R   X:-214.56866  2.50122  0.00029  8/11/14 3:10:49 pm
                          Y: 173.04842
                          Z: 188.80952
  8 8 X- A=-12.5 B=-  R   X:-214.61168  2.50076  0.00018  8/11/14 3:11:25 pm
                          Y: -49.25864
                          Z: 188.62241
  9 9 Y- A=90.0 B=-5  R   X: -62.02928  2.50083  0.00024  8/11/14 3:11:57 pm
                          Y: 247.29939
                          Z:  46.73211
```

Appendix F: **CMM Certificate of Calibration**

Certificate of Calibration

Certificate ID: W54796

Manufacturer	Carl Zeiss
Model	CONTURA G2 RDS
Serial Number	201005502324
Customer	Dotson Co 200 W Rock St Mankato 56001 USA
Job Number	W54796

The equipment identified in this certificate was calibrated with standards that are traceable to national metrology institutes (e.g. NIST) through calibration laboratories accredited to ISO 17025. All results are reported in units of measure as defined by the International System of Units (SI).

The user is responsible for definition of appropriate intervals of calibration.

Calibration Certificate pages	1 of 17
Date of Calibration	8/9/2014
Calibration Interval	12 months*
Calibration Procedure	CL-1001

**Unless agreed upon by customer, this is manufacturer's recommended interval only.*

Calibration certificates without signature are not valid.

Jenae Smith — Field Service Tech

Signature / Name
Jenae Smith

Title:

The most noteworthy contributor to the uncertainty budget of a CMM is the deviation of temperature away from the standard of 20 degrees Celsius.

Unless otherwise annotated in protocol results, machine condition is in good working order.
The reported results relate only to the item(s) specified above. All measurements performed at 95% confide level (k=2).

Carl Zeiss Industrial Metrology
6250 Sycamore Lane North
Maple Grove, MN 55369

Telephone (800)327-9735
Fax (763)535-9792
E-Mail imt@zeiss.com

1. Calibration task

Indication error **E** for length measurements and probing error **P** are measured on the coordinate measuring machine.

For sensor systems with scanning capability, roundness form measuring error **RONt (MZCI)** was measured.
If a rotary table is installed, the four-axis errors **FR**, **FT** and **FA** were measured if this measurement was ordered.

The coordinate measuring machine had the following configuration at the time of calibration:

Controller: C99N #
Probe: TL3 #
Measurement SW: CALYPSO 5.4
Reference sphere: #I4144 r=12.4939
X measuring range: 1000mm
Y measuring range: 1200mm
Z measuring range: 600mm

2. Calibration procedure

Calibration of the metrological features of the coordinate measuring machine was performed according to Carl Zeiss IMT procedure CL-1001. This procedure is established and validated using international metrological methods.

Length measurement accuracies **E** were determined via mechanical probings on parallel or stepped gauge blocks.

The roundness form measurement errors **RONt (MZCI)** were determined by measuring a master ring in the scanning mode with D = 50mm.

The four-axis measurement deviations **FR** (radial), **FT** (tangential) and **FA** (axial) were determined using two ceramic spheres with D = 30mm. The ceramic spheres were clamped with a horizontal distance from the rotary axis of r = 206mm and a horizontal distance of d = 412mm as well as a vertical distance of h = 206mm.

The calibration is performed at the customer site specified on page 1. In the event that customer and machine location are different, the customer location will be detailed in Section 3..

The calibration standards used are specified in the relevant sections of the measurement result documentation.

3. Ambient conditions

The calibration was performed on-site. The coordinate measuring machine is installed at the following location:

Dotson Co
200 W Rock St
Mankato 56001 USA

4. Measurement results

The measurement results apply only to the specified time of measurement. They also apply only to the relevant installation site and machine settings at the time of calibration. All settings and correction values were documented by the calibration laboratory.

4.1 Indication error for length measurements E

The following parallel and stepped gauge blocks are used to determine indication errors:

GCS #: GSC 7324 Valid to: 12/11/2014
GCS #:

The following temperature measuring device was utilized to perform temperature measurement to calculate deviation from a reference temperature of 20°C (if applicable).

GCS #: 65007061188

The determined indication errors **E** and the maximum permissible indication error for length measurements **MPE_E** are represented in the following diagrams.

The maximum permissible indication error amounts to:

MPE_E = +/- (1.9 + L/300) µm

ZEISS

indication error in pos. 1 (X axis (top))

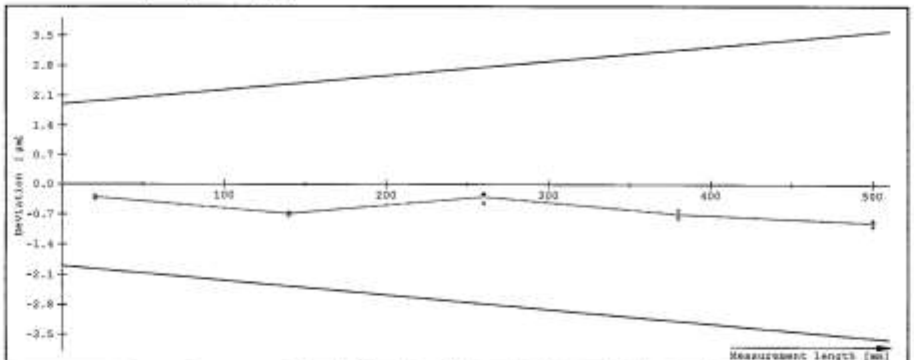

	X axis	Y axis	Z axis	test piece	Mon. factor = 0.31
temperature of material measure in °C	20.00	20.00	20.00	21.78	
position of test piece in mm	240	-598	-118	$MPE\text{-}E_0 = 1.9 + L/300$	

Measuring length L (mm)		Deviation (mm)		
nominal value	actual value	mean value	minimum	maximum
19.9876	19.9873	-0.0003	-0.0003	-0.0003
139.9596	139.9589	-0.0007	-0.0007	-0.0007
259.9356	259.9353	-0.0003	-0.0004	-0.0002
379.9735	379.9728	-0.0007	-0.0008	-0.0006
499.8984	499.8975	-0.0009	-0.0010	-0.0008

W54796

indication error in pos. 2 (X axis (bottom))

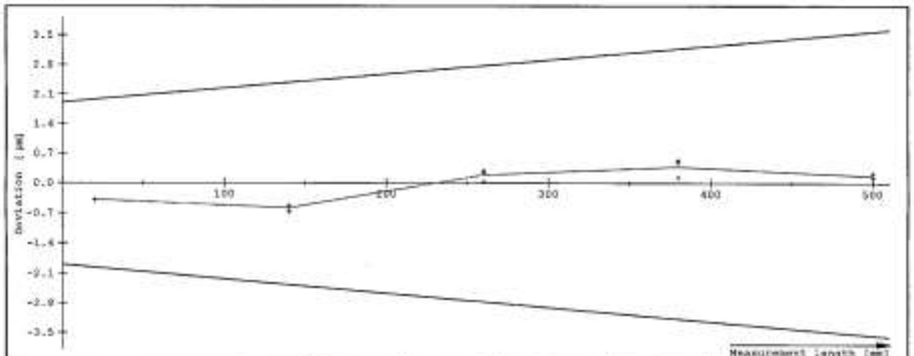

	X axis	Y axis	Z axis	test piece	Mon. factor = 0.28
temperature of material measure in °C	20.00	20.00	20.00	21.75	
position of test piece in mm	246	-500	-452	$MPE\text{-}E_0 = 1.9 + L/300$	

Measuring length L (mm)		Deviation (mm)		
nominal value	actual value	mean value	minimum	maximum
19.9874	19.9872	-0.0004	-0.0004	-0.0004
139.9536	139.9530	-0.0006	-0.0007	-0.0005
259.9356	259.9358	0.0002	0.0000	0.0003
379.9735	379.9738	0.0004	0.0001	0.0005
499.8984	499.8986	0.0002	0.0001	0.0002

ZEISS

W54796

indication error in pos. 3 (Y axis (right))

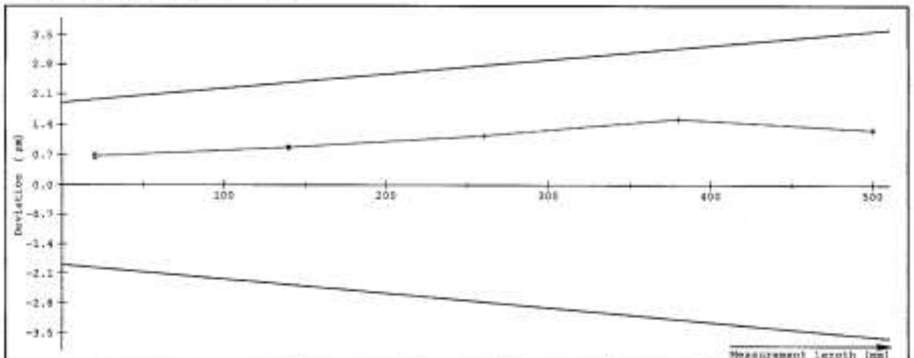

	X axis	Y axis	Z axis	test piece	
temperature of material measure in °C	20.00	20.00	20.00	22.03	Mon. factor = 0.49
position of test piece in mm	922	-1136	-452	$MPE\text{-}E_0 = 1.9 + L/300$	

Measuring length L (mm)		Deviation (mm)		
nominal value	actual value	mean value	minimum	maximum
19.9876	19.9883	0.0007	0.0006	0.0007
139.9596	139.9604	0.0009	0.0008	0.0009
259.9356	259.9368	0.0011	0.0011	0.0011
379.9735	379.9750	0.0015	0.0015	0.0015
499.8984	499.8997	0.0013	0.0012	0.0013

ZEISS

W54796

indication error in pos. 4 (Y axis (left))

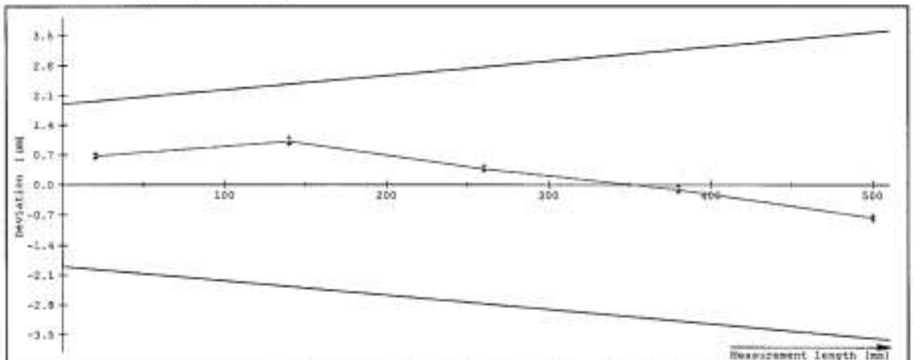

	X axis	Y axis	Z axis	test piece	Mon. factor = 0.47
temperature of material measure in °C	20.00	20.00	20.00	21.95	
position of test piece in mm	23	-585	-432	MPE-E_0 = 1.9 + L/300	

Measuring length L (mm)		Deviation (mm)		
nominal value	actual value	mean value	minimum	maximum
19.9876	19.9883	0.0007	0.0006	0.0007
139.9596	139.9606	0.0010	0.0009	0.0011
259.9356	259.9360	0.0004	0.0003	0.0004
379.9735	379.9733	-0.0001	-0.0002	0.0000
499.9984	499.9976	-0.0008	-0.0008	-0.0007

W54796

Indication error in pos. 5 (Z axis)

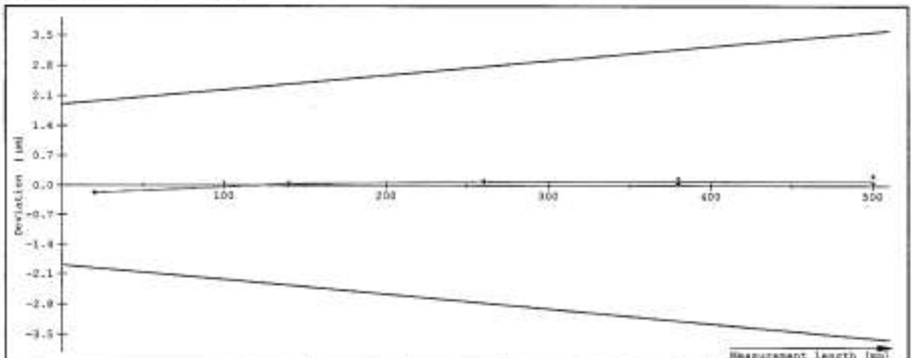

	X axis	Y axis	Z axis	test piece	
temperature of material measure in °C	20.00	20.00	20.00	21.76	Mon. factor = 0.10
position of test piece in mm	516	-804	-351	MPE-E_0 = 1.9 + L/300	

Measuring length L (mm)		Deviation (mm)		
nominal value	actual value	mean value	minimum	maximum
19.9876	19.9874	-0.0002	-0.0002	-0.0002
139.9596	139.9596	0.0000	0.0000	0.0001
259.9356	259.9357	0.0001	0.0001	0.0001
379.9735	379.9736	0.0001	0.0000	0.0002
499.9984	499.9985	0.0001	0.0000	0.0002

ZEISS

W54796

indication error in pos. 6 (Spatial (front-right))

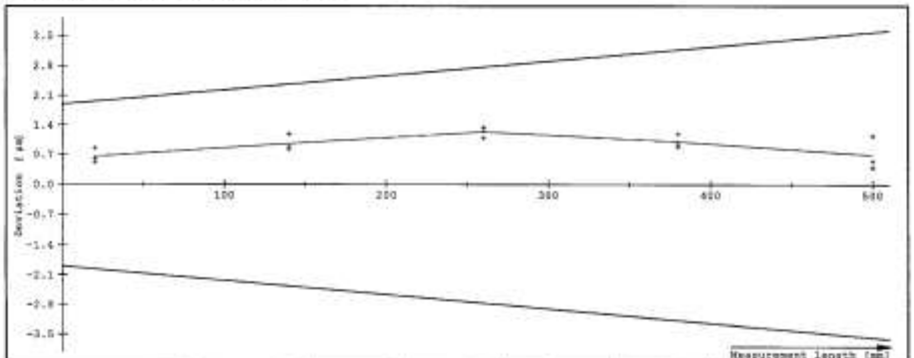

	X axis	Y axis	Z axis	test piece	Mon. factor = 0.50
temperature of material measure in °C	20.00	20.00	20.00	21.76	
position of test piece in mm	696	-882	-361	$MPE\text{-}E_0 = 1.9 + L/300$	

Measuring length L (mm)		Deviation (mm)		
nominal value	actual value	mean value	minimum	maximum
19.9876	19.9883	0.0007	0.0005	0.0009
139.9596	139.9605	0.0010	0.0008	0.0012
259.9356	259.9369	0.0012	0.0011	0.0013
379.9735	379.9744	0.0010	0.0009	0.0012
499.8984	499.8991	0.0007	0.0004	0.0011

indication error in pos. 7 (Spatial (front-left))

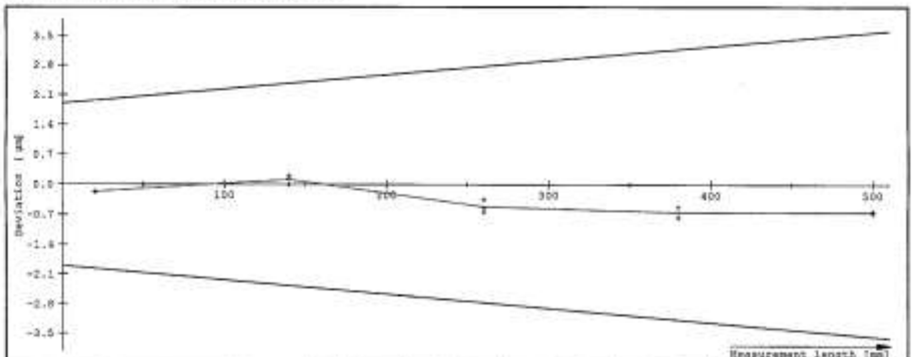

	X axis	Y axis	Z axis	test piece	
temperature of material measure in °C	20.00	20.00	20.00	21.97	Mon. factor = 0.24
position of test piece in mm	345	-857	-361	$MPE\text{-}E_0 = 1.9 + L/300$	

Measuring length L (mm)		Deviation (mm)		
nominal value	actual value	mean value	minimum	maximum
19.9876	19.9874	-0.0002	-0.0002	-0.0002
139.9596	139.9597	0.0001	0.0000	0.0002
259.9356	259.9351	-0.0005	-0.0006	-0.0004
379.9735	379.9728	-0.0006	-0.0008	-0.0005
499.8964	499.8978	-0.0006	-0.0007	-0.0006

ZEISS

indication error in pos. 8 (Spatial (rear-left))

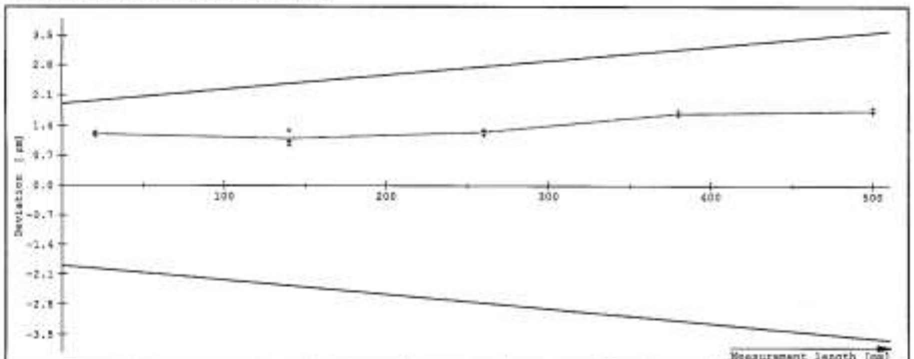

	X axis	Y axis	Z axis	test piece	Mon. factor = 0.63
temperature of material measure in °C	20.00	20.00	20.00	22.00	
position of test piece in mm	381	-356	-361	$MPE\text{-}E_0 = 1.9 + L/300$	

Measuring length L (mm)		Deviation (mm)		
nominal value	actual value	mean value	minimum	maximum
19.9876	19.9888	0.0012	0.0012	0.0012
139.9596	139.9606	0.0011	0.0010	0.0013
259.9356	259.9369	0.0012	0.0012	0.0013
379.9735	379.9751	0.0017	0.0016	0.0017
499.8984	499.9001	0.0017	0.0017	0.0018

indication error in pos. 9 (Spatial (rear-right))

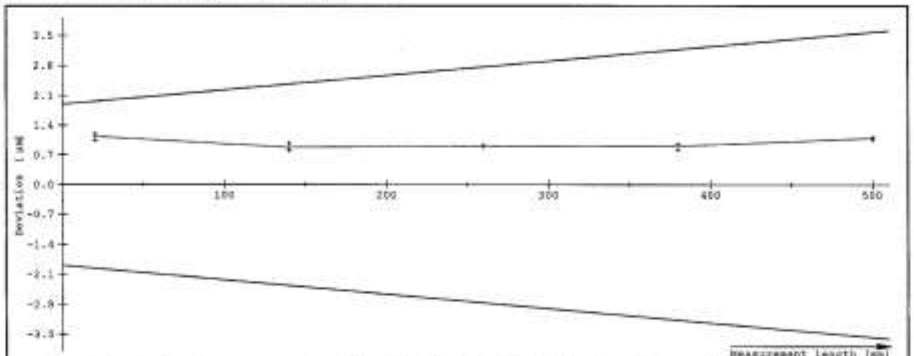

	X axis	Y axis	Z axis	test piece	Mon. factor = 0.61
temperature of material measure in °C	20.00	20.00	20.00	22.01	
position of test piece in mm	734	-382	-361	MPE-E_0 = 1.9 + L/300	

Measuring length L (mm)		Deviation (mm)		
nominal value	actual value	mean value	minimum	maximum
19.9876	19.9887	0.0011	0.0010	0.0012
139.9596	139.9604	0.0009	0.0008	0.0010
259.9356	259.9365	0.0009	0.0009	0.0009
379.9735	379.9744	0.0009	0.0008	0.0009
499.8904	499.8995	0.0011	0.0011	0.0011

Certificate of conformity
If confirmed below, the coordinate measuring machine fulfills the specified requirements. The performance of the coordinate measuring machine has been calibrated according to relevant specifications.

The coordinate measuring machine meets the original manufacturer's specification.

5.

Roundness form measurement error RONt (MZCI)

The following master ring is used to determine roundness form measurement error **RONt (MZCI)**:

GCS number: 4149 Valid to: 6/17/2015

Max. permissible roundness error: t = **1.9 µm**

Measurement results:

In the X/Y plane:	**t = 0.5 µm**	(T = 21.80°C; stylus L = 40mm and D = 8.0mm)
In the X/Z plane:	**t = 0.8 µm**	(T = 21.80°C; stylus L = 40mm and D = 8.0mm)
In the Y/Z plane:	**t = 1.1 µm**	(T = 21.80°C; stylus L = 40mm and D = 8.0mm)

ZEISS

W54796

Roundness form measurement error RONt (MZCI) XY-Plane

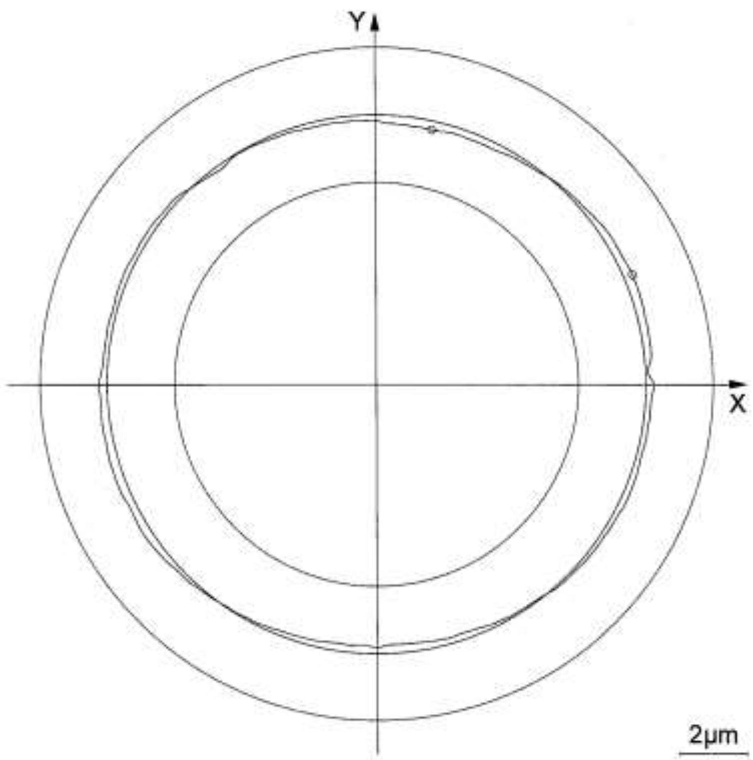

ZEISS

W54796

Roundness form measurement error RONt (MZCI) YZ-Plane

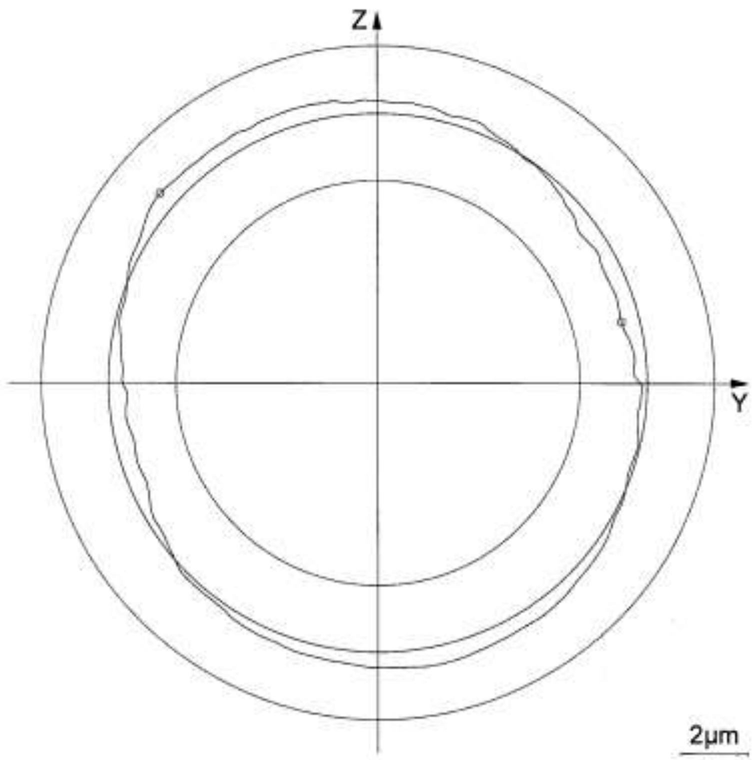

W54796

Roundness form measurement error RONt (MZCI) ZX-Plane

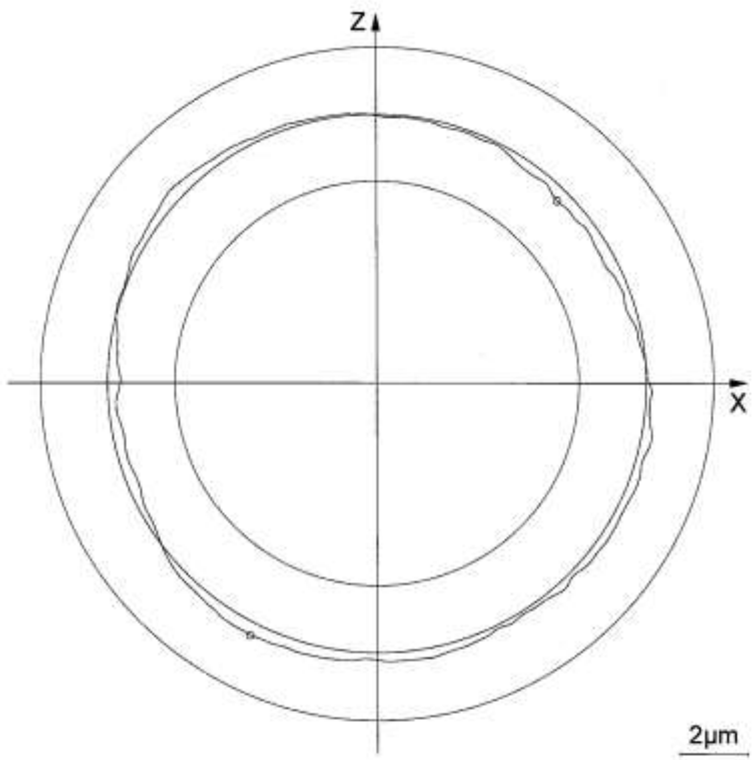

Appendix G: **Environmental Data**

Date - Time	Temperature(°F)	Humidity(%)	Relative Pressure(inHg)	Absolute Pressure(inHg)
7/21/2014 - 8:26	73.8	63	29.8	28.88
7/21/2014 - 9:00	73.9	62	29.79	28.87
7/21/2014 - 9:30	73.9	61	29.8	28.87
7/21/2014 - 9:57	73.9	62	29.79	28.87
7/21/2014 - 10:27	73.8	63	29.8	28.87
7/21/2014 - 10:56	73.6	62	29.79	28.87
7/21/2014 - 11:26	73.8	62	29.79	28.87
7/21/2014 - 11:55	74.1	62	29.78	28.86
7/21/2014 - 12:28	73.9	62	29.78	28.86
7/21/2014 - 13:05	73.6	63	29.78	28.85
7/21/2014 - 13:36	73.4	64	29.77	28.85
7/21/2014 - 13:59	73	64	29.76	28.84
7/21/2014 - 14:33	72.9	64	29.75	28.83
7/21/2014 - 14:55	72.7	64	29.76	28.83
7/21/2014 - 15:25	72.7	64	29.76	28.84
7/21/2014 - 15:56	72.9	64	29.76	28.84
7/21/2014 - 16:25	72.9	64	29.78	28.85
7/21/2014 - 17:05	72.7	64	29.78	28.85
7/21/2014 - 17:26	72.7	64	29.77	28.84
7/21/2014 - 17:57	72.3	65	29.76	28.84
7/21/2014 - 18:25	72.3	65	29.78	28.85
7/21/2014 - 18:55	72.3	65	29.77	28.84
7/21/2014 - 19:25	72.1	65	29.76	28.83
7/21/2014 - 19:55	72.5	65	29.75	28.83
7/21/2014 - 20:25	72.9	64	29.74	28.82
7/21/2014 - 21:08	73.2	64	29.73	28.8
7/21/2014 - 21:26	73.8	63	29.72	28.79
7/21/2014 - 22:05	73.9	63	29.72	28.79
7/21/2014 - 22:25	73.9	63	29.7	28.78
7/21/2014 - 22:55	73.9	64	29.7	28.78
7/21/2014 - 23:25	73.9	64	29.7	28.77
7/21/2014 - 23:55	73.8	64	29.71	28.78
7/22/2014 - 0:25	73.4	64	29.71	28.79
7/22/2014 - 0:55	73.4	64	29.72	28.79
7/22/2014 - 1:25	73	63	29.72	28.79
7/22/2014 - 1:57	73.4	65	29.72	28.79
7/22/2014 - 2:28	73.2	64	29.73	28.8
7/22/2014 - 2:56	73.2	64	29.73	28.81
7/22/2014 - 3:28	73.4	65	29.73	28.81
7/22/2014 - 3:56	73.4	65	29.73	28.8

7/22/2014 - 4:42	73.2	64	29.73	28.81
7/22/2014 - 5:12	73	64	29.75	28.82
7/22/2014 - 5:42	73.2	64	29.78	28.86
7/22/2014 - 6:12	73.4	65	29.8	28.87
7/22/2014 -6:36	73.2	63	29.72	28.87
7/22/2014 -7:06	73	64	29.79	28.94
7/22/2014 - 7:36	73.2	63	29.8	28.95
7/22/2014 - 8:06	73.4	63	29.8	28.95
7/22/2014 - 8:36	73.2	63	29.8	28.95
7/22/2014 - 9:06	73.8	63	29.77	28.92
7/22/2014 - 9:36	73.8	62	29.8	28.95
7/22/2014 - 10:06	73.6	63	29.8	28.95
7/22/2014 - 10:36	73.4	63	29.81	28.96
7/22/2014 - 11:06	73.8	63	29.81	28.96
7/22/2014 - 11:36	73.8	63	29.83	28.98
7/22/2014 - 12:06	73.2	62	29.83	28.98
7/22/2014 - 12:36	73.2	62	29.85	29
7/22/2014 - 13:06	73.4	63	29.86	29.01
7/22/2014 - 13:36	73.4	63	29.88	29.03
7/22/2014 - 14:06	73.8	62	29.87	29.02
7/22/2014 - 14:36	73.6	62	29.87	29.02
7/22/2014 - 15:06	73.2	62	29.88	29.03
7/22/2014 - 15:36	73.4	62	29.88	29.03
7/22/2014 - 16:06	73.6	62	29.89	29.04
7/22/2014 - 16:36	73.6	62	29.89	29.04
7/22/2014 - 17:06	73.2	62	29.89	29.04
7/22/2014 - 17:36	73.2	62	29.91	29.06
7/22/2014 - 18:06	73.2	62	29.92	29.07
7/22/2014 - 18:36	73	62	29.92	29.07
7/22/2014 - 19:06	73.8	61	29.93	29.08
7/22/2014 - 19:36	73.8	61	29.93	29.08
7/22/2014 - 20:06	73.9	61	29.93	29.08
7/22/2014 - 20:36	73.6	60	29.94	29.09
7/22/2014 - 21:06	73	61	29.95	29.1
7/22/2014 - 21:36	73.2	61	29.96	29.11
7/22/2014 - 22:06	73.4	59	29.96	29.11
7/22/2014 - 22:36	73.8	59	29.97	29.12
7/22/2014 - 23:06	73.8	60	29.97	29.12
7/22/2014 - 23:36	73.6	60	29.98	29.13
7/23/2014 - 0:06	73.2	61	29.99	29.14
7/23/2014 - 0:36	73.4	60	30	29.15
7/23/2014 - 1:06	73.4	60	30	29.15

7/23/2014 - 1:36	73.4	60	30.01	29.16
7/23/2014 - 2:06	73	61	30.01	29.16
7/23/2014 - 2:36	73	61	30.01	29.16
7/23/2014 - 3:06	73.2	61	30.01	29.16
7/23/2014 - 3:36	73.4	60	30.02	29.17
7/23/2014 - 4:06	73.4	60	30.03	29.18
7/23/2014 - 4:36	73.4	60	30.03	29.18
7/23/2014 - 5:06	73	61	30.02	29.17
7/23/2014 - 5:36	73.2	61	30.03	29.18
7/23/2014 - 6:06	73.4	60	30.05	29.2
7/23/2014 - 6:36	73.4	60	30.06	29.21
7/23/2014 - 7:06	73.6	59	30.06	29.21
7/23/2014 - 7:36	73.6	59	30.07	29.22
7/23/2014 - 8:06	73.4	59	30.07	29.22
7/23/2014 - 8:36	73.6	59	30.08	29.23
7/23/2014 - 9:06	73.8	58	30.08	29.23
7/23/2014 - 9:36	73.8	59	30.08	29.23
7/23/2014 - 10:06	74.1	59	30.07	29.22
7/23/2014 - 10:36	74.3	58	30.06	29.21
7/23/2014 - 11:06	74.3	58	30.06	29.21
7/23/2014 - 11:36	74.1	58	30.06	29.21
7/23/2014 - 12:06	73.9	55	30.07	29.22
7/23/2014 - 12:36	73.4	56	30.07	29.22
7/23/2014 - 13:06	73	57	30.07	29.22
7/23/2014 - 13:36	72.9	58	30.07	29.22
7/23/2014 - 14:06	72.5	58	30.06	29.21
7/23/2014 - 14:36	72.3	58	30.06	29.21
7/23/2014 - 15:06	72.3	58	30.05	29.2
7/23/2014 - 15:36	72.9	57	30.05	29.2
7/23/2014 - 16:06	73	56	30.04	29.19
7/23/2014 - 16:36	73.6	56	30.03	29.18
7/23/2014 - 17:06	73.9	55	30.01	29.16
7/23/2014 - 17:36	73.9	55	30.01	29.16
7/23/2014 - 18:06	73.9	55	30	29.15
7/23/2014 - 18:36	73.6	55	30	29.15
7/23/2014 - 19:06	73.8	55	29.99	29.14
7/23/2014 - 19:36	73.6	55	29.99	29.14
7/23/2014 - 20:06	73.4	55	29.98	29.13
7/23/2014 - 20:36	73.8	56	29.98	29.13
7/23/2014 - 21:06	73.9	55	29.98	29.13
7/23/2014 - 21:36	73.9	55	29.98	29.13
7/23/2014 - 22:06	73.8	55	29.98	29.13

7/23/2014 - 22:36	73.6	56	29.98	29.13
7/23/2014 - 23:06	73.8	56	29.98	29.13
7/23/2014 - 23:36	73.8	56	29.98	29.13
7/24/2014 - 0:06	73.6	56	29.98	29.13
7/24/2014 - 0:36	73.9	56	29.98	29.13
7/24/2014 - 1:06	73.4	56	29.98	29.13
7/24/2014 - 1:36	73.6	56	29.99	29.14
7/24/2014 - 2:06	73.4	57	29.99	29.14
7/24/2014 - 2:36	73.6	57	29.98	29.13
7/24/2014 - 3:06	73.8	57	29.97	29.12
7/24/2014 - 3:36	73.8	57	29.98	29.13
7/24/2014 - 4:06	73.8	57	29.97	29.12
7/24/2014 - 4:36	73.6	58	29.98	29.13
7/24/2014 - 5:06	73.4	58	29.98	29.13
7/24/2014 - 5:36	73.2	59	29.98	29.13
7/24/2014 - 6:06	73.6	58	29.97	29.12
7/24/2014 - 6:36	73.4	58	29.96	29.11
7/24/2014 - 7:06	73.2	58	29.95	29.1
7/24/2014 - 7:37	73.4	58	29.96	29.11
7/24/2014 - 8:07	73.4	57	29.96	29.11
7/24/2014 - 8:37	73.4	58	29.97	29.12
7/24/2014 - 9:07	73.6	57	29.96	29.11
7/24/2014 - 9:37	73.8	57	29.96	29.1
7/24/2014 - 10:07	73.8	57	29.95	29.1
7/24/2014 - 10:37	73.8	57	29.93	29.08
7/24/2014 - 11:07	73.6	58	29.93	29.08
7/24/2014 - 11:37	73.8	58	29.92	29.07
7/24/2014 - 12:07	73.8	58	29.9	29.05
7/24/2014 - 12:37	73.9	57	29.89	29.04
7/24/2014 - 13:07	73.8	58	29.88	29.03
7/24/2014 - 13:37	73.4	58	29.85	29
7/24/2014 - 14:07	73.6	58	29.84	28.99
7/24/2014 - 14:37	73.6	58	29.84	28.99
7/24/2014 - 15:07	73.4	59	29.88	29.03
7/24/2014 - 15:37	73.2	60	29.91	29.06
7/24/2014 - 16:07	73.2	60	29.91	29.06
7/24/2014 - 16:37	73.4	59	29.89	29.04
7/24/2014 - 17:07	73.6	59	29.89	29.04
7/24/2014 - 17:37	73.8	59	29.67	28.82
7/24/2014 - 18:07	73.8	59	29.77	28.92
7/24/2014 - 18:37	73.4	60	29.75	28.9
7/24/2014 - 19:07	73	61	29.74	28.89

7/24/2014 - 19:37	73.2	61	29.72	28.87
7/24/2014 - 20:07	73.6	60	29.72	28.87
7/24/2014 - 20:37	73.6	59	29.73	28.88
7/24/2014 - 21:07	73.6	59	29.75	28.9
7/24/2014 - 21:37	73.4	59	29.76	28.91
7/24/2014 - 22:07	73.4	59	29.78	28.93
7/24/2014 - 22:37	73.6	59	29.78	28.92
7/24/2014 - 23:07	73.8	59	29.77	28.92
7/24/2014 - 23:37	73.8	59	29.75	28.9
7/25/2014 - 0:07	73.8	60	29.74	28.89
7/25/2014 - 0:37	73.6	60	29.72	28.87
7/25/2014 - 1:07	73.4	60	29.7	28.85
7/25/2014 - 1:37	73.4	60	29.67	28.82
7/25/2014 - 2:07	73.6	61	29.72	28.87
7/25/2014 - 2:37	73.6	60	29.7	28.84
7/25/2014 - 3:07	73.4	60	29.67	28.82
7/25/2014 - 3:37	73.2	61	29.64	28.79
7/25/2014 - 4:07	73.4	61	29.64	28.79
7/25/2014 - 4:37	73.6	61	29.7	28.85
7/25/2014 - 5:07	73.6	61	29.72	28.87
7/25/2014 - 5:37	73.4	61	29.65	28.8
7/25/2014 - 6:07	73.2	62	29.6	28.75
7/25/2014 - 6:37	73.4	62	29.64	28.79
7/25/2014 - 7:07	73.6	61	29.62	28.77
7/25/2014 - 7:37	73.4	61	29.63	28.78
7/25/2014 - 8:07	73.6	61	29.62	28.77
7/25/2014 - 8:37	73.6	61	29.64	28.79
7/25/2014 - 9:07	73.4	61	29.65	28.8
7/25/2014 - 9:37	73.6	61	29.64	28.79
7/25/2014 - 10:07	73.8	61	29.65	28.8
7/25/2014 - 10:37	73.6	60	29.65	28.8
7/25/2014 - 11:07	73.4	61	29.65	28.79
7/25/2014 - 11:37	73.6	60	29.64	28.79
7/25/2014 - 12:07	73.4	60	29.63	28.78
7/25/2014 - 12:37	73.8	60	29.62	28.77
7/25/2014 - 13:07	73.8	60	29.62	28.77
7/25/2014 - 13:37	73.8	60	29.62	28.77
7/25/2014 - 14:07	73.8	61	29.62	28.77
7/25/2014 - 14:37	73.6	60	29.62	28.77
7/25/2014 - 15:07	73.4	61	29.62	28.77
7/25/2014 - 15:37	73.6	61	29.62	28.77
7/25/2014 - 16:07	73.8	61	29.61	28.76

7/25/2014 - 16:37	73.8	61	29.61	28.76
7/25/2014 - 17:07	73.8	61	29.61	28.76
7/25/2014 - 17:37	73.8	61	29.61	28.76
7/25/2014 - 18:07	73.4	62	29.62	28.77
7/25/2014 - 18:37	73.6	62	29.6	28.75
7/25/2014 - 19:07	73.8	61	29.6	28.75
7/25/2014 - 19:37	73.9	61	29.6	28.74
7/25/2014 - 20:07	73.8	61	29.59	28.74
7/25/2014 - 20:37	73.8	61	29.59	28.74
7/25/2014 - 21:07	73.8	61	29.6	28.75
7/25/2014 - 21:37	73.6	60	29.62	28.77
7/25/2014 - 22:07	73.8	61	29.62	28.77
7/25/2014 - 22:37	73.9	61	29.62	28.77
7/25/2014 - 23:07	73.9	61	29.63	28.78
7/25/2014 - 23:37	73.9	62	29.64	28.79
7/26/2014 - 0:07	73.8	62	29.64	28.79
7/26/2014 - 0:37	73.6	63	29.64	28.79
7/26/2014 - 1:07	73.2	63	29.64	28.79
7/26/2014 - 1:37	73.2	63	29.64	28.79
7/26/2014 - 2:07	73.6	63	29.63	28.78
7/26/2014 - 2:37	73.8	63	29.64	28.79
7/26/2014 - 3:07	73.4	63	29.65	28.8
7/26/2014 - 3:37	73.6	63	29.65	28.8
7/26/2014 - 4:07	73	63	29.64	28.79
7/26/2014 - 4:37	73.4	63	29.64	28.79
7/26/2014 - 5:07	73.6	64	29.64	28.79
7/26/2014 - 5:37	73.6	63	29.63	28.78
7/26/2014 - 6:07	73.4	64	29.66	28.81
7/26/2014 - 6:37	73.2	63	29.65	28.8
7/26/2014 - 7:07	73.2	63	29.66	28.81
7/26/2014 - 7:37	73.4	63	29.7	28.84
7/26/2014 - 8:07	73.6	64	29.68	28.83
7/26/2014 - 8:37	73.6	64	29.63	28.78
7/26/2014 - 9:07	73.6	64	29.63	28.78
7/26/2014 - 9:37	73.4	64	29.65	28.8
7/26/2014 - 10:07	73.4	63	29.67	28.82
7/26/2014 - 10:37	73.4	63	29.65	28.8
7/26/2014 - 11:07	73.6	63	29.68	28.83
7/26/2014 - 11:37	73.6	63	29.69	28.84
7/26/2014 - 12:07	73.6	63	29.72	28.87
7/26/2014 - 12:37	73	62	29.74	28.89
7/26/2014 - 13:07	73.4	62	29.7	28.85

7/26/2014 - 13:37	73.2	62	29.67	28.82
7/26/2014 - 14:07	73.6	62	29.66	28.81
7/26/2014 - 14:37	73.9	62	29.65	28.8
7/26/2014 - 15:07	73.9	62	29.65	28.8
7/26/2014 - 15:37	73.8	62	29.64	28.79
7/26/2014 - 16:07	73.6	62	29.67	28.82
7/26/2014 - 16:37	73.8	62	29.66	28.81
7/26/2014 - 17:07	73.8	62	29.66	28.81
7/26/2014 - 17:37	73.8	62	29.65	28.8
7/26/2014 - 18:07	73.8	63	29.65	28.8
7/26/2014 - 18:37	73.6	62	29.65	28.8
7/26/2014 - 19:07	73	63	29.65	28.8
7/26/2014 - 19:37	73.4	63	29.66	28.81
7/26/2014 - 20:07	73.6	63	29.65	28.8
7/26/2014 - 20:37	73.2	63	29.66	28.81
7/26/2014 - 21:07	73	63	29.66	28.81
7/26/2014 - 21:37	73.2	63	29.67	28.82
7/26/2014 - 22:07	73.4	64	29.67	28.82
7/26/2014 - 22:37	73.6	63	29.68	28.83
7/26/2014 - 23:07	73.6	64	29.68	28.83
7/26/2014 - 23:37	73.2	63	29.68	28.83
7/27/2014 - 0:07	73.2	63	29.69	28.84
7/27/2014 - 0:37	73.2	63	29.69	28.84
7/27/2014 - 1:07	73.6	63	29.69	28.84
7/27/2014 - 1:37	73.6	63	29.69	28.84
7/27/2014 - 2:07	73.4	63	29.69	28.84
7/27/2014 - 2:37	73.2	62	29.69	28.84
7/27/2014 - 3:07	73	62	29.69	28.84
7/27/2014 - 3:37	73	63	29.68	28.83
7/27/2014 - 4:07	73.6	62	29.68	28.83
7/27/2014 - 4:37	73.2	62	29.67	28.82
7/27/2014 - 5:07	73.4	62	29.67	28.82
7/27/2014 - 5:37	73.4	61	29.68	28.83
7/27/2014 - 6:07	73.4	61	29.68	28.83
7/27/2014 - 6:37	73.6	60	29.69	28.84
7/27/2014 - 7:07	73.6	60	29.7	28.84
7/27/2014 - 7:37	73.6	60	29.71	28.86
7/27/2014 - 8:07	73.6	60	29.71	28.86
7/27/2014 - 8:37	73.4	60	29.71	28.86
7/27/2014 - 9:07	73.4	60	29.72	28.87
7/27/2014 - 9:37	73.6	60	29.73	28.88
7/27/2014 - 10:07	73.8	60	29.73	28.88

7/27/2014 - 10:37	73.6	60	29.75	28.9
7/27/2014 - 11:07	73.6	60	29.75	28.9
7/27/2014 - 11:37	73.6	60	29.77	28.92
7/27/2014 - 12:07	73.4	60	29.78	28.92
7/27/2014 - 12:37	73.4	60	29.78	28.93
7/27/2014 - 13:07	73.6	60	29.78	28.93
7/27/2014 - 13:37	73.2	61	29.79	28.94
7/27/2014 - 14:07	73.4	60	29.79	28.94
7/27/2014 - 14:37	73.2	61	29.81	28.96
7/27/2014 - 15:07	73.2	62	29.81	28.96
7/27/2014 - 15:37	73.4	61	29.82	28.97
7/27/2014 - 16:07	73.4	61	29.82	28.97
7/27/2014 - 16:37	73.4	61	29.82	28.97
7/27/2014 - 17:07	73.4	61	29.83	28.98
7/27/2014 - 17:37	73.2	62	29.84	28.99
7/27/2014 - 18:07	73.4	61	29.85	29
7/27/2014 - 18:37	73.2	62	29.85	29
7/27/2014 - 19:07	73.4	61	29.86	29.01
7/27/2014 - 19:37	73.4	61	29.87	29.02
7/27/2014 - 20:07	73.2	62	29.88	29.03
7/27/2014 - 20:37	73.4	62	29.88	29.03
7/27/2014 - 21:07	73.2	62	29.9	29.05
7/27/2014 - 21:37	73.4	62	29.91	29.06
7/27/2014 - 22:07	73.4	62	29.92	29.07
7/27/2014 - 22:37	73	62	29.93	29.08
7/27/2014 - 23:07	73.2	62	29.94	29.09
7/27/2014 - 23:37	73	62	29.95	29.1
7/28/2014 - 0:07	73.6	62	29.96	29.11
7/28/2014 - 0:37	73.6	62	29.96	29.11
7/28/2014 - 1:07	73.6	62	29.96	29.11
7/28/2014 - 1:37	73.4	61	29.97	29.12
7/28/2014 - 2:07	73.2	62	29.98	29.13
7/28/2014 - 2:37	73.4	62	29.98	29.13
7/28/2014 - 3:07	73.4	62	29.97	29.12
7/28/2014 - 3:37	73.6	61	29.98	29.13
7/28/2014 - 4:07	73.6	61	29.98	29.13
7/28/2014 - 4:37	73.6	61	29.99	29.14
7/28/2014 - 5:07	73.4	62	30	29.15
7/28/2014 - 5:37	73.2	62	30.01	29.16
7/28/2014 - 6:07	73.2	63	30.02	29.17
7/28/2014 - 6:37	73.2	63	30.02	29.17
7/28/2014 - 7:07	72.7	63	30.03	29.18

7/28/2014 - 7:37	72.7	63	30.03	29.18
7/28/2014 - 8:07	72.9	64	30.04	29.18
7/28/2014 - 8:37	73	63	30.04	29.18
7/28/2014 - 9:07	73.2	63	30.04	29.19
7/28/2014 - 9:37	73.4	61	30.04	29.19
7/28/2014 - 10:07	73.6	62	30.04	29.19
7/28/2014 - 10:37	73.9	61	30.04	29.19
7/28/2014 - 11:07	74.1	61	30.04	29.19
7/28/2014 - 11:37	73.9	60	30.04	29.19
7/28/2014 - 11:56	73.8	60	30.04	29.18
7/28/2014 - 12:26	73.4	60	30.04	29.18
7/28/2014 - 12:56	73.2	61	30.03	29.18
7/28/2014 - 13:26	73	61	30.03	29.18
7/28/2014 - 13:56	73	60	30.02	29.17
7/28/2014 - 14:26	73	60	30.02	29.17
7/28/2014 - 14:56	73	59	30.01	29.16
7/28/2014 - 15:26	72.7	58	30.01	29.16
7/28/2014 - 15:56	73	58	30.01	29.16
7/28/2014 - 16:26	73	57	30.01	29.16
7/28/2014 - 16:56	72.5	57	30.01	29.16
7/28/2014 - 17:26	72.7	57	30.01	29.16
7/28/2014 - 17:56	72.5	57	30	29.15
7/28/2014 - 18:26	72.3	57	29.99	29.14
7/28/2014 - 18:56	73	56	29.98	29.13
7/28/2014 - 19:26	73.4	56	29.98	29.13
7/28/2014 - 19:56	73.6	56	29.97	29.12
7/28/2014 - 20:26	73.6	56	29.97	29.12
7/28/2014 - 20:56	73.8	56	29.97	29.12
7/28/2014 - 21:26	73.8	55	29.98	29.13
7/28/2014 - 21:56	73.6	55	29.98	29.13
7/28/2014 - 22:26	73.8	56	29.98	29.13
7/28/2014 - 22:56	73.8	56	29.98	29.13
7/28/2014 - 23:26	73.6	57	29.98	29.13
7/28/2014 - 23:56	73.6	57	29.98	29.13
7/29/2014 - 0:26	73.4	57	29.98	29.13
7/29/2014 - 0:56	73.4	57	29.98	29.13
7/29/2014 - 1:26	73.2	58	29.99	29.14
7/29/2014 - 1:56	73.2	58	29.98	29.13
7/29/2014 - 2:26	73.2	57	29.98	29.13
7/29/2014 - 2:56	72.9	58	29.98	29.13
7/29/2014 - 3:26	72.7	58	29.98	29.13
7/29/2014 - 3:56	72.9	59	29.98	29.13

7/29/2014 - 4:26	72.1	59	29.98	29.13
7/29/2014 - 4:56	72.3	59	29.99	29.14
7/29/2014 - 5:26	72.9	59	29.98	29.13
7/29/2014 - 5:56	73	58	29.98	29.13
7/29/2014 - 6:26	72.7	57	29.98	29.13
7/29/2014 - 6:56	72.7	57	29.98	29.13
7/29/2014 - 7:26	73	57	29.99	29.14
7/29/2014 - 7:56	73	57	29.99	29.14
7/29/2014 - 8:26	73.4	57	29.99	29.14
7/29/2014 - 8:56	73.6	57	29.99	29.14
7/29/2014 - 9:26	73.4	59	29.98	29.13
7/29/2014 - 9:56	73.6	58	29.98	29.13
7/29/2014 - 10:26	73.9	57	29.98	29.13
7/29/2014 - 10:56	74.1	57	29.97	29.12
7/29/2014 - 11:26	74.1	56	29.98	29.13
7/29/2014 - 11:56	74.1	56	29.97	29.12
7/29/2014 - 12:26	74.3	56	29.96	29.11
7/29/2014 - 12:56	74.3	55	29.96	29.1
7/29/2014 - 13:26	74.3	55	29.95	29.1
7/29/2014 - 13:56	74.3	55	29.95	29.1
7/29/2014 - 14:26	73.9	55	29.94	29.09
7/29/2014 - 14:56	74.1	55	29.93	29.08
7/29/2014 - 15:26	73.9	55	29.93	29.08
7/29/2014 - 15:56	73.4	54	29.93	29.08
7/29/2014 - 16:26	73	54	29.93	29.08
7/29/2014 - 16:56	72.7	54	29.92	29.07
7/29/2014 - 17:26	72.5	54	29.92	29.07
7/29/2014 - 17:56	72.7	54	29.91	29.05
7/29/2014 - 18:26	73	54	29.9	29.05
7/29/2014 - 18:56	73.2	54	29.9	29.05
7/29/2014 - 19:26	73.4	54	29.88	29.03
7/29/2014 - 19:56	73	54	29.89	29.04
7/29/2014 - 20:26	73	54	29.88	29.03
7/29/2014 - 20:56	73	54	29.89	29.04
7/29/2014 - 21:26	73	55	29.9	29.05
7/29/2014 - 21:56	73	55	29.91	29.06
7/29/2014 - 22:26	73	55	29.91	29.06
7/29/2014 - 22:56	73.2	56	29.91	29.06
7/29/2014 - 23:26	73.2	57	29.91	29.06
7/29/2014 - 23:56	73.2	58	29.91	29.06
7/30/2014 - 0:26	73.2	58	29.91	29.06
7/30/2014 - 0:56	73.4	58	29.91	29.05

7/30/2014 - 1:26	73.2	58	29.91	29.05
7/30/2014 - 1:56	73	58	29.91	29.05
7/30/2014 - 2:26	73	59	29.9	29.05
7/30/2014 - 2:56	73	59	29.91	29.06
7/30/2014 - 3:26	72.7	61	29.92	29.07
7/30/2014 - 3:56	72.3	61	29.92	29.07
7/30/2014 - 4:26	72.3	61	29.93	29.08
7/30/2014 - 4:56	72.5	60	29.92	29.07
7/30/2014 - 5:26	72.5	60	29.93	29.08
7/30/2014 - 5:56	72.5	59	29.93	29.08
7/30/2014 - 6:26	72.5	59	29.93	29.08
7/30/2014 - 6:56	72.5	59	29.93	29.08
7/30/2014 - 7:26	72.5	59	29.94	29.09
7/30/2014 - 7:56	72.5	60	29.95	29.1
7/30/2014 - 8:26	72.5	61	29.95	29.1
7/30/2014 - 8:56	72.5	61	29.95	29.1
7/30/2014 - 9:26	72.7	61	29.94	29.09
7/30/2014 - 9:56	72.9	59	29.94	29.09
7/30/2014 - 10:26	73.4	58	29.93	29.08
7/30/2014 - 10:56	73.8	58	29.93	29.08
7/30/2014 - 11:26	73.9	58	29.93	29.08
7/30/2014 - 11:56	73.9	58	29.93	29.08
7/30/2014 - 12:26	73.8	58	29.92	29.07
7/30/2014 - 12:56	73.6	58	29.92	29.07
7/30/2014 - 13:26	73.4	58	29.92	29.07
7/30/2014 - 13:56	73	58	29.91	29.06
7/30/2014 - 14:26	73.2	58	29.91	29.05
7/30/2014 - 14:56	73	58	29.91	29.05
7/30/2014 - 15:26	73	57	29.9	29.05
7/30/2014 - 15:56	73.2	57	29.89	29.04
7/30/2014 - 16:26	73.4	56	29.9	29.05
7/30/2014 - 16:56	73.2	57	29.89	29.04
7/30/2014 - 17:26	73.2	57	29.89	29.04
7/30/2014 - 17:56	73.2	57	29.89	29.04
7/30/2014 - 18:26	73	57	29.89	29.04
7/30/2014 - 18:56	73.2	57	29.89	29.04
7/30/2014 - 19:26	73	57	29.89	29.04
7/30/2014 - 19:56	73	57	29.88	29.03
7/30/2014 - 20:26	73	57	29.88	29.03
7/30/2014 - 20:56	73	57	29.88	29.03
7/30/2014 - 21:26	73.2	56	29.89	29.04
7/30/2014 - 21:56	73.2	56	29.89	29.04

7/30/2014 - 22:26	73.4	57	29.89	29.04
7/30/2014 - 22:56	73.4	58	29.89	29.04
Average:	73.39	60.00	29.85	28.99

Appendix H: **Weather Station WS2080 Specifications**

Measurement	Range	Accuracy	Resolution
Indoor Temperature	32 to 140 °F	± 2 °F	0.1 °F
Outdoor Temperature	-40 to 149 °F	± 2 °F	0.1 °F
Indoor Humidity	10 to 99%	± 5%	1 %
Outdoor Humidity	10 to 99%	± 5%	1 %
Barometric Pressure	8.85 to 32.50 inHg	± 0.08 inHg (within range of 27.13 to 32.50 inHg)	0.01 inHg
Rain	0 to 394 in.	± 10%	0.01 in
Wind Direction	0 - 360 °	22.5° (16 point compass)	22.5° (16 point compass)
Wind Speed	0 to 112 mph	± 2.2 mph or 10% (whichever is greater)	0.1 mph

Appendix I: **Raw SPSS Data (columns 1-9)**

wall_thick	raster_res	position	dia_sm_top	dia_sm_mid	dia_sm_bot	thick_top	Thick_mid	Thick_bot
1	1	4	0.49881	0.49974	0.49916	0.06395	0.06498	0.06441
1	1	6	0.49848	0.49868	0.49932	0.06382	0.06415	0.0647
1	1	9	0.50142	0.50213	0.50261	0.06197	0.06169	0.06209
1	1	14	0.50396	0.50346	0.5032	0.06339	0.06303	0.06265
1	1	17	0.50482	0.50514	0.5051	0.06384	0.06343	0.06371
1	1	24	0.49821	0.49933	0.4995	0.0622	0.06315	0.06341
1	1	28	0.49805	0.49933	0.49889	0.06224	0.06305	0.06255
1	1	29	0.5021	0.5033	0.50292	0.06104	0.06201	0.062
1	1	35	0.49784	0.49759	0.49811	0.06381	0.06387	0.06435
1	1	38	0.49732	0.5975	0.49689	0.06357	0.06491	0.06396
1	1	42	0.50532	0.5063	0.5053	0.06334	0.06375	0.06316
1	1	48	0.49689	0.49752	0.49716	0.06163	0.06214	0.06185
1	1	51	0.50507	0.50526	0.50553	0.06368	0.06362	0.06481
1	1	54	0.50598	0.50692	0.50582	0.06367	0.06399	0.06397
1	1	59	0.49681	0.4976	0.49803	0.06383	0.06411	0.065
1	1	62	0.5053	0.50482	0.50528	0.06365	0.0635	0.06386
1	1	66	0.50348	0.50501	0.50624	0.06331	0.06346	0.06458
1	1	69	0.50224	0.50309	0.50378	0.06248	0.06246	0.06304
1	1	75	0.50362	0.50417	0.50559	0.06355	0.063	0.06493
1	1	80	0.49759	0.49864	0.49774	0.06177	0.06285	0.06234
1	1	81	0.50387	0.50317	0.50343	0.06386	0.06349	0.06392
1	1	87	0.49738	0.49595	0.49802	0.06191	0.06352	0.06243
1	1	92	0.49961	0.49946	0.49939	0.06184	0.06213	0.06233
1	1	93	0.50249	0.50269	0.5031	0.06199	0.06184	0.06289
1	2	3	0.49699	0.49761	0.49823	0.06368	0.06399	0.06444
1	2	5	0.50287	0.50284	0.50258	0.06191	0.06204	0.06207
1	2	10	0.50368	0.50366	0.50392	0.06237	0.06246	0.06258
1	2	15	0.49732	0.49877	0.49774	0.06341	0.06475	0.06438
1	2	20	0.49817	0.4991	0.49922	0.0636	0.06343	0.0633
1	2	23	0.50492	0.50571	0.50496	0.06319	0.06426	0.06362
1	2	25	0.50347	0.50394	0.50373	0.06236	0.06265	0.06284
1	2	31	0.49781	0.49866	0.49834	0.06452	0.06462	0.0644
1	2	33	0.50478	0.50565	0.50519	0.06397	0.0643	0.06444
1	2	37	0.50446	0.50533	0.50496	0.06316	0.06326	0.06305
1	2	41	0.504	0.50458	0.50413	0.0631	0.06317	0.06313
1	2	46	0.49819	0.49961	0.49926	0.06443	0.06469	0.06514
1	2	52	0.49749	0.49848	0.49904	0.06398	0.06402	0.06412
1	2	55	0.50482	0.50502	0.50528	0.06308	0.06343	0.0643
1	2	58	0.50511	0.50538	0.50595	0.06306	0.06384	0.06441

1	2	63	0.49765	0.49823	0.49825	0.06394	0.06442	0.06454
1	2	67	0.49762	0.49758	0.49766	0.0642	0.06424	0.06366
1	2	72	0.49877	0.49966	0.49926	0.06236	0.06364	0.06294
1	2	73	0.50228	0.50321	0.50325	0.06193	0.06224	0.06258
1	2	78	0.50412	0.50403	0.50524	0.06377	0.06332	0.06435
1	2	84	0.49898	0.4995	0.49904	0.06297	0.06345	0.06365
1	2	88	0.4998	0.49946	0.50073	0.06224	0.06334	0.06414
1	2	91	0.5038	0.50486	0.50386	0.06406	0.06447	0.0644
1	2	94	0.50406	0.50447	0.50479	0.06393	0.06418	0.06409
2	1	2	0.49715	0.49787	0.49754	0.12357	0.12306	0.12303
2	1	8	0.49965	0.49919	0.49944	0.12305	0.12312	0.12368
2	1	12	0.49838	0.49891	0.49857	0.12259	0.12256	0.12308
2	1	13	0.50065	0.50082	0.50109	0.1202	0.12059	0.12129
2	1	19	0.50445	0.50549	0.50457	0.12325	0.124	0.12374
2	1	21	0.50417	0.5044	0.50426	0.12284	0.12328	0.12303
2	1	27	0.4974	0.49719	0.49705	0.12259	0.1226	0.12255
2	1	30	0.50419	0.50464	0.50387	0.12253	0.12276	0.12266
2	1	36	0.49912	0.49844	0.49811	0.12352	0.12334	0.12292
2	1	40	0.49948	0.49995	0.4991	0.1232	0.12318	0.12321
2	1	43	0.50513	0.505	0.50449	0.12339	0.12315	0.12348
2	1	47	0.50481	0.50577	0.50475	0.12306	0.12397	0.12358
2	1	49	0.50359	0.50497	0.50404	0.1234	0.12395	0.12394
2	1	56	0.49945	0.4994	0.49993	0.12285	0.12309	0.12308
2	1	57	0.50277	0.5029	0.50307	0.12213	0.12191	0.12238
2	1	61	0.50204	0.50231	0.50251	0.12171	0.12124	0.12158
2	1	68	0.50033	0.49968	0.50012	0.12424	0.12406	0.12345
2	1	70	0.50315	0.50387	0.50343	0.12258	0.12289	0.12309
2	1	76	0.50001	0.49921	0.49908	0.12239	0.12296	0.12281
2	1	79	0.50437	0.50427	0.50447	0.12351	0.12294	0.12403
2	1	82	0.50506	0.50457	0.50521	0.12424	0.12419	0.12504
2	1	86	0.5048	0.50464	0.5049	0.12413	0.12346	0.12392
2	1	89	0.50199	0.50188	0.50152	0.12179	0.12154	0.12154
2	1	95	0.49847	0.499	0.49878	0.12456	0.12338	0.12326
2	2	1	0.50335	0.504	0.5036	0.12252	0.12296	0.12258
2	2	7	0.50342	0.50386	0.50357	0.12266	0.12274	0.12291
2	2	11	0.49788	0.49727	0.49755	0.12245	0.12255	0.12331
2	2	16	0.49778	0.49793	0.49804	0.12222	0.12234	0.12259
2	2	18	0.49759	0.49812	0.49701	0.12182	0.12251	0.12193
2	2	22	0.49824	0.49861	0.49855	0.12229	0.12244	0.12273
2	2	26	0.49784	0.4992	0.49827	0.12235	0.12297	0.12288
2	2	32	0.49689	0.49828	0.49757	0.12115	0.1218	0.12178
2	2	34	0.50532	0.50508	0.50561	0.12368	0.12364	0.12356

2	2	39	0.49713	0.49838	0.49789	0.12173	0.12231	0.1227
2	2	44	0.49852	0.49897	0.49903	0.12175	0.12225	0.12216
2	2	45	0.50212	0.50195	0.50262	0.12086	0.12122	0.12112
2	2	50	0.49644	0.49704	0.49663	0.12244	0.12279	0.12189
2	2	53	0.50342	0.50339	0.50375	0.1228	0.12227	0.12268
2	2	60	0.49906	0.49838	0.49926	0.12232	0.1215	0.12259
2	2	64	0.49768	0.49908	0.49897	0.12099	0.12202	0.12248
2	2	65	0.50256	0.50286	0.50243	0.12249	0.12325	0.12298
2	2	71	0.49896	0.49898	0.50029	0.12273	0.12274	0.12413
2	2	74	0.49942	0.50018	0.49973	0.12201	0.12288	0.12286
2	2	77	0.50277	0.503	0.50168	0.122	0.12186	0.1216
2	2	83	0.49759	0.4972	0.49859	0.12293	0.1237	0.12236
2	2	85	0.50255	0.50321	0.50363	0.12201	0.12251	0.12276
2	2	90	0.50318	0.50479	0.50356	0.12208	0.12329	0.12305
2	2	96	0.49859	0.49919	0.49912	0.12085	0.12245	0.12252

Raw SPSS Data (columns 10-18)

cyl_sm	fillet_rad	cyl_lg	dia_lg_top	dia_lg_mid	dia_lg_bot	concentricity	dia_sm_ave	dia_lg_ave
0.00774	0.28363	0.01075	1.00019	0.9999	1.0022	0.00312	0.49924	1.00076
0.00874	0.27608	0.00795	1.00167	0.99998	0.99985	0.01033	0.49883	1.00050
0.00668	0.28905	0.00811	1.00808	1.00568	1.00597	0.00515	0.50205	1.00658
0.00753	0.28713	0.00801	1.01074	1.00752	1.00683	0.00435	0.50354	1.00836
0.01022	0.2862	0.00579	0.99781	0.99988	0.99802	0.0132	0.50502	0.99857
0.00635	0.28795	0.00774	1.00049	0.99995	1.00017	0.00028	0.49901	1.00020
0.00666	0.28091	0.0071	1.00046	1.00048	1	0.00616	0.49876	1.00031
0.0065	0.29108	0.00366	1.00381	1.00272	1.00238	0.01075	0.50277	1.00297
0.0077	0.28331	0.01116	1.0006	1.00026	1.00184	0.00515	0.49785	1.00090
0.00774	0.28563	0.00993	1.00145	1.00033	1.00175	0.00887	0.53057	1.00118
0.00777	0.28938	0.00831	1.01195	1.00963	1.0104	0.00592	0.50564	1.01066
0.00479	0.28428	0.00693	0.99983	0.99887	0.99976	0.00353	0.49719	0.99949
0.00671	0.29421	0.0085	1.01234	1.01092	1.01441	0.00654	0.50529	1.01256
0.0087	0.29045	0.01035	1.01631	1.01066	1.01109	0.00714	0.50624	1.01269
0.00735	0.28203	0.0097	1.00102	1.00067	1.00174	0.00294	0.49748	1.00114
0.00742	0.28935	0.00831	1.01266	1.00982	1.00903	0.00713	0.50513	1.01050
0.00694	0.28879	0.01155	1.01714	1.01246	1.01205	0.01391	0.50491	1.01388
0.00649	0.28699	0.0077	1.00912	1.00775	1.0079	0.01181	0.50304	1.00826
0.00758	0.28985	0.00741	1.01	1.0087	1.00982	0.00667	0.50446	1.00951
0.00584	0.28452	0.00724	1.00134	1.00319	1.00077	0.00648	0.49799	1.00177
0.00629	0.29333	0.01263	1.0129	1.01327	1.0122	0.02223	0.50349	1.01279
0.00692	0.28666	0.0108	1.00251	1.0021	1.00137	0.01271	0.49712	1.00199
0.00547	0.28884	0.00774	1.00249	1.00126	1.00098	0.01098	0.49949	1.00158
0.00655	0.29405	0.0066	1.00835	1.00645	1.00839	0.01447	0.50276	1.00773
0.0071	0.28889	0.00829	0.99671	0.99882	1.00114	0.00531	0.49761	0.99889
0.00501	0.28769	0.00669	1.00848	1.008	1.00519	0.00397	0.50276	1.00722
0.00397	0.2898	0.00682	1.01032	1.0087	1.00872	0.00392	0.50375	1.00925
0.00832	0.28829	0.00843	0.99862	1.00072	1.00331	0.00646	0.49794	1.00088
0.00558	0.28018	0.00557	1.00325	1.00419	1.00498	0.01399	0.49883	1.00414
0.0076	0.29607	0.0075	1.01012	1.00736	1.00905	0.00238	0.50520	1.00884
0.00721	0.2953	0.00572	1.00588	1.00441	1.00469	0.01306	0.50371	1.00499
0.00758	0.28993	0.00793	1.00077	1.00005	1.00089	0.01707	0.49827	1.00057
0.00985	0.29492	0.01129	1.01117	1.00987	1.01129	0.00794	0.50521	1.01078
0.00657	0.29549	0.00924	1.01152	1.01049	1.01097	0.01428	0.50492	1.01099
0.0091	0.30244	0.00687	1.00434	1.00372	1.00478	0.0121	0.50424	1.00428
0.00761	0.2923	0.011	1.00299	1.00236	1.00342	0.01148	0.49902	1.00292
0.00679	0.28921	0.01108	1.00008	1.00194	1.00189	0.00168	0.49834	1.00130
0.00811	0.29522	0.00884	1.01424	1.01019	1.00685	0.0028	0.50504	1.01043
0.00782	0.29391	0.01002	1.01349	1.00895	1.00954	0.00744	0.50548	1.01066
0.00859	0.28879	0.01004	1.0014	1.00179	1.00281	0.00483	0.49804	1.00200
0.00714	0.28875	0.01005	1.00144	1.00114	1.00148	0.00842	0.49762	1.00135
0.00809	0.29014	0.00953	1.00246	1.00258	1.00373	0.00714	0.49923	1.00292

0.00751	0.29142	0.00797	1.01013	1.00786	1.00815	0.01468	0.50291	1.00871
0.00719	0.29046	0.00945	1.0141	1.01051	1.0112	0.01157	0.50446	1.01194
0.0069	0.29462	0.01238	1.00531	1.00309	1.00324	0.00381	0.49917	1.00388
0.00718	0.28493	0.00958	1.00134	1.00354	1.00305	0.01221	0.50000	1.00264
0.00665	0.30102	0.00696	1.00847	1.0084	1.00918	0.00696	0.50417	1.00868
0.00697	0.30035	0.0081	1.01237	1.00952	1.00953	0.01223	0.50444	1.01047
0.00825	0.2677	0.01032	1.01295	1.01366	1.01313	0.00848	0.49752	1.01325
0.00677	0.283	0.01014	1.00297	1.00102	1.00176	0.01404	0.49943	1.00192
0.00586	0.28277	0.00742	1.00066	1.00098	1.00015	0.01171	0.49862	1.00060
0.00325	0.28844	0.00694	1.00736	1.00616	1.00688	0.00827	0.50085	1.00680
0.00694	0.28889	0.00669	1.00703	1.0079	1.00913	0.00494	0.50484	1.00802
0.00579	0.29164	0.00527	1.00452	1.00465	1.00473	0.01402	0.50428	1.00463
0.00671	0.28308	0.0091	1.0016	0.99915	1.00066	0.02124	0.49721	1.00047
0.00504	0.29247	0.0051	1.00756	1.00627	1.00692	0.01173	0.50423	1.00692
0.00702	0.28699	0.01048	1.00108	0.99989	1.00106	0.00193	0.49856	1.00068
0.00665	0.28651	0.00981	1.00282	1.00051	1.00119	0.01539	0.49951	1.00151
0.00553	0.28619	0.0083	1.01153	1.00808	1.00894	0.00443	0.50487	1.00952
0.00591	0.28844	0.0075	1.00813	1.00917	1.00982	0.00368	0.50511	1.00904
0.00883	0.28382	0.01271	1.01484	1.01072	1.01425	0.01414	0.50420	1.01327
0.00641	0.28535	0.01088	1.00376	1.00244	1.00322	0.01386	0.49959	1.00314
0.00489	0.28687	0.00772	1.01133	1.00767	1.00872	0.01	0.50291	1.00924
0.00528	0.28667	0.00669	1.00542	1.0037	1.00646	0.00963	0.50229	1.00519
0.00807	0.28212	0.01136	1.00385	1.00572	1.00439	0.01745	0.50004	1.00465
0.00571	0.2845	0.00827	1.01195	1.00886	1.0102	0.01443	0.50348	1.01034
0.0065	0.28577	0.01255	1.00333	1.00429	1.0033	0.01671	0.49943	1.00364
0.00567	0.28662	0.00822	1.01114	1.00982	1.00902	0.00826	0.50437	1.00999
0.01033	0.295	0.0076	1.00544	1.00559	1.00582	0.00517	0.50495	1.00562
0.0073	0.29215	0.0066	1.00225	1.00535	1.00596	0.00975	0.50478	1.00452
0.00461	0.29264	0.00714	1.01209	1.00644	1.00775	0.01353	0.50180	1.00876
0.00657	0.28976	0.00977	1.00213	1.00241	1.0027	0.02045	0.49875	1.00241
0.00549	0.2837	0.00981	1.01012	1.00933	1.01014	0.00629	0.50365	1.00986
0.00722	0.28525	0.00714	1.00753	1.00767	1.00976	0.00666	0.50362	1.00832
0.00838	0.28075	0.0079	0.99789	0.99957	1.00108	0.00387	0.49757	0.99951
0.00576	0.28468	0.00574	0.99953	0.99957	0.99719	0.00944	0.49792	0.99876
0.00737	0.28214	0.00797	0.9981	0.99711	0.9995	0.01843	0.49757	0.99824
0.00797	0.28642	0.00853	0.99934	0.99953	0.99975	0.02106	0.49847	0.99954
0.00828	0.27858	0.00788	1.00497	1.00025	1.00216	0.02101	0.49844	1.00246
0.0048	0.2914	0.00595	0.99871	0.99844	0.99892	0.01255	0.49758	0.99869
0.00647	0.28984	0.00911	1.01278	1.01103	1.01058	0.01367	0.50534	1.01146
0.00645	0.28725	0.01077	0.99921	0.99903	1.00198	0.00378	0.49780	1.00007
0.00538	0.28485	0.00812	1.00161	0.99989	1.00096	0.00719	0.49884	1.00082
0.00417	0.29086	0.00527	1.0078	1.00638	1.00635	0.00904	0.50223	1.00684
0.00755	0.28651	0.01044	0.99881	0.99973	1.00109	0.00888	0.49670	0.99988
0.00587	0.28932	0.0095	1.01362	1.00913	1.01046	0.01299	0.50352	1.01107
0.0062	0.28583	0.00921	1.00305	1.00035	0.99939	0.01	0.49890	1.00093

0.00593	0.28656	0.00934	1.00012	1.00145	0.99969	0.00896	0.49858	1.00042
0.00624	0.28686	0.00963	1.00952	1.00977	1.00876	0.01317	0.50262	1.00935
0.00622	0.28416	0.01117	1.00156	1.00253	1.00291	0.00398	0.49941	1.00233
0.0073	0.28031	0.01101	1.00104	1.00078	1.00142	0.01402	0.49978	1.00108
0.00578	0.28818	0.00799	1.00937	1.00555	1.00614	0.011	0.50248	1.00702
0.00632	0.28369	0.01123	1.00238	1.00118	1.00208	0.01436	0.49779	1.00188
0.00531	0.29232	0.00807	1.01121	1.00941	1.00992	0.01616	0.50313	1.01018
0.00551	0.2908	0.00805	1.01233	1.01032	1.01117	0.01329	0.50384	1.01127
0.00452	0.28596	0.00732	1.00153	1.00021	1.00206	0.01111	0.49897	1.00127

Appendix J: **ANOVA results**

(#1) Diameter Small (0.5")

Univariate Analysis of Variance

Between-Subjects Factors

		Value Label	N
Wall_Thick	1	(.06)	48
	2	(.12)	48
Raster_Res	1	Fine	48
	2	Normal	48

Tests of Between-Subjects Effects

Dependent Variable:Dia_sm_top

Source	Type III Sum of Squares	df	Mean Square	F	Sig.
Corrected Model	4.144E-5[a]	3	1.381E-5	1.589	.197
Intercept	24.097	1	24.097	2771820.852	.000
Wall_Thick	3.725E-6	1	3.725E-6	.428	.514
Raster_Res	1.489E-5	1	1.489E-5	1.713	.194
Wall_Thick * Raster_Res	2.282E-5	1	2.282E-5	2.625	.109
Error	.001	92	8.694E-6		
Total	24.098	96			
Corrected Total	.001	95			

a. R Squared = .049 (Adjusted R Squared = .018)

Dependent Variable:Dia_sm_mid

Source	Type III Sum of Squares	df	Mean Square	F	Sig.
Corrected Model	.000[a]	3	.000	1.194	.317
Intercept	24.236	1	24.236	232545.442	.000
Wall_Thick	.000	1	.000	1.659	.201
Raster_Res	.000	1	.000	1.609	.208
Wall_Thick * Raster_Res	3.271E-5	1	3.271E-5	.314	.577
Error	.010	92	.000		
Total	24.246	96			
Corrected Total	.010	95			

a. R Squared = .037 (Adjusted R Squared = .006)

Tests of Between-Subjects Effects

Dependent Variable:Dia_sm_bot

Source	Type III Sum of Squares	df	Mean Square	F	Sig.
Corrected Model	3.798E-5[a]	3	1.266E-5	1.472	.227
Intercept	24.132	1	24.132	2805090.470	.000
Wall_Thick	1.494E-5	1	1.494E-5	1.737	.191
Raster_Res	8.431E-6	1	8.431E-6	.980	.325
Wall_Thick * Raster_Res	1.461E-5	1	1.461E-5	1.698	.196
Error	.001	92	8.603E-6		
Total	24.133	96			
Corrected Total	.001	95			

a. R Squared = .046 (Adjusted R Squared = .015)

(#2) Diameter Large (1”)

Tests of Between-Subjects Effects

Dependent Variable:Dia_lg_top

Source	Type III Sum of Squares	df	Mean Square	F	Sig.
Corrected Model	7.288E-5[a]	3	2.429E-5	.883	.453
Intercept	97.103	1	97.103	3530677.470	.000
Wall_Thick	1.232E-5	1	1.232E-5	.448	.505
Raster_Res	2.387E-5	1	2.387E-5	.868	.354
Wall_Thick * Raster_Res	3.669E-5	1	3.669E-5	1.334	.251
Error	.003	92	2.750E-5		
Total	97.106	96			
Corrected Total	.003	95			

a. R Squared = .028 (Adjusted R Squared = -.004)

Tests of Between-Subjects Effects

Dependent Variable:Dia_lg_mid

Source	Type III Sum of Squares	df	Mean Square	F	Sig.
Corrected Model	7.268E-5[a]	3	2.423E-5	1.354	.262
Intercept	96.901	1	96.901	5414063.692	.000
Wall_Thick	1.066E-5	1	1.066E-5	.596	.442
Raster_Res	1.387E-5	1	1.387E-5	.775	.381
Wall_Thick * Raster_Res	4.815E-5	1	4.815E-5	2.690	.104
Error	.002	92	1.790E-5		
Total	96.902	96			
Corrected Total	.002	95			

a. R Squared = .042 (Adjusted R Squared = .011)

Tests of Between-Subjects Effects

Dependent Variable:Dia_lg_bot

Source	Type III Sum of Squares	df	Mean Square	F	Sig.
Corrected Model	6.985E-5[a]	3	2.328E-5	1.290	.283
Intercept	96.998	1	96.998	5373113.740	.000
Wall_Thick	3.519E-6	1	3.519E-6	.195	.660
Raster_Res	1.103E-5	1	1.103E-5	.611	.436
Wall_Thick * Raster_Res	5.530E-5	1	5.530E-5	3.063	.083
Error	.002	92	1.805E-5		
Total	97.000	96			
Corrected Total	.002	95			

a. R Squared = .040 (Adjusted R Squared = .009)

(#3) Fillet Radius (0.3”)

Tests of Between-Subjects Effects

Dependent Variable:Fillet_rad

Source	Type III Sum of Squares	df	Mean Square	F	Sig.
Corrected Model	.001[a]	3	.000	8.575	.000
Intercept	7.962	1	7.962	370848.129	.000
Wall_Thick	.000	1	.000	12.453	.001
Raster_Res	.000	1	.000	5.374	.023
Wall_Thick * Raster_Res	.000	1	.000	7.898	.006
Error	.002	92	2.147E-5		
Total	7.965	96			
Corrected Total	.003	95			

a. R Squared = .219 (Adjusted R Squared = .193)

(#4) Cylindricity Small (.5")

Tests of Between-Subjects Effects

Dependent Variable:Cyl_sm

Source	Type III Sum of Squares	df	Mean Square	F	Sig.
Corrected Model	1.782E-5[a]	3	5.941E-6	3.772	.013
Intercept	.004	1	.004	2789.904	.000
Wall_Thick	1.729E-5	1	1.729E-5	10.977	.001
Raster_Res	1.350E-9	1	1.350E-9	.001	.977
Wall_Thick * Raster_Res	5.340E-7	1	5.340E-7	.339	.562
Error	.000	92	1.575E-6		
Total	.005	96			
Corrected Total	.000	95			

a. R Squared = .110 (Adjusted R Squared = .080)

(#5) Cylindricity Large (1")

Tests of Between-Subjects Effects

Dependent Variable:Cyl_lg

Source	Type III Sum of Squares	df	Mean Square	F	Sig.
Corrected Model	6.115E-7[a]	3	2.038E-7	.056	.983
Intercept	.007	1	.007	1953.286	.000
Wall_Thick	1.751E-9	1	1.751E-9	.000	.983
Raster_Res	3.688E-7	1	3.688E-7	.101	.751
Wall_Thick * Raster_Res	2.410E-7	1	2.410E-7	.066	.798
Error	.000	92	3.648E-6		
Total	.007	96			
Corrected Total	.000	95			

a. R Squared = .002 (Adjusted R Squared = -.031)

(#6) Concentricity (small diameter compared to large diameter)

Tests of Between-Subjects Effects

Dependent Variable:Concentricity

Source	Type III Sum of Squares	df	Mean Square	F	Sig.
Corrected Model	.000[a]	3	6.698E-5	2.841	.042
Intercept	.009	1	.009	398.448	.000
Wall_Thick	.000	1	.000	8.486	.004
Raster_Res	1.335E-7	1	1.335E-7	.006	.940
Wall_Thick * Raster_Res	7.073E-7	1	7.073E-7	.030	.863
Error	.002	92	2.358E-5		
Total	.012	96			
Corrected Total	.002	95			

a. R Squared = .085 (Adjusted R Squared = .055)

Appendix K: **Kruskal-Wallis Test Results**

Test Statistics[a,b]

	Dia_sm_top	Dia_sm_mid	Dia_sm_bot	Dia_lg_top	Dia_lg_mid	Dia_lg_bot
Chi-Square	.323	2.073	2.063	.227	.887	.318
df	1	1	1	1	1	1
Asymp. Sig.	.570	.150	.151	.634	.346	.573

a. Kruskal Wallis Test

b. Grouping Variable: Wall_Thick

Test Statistics[a,b]

	Dia_sm_top	Dia_sm_mid	Dia_sm_bot	Dia_lg_top	Dia_lg_mid	Dia_lg_bot
Chi-Square	1.959	1.798	1.023	1.045	.668	.210
df	1	1	1	1	1	1
Asymp. Sig.	.162	.180	.312	.307	.414	.647

a. Kruskal Wallis Test

b. Grouping Variable: Raster_Res

Test Statistics[a,b]

	Fillet_rad
Chi-Square	10.633
df	1
Asymp. Sig.	.001

a. Kruskal Wallis Test

b. Grouping Variable: Wall_Thick

Test Statistics[a,b]

	Fillet_rad
Chi-Square	3.106
df	1
Asymp. Sig.	.078

a. Kruskal Wallis Test

b. Grouping Variable: Raster_Res

Test Statistics[a,b]

	Cyl_sm	Cyl_lg
Chi-Square	12.761	.001
df	1	1
Asymp. Sig.	.000	.980

a. Kruskal Wallis Test

b. Grouping Variable: Wall_Thick

Test Statistics[a,b]

	Cyl_sm	Cyl_lg
Chi-Square	.052	.256
df	1	1
Asymp. Sig.	.820	.613

a. Kruskal Wallis Test

b. Grouping Variable: Raster_Res

Test Statistics[a,b]

	Concentricity
Chi-Square	8.084
df	1
Asymp. Sig.	.004

a. Kruskal Wallis Test

b. Grouping Variable: Wall_Thick

Test Statistics[a,b]

	Concentricity
Chi-Square	.015
df	1
Asymp. Sig.	.904

a. Kruskal Wallis Test

b. Grouping Variable: Raster_Res

Appendix L: **Simple Effects Test Results**

Estimates

Dependent Variable: Fillet_rad

Wall_Thick	Raster_Res	Mean	Std. Error	95% Confidence Interval Lower Bound	95% Confidence Interval Upper Bound
(.06)	Fine	.287	.001	.285	.289
	Normal	.292	.001	.290	.294
(.12)	Fine	.287	.001	.285	.288
	Normal	.286	.001	.284	.288

Pairwise Comparisons

Dependent Variable: Fillet_rad

Wall_Thick	(I) Raster_Res	(J) Raster_Res	Mean Difference (I-J)	Std. Error	Sig.[a]	95% Confidence Interval for Difference[a] Lower Bound	95% Confidence Interval for Difference[a] Upper Bound
(.06)	Fine	Normal	-.005*	.001	.000	-.008	-.002
	Normal	Fine	.005*	.001	.000	.002	.008
(.12)	Fine	Normal	.000	.001	.729	-.002	.003
	Normal	Fine	.000	.001	.729	-.003	.002

Based on estimated marginal means

*. The mean difference is significant at the .05 level.

a. Adjustment for multiple comparisons: Bonferroni.

Univariate Tests

Dependent Variable: Fillet_rad

Wall_Thick		Sum of Squares	df	Mean Square	F	Sig.	Partial Eta Squared
(.06)	Contrast	.000	1	.000	13.151	.000	.125
	Error	.002	92	.000			
(.12)	Contrast	.000	1	.000	.121	.729	.001
	Error	.002	92	.000			

Each F tests the simple effects of Raster_Res within each level combination of the other effects shown. These tests are based on the linearly independent pairwise comparisons among the estimated marginal means.

Appendix M: **Histogram Results**

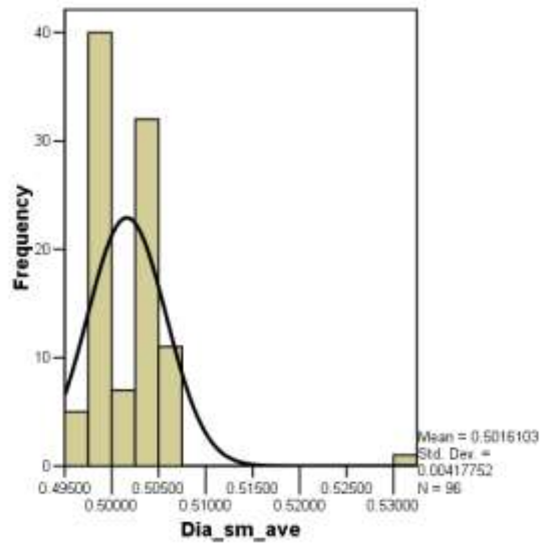

Bimodal Distribution of 0.5” Average Diameter with Superimposed Normal Curve

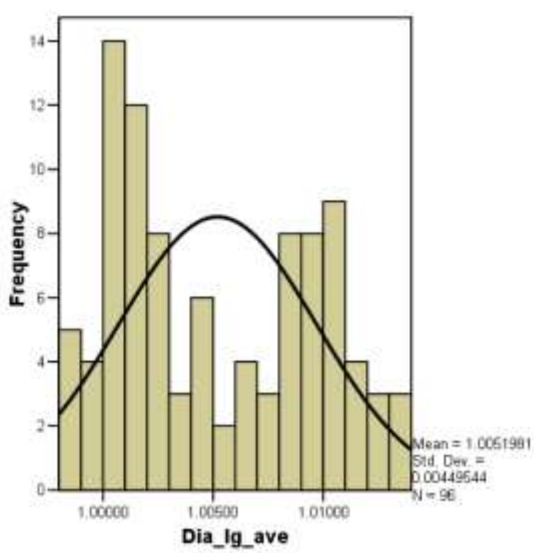

Bimodal Distribution of 1” Average Diameter with Superimposed Normal Curve

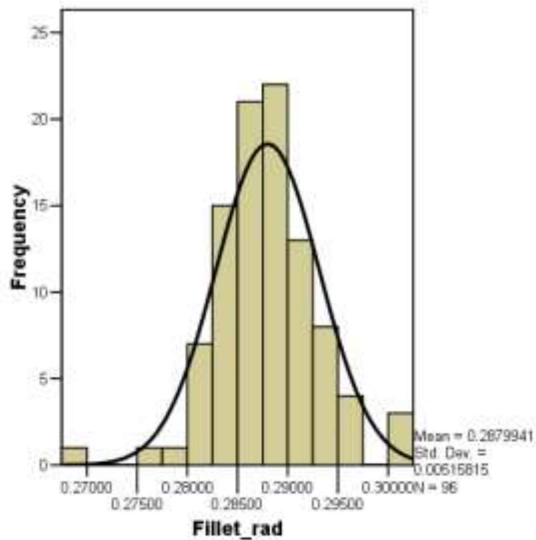

Histogram of 0.3" Radius Fillet with Superimposed Normal Curve

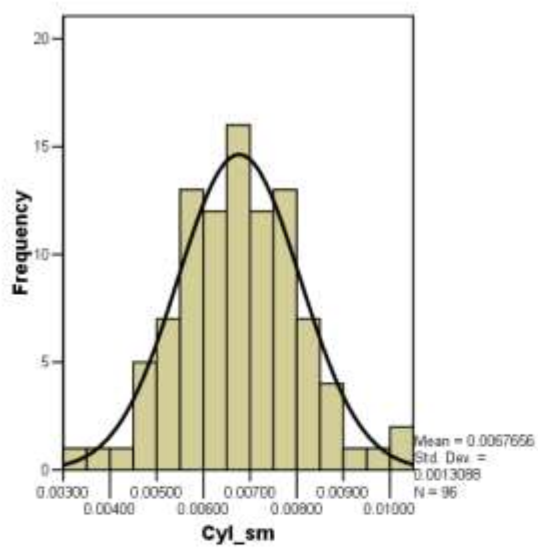

Histogram of 0.5" Diameter Cylindricity with Superimposed Normal Curve

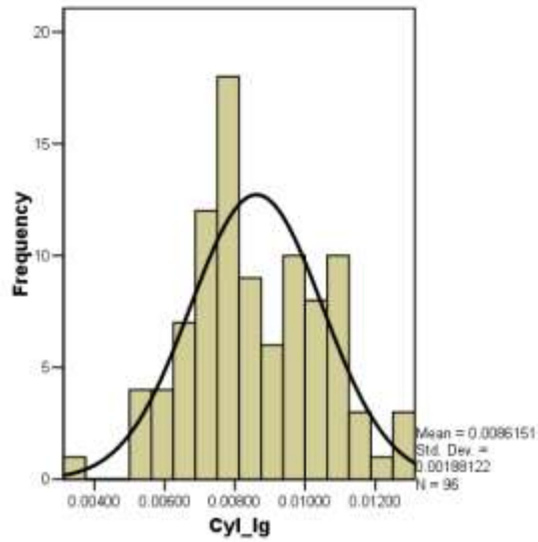

Bimodal Distribution of 1” Dia. Cylindricity with Superimposed Normal Curve

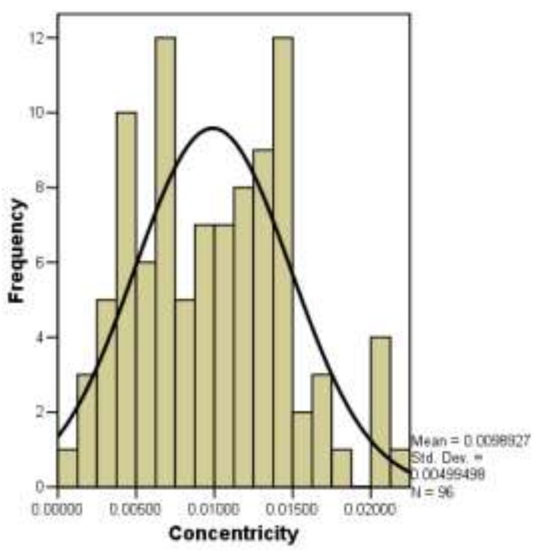

Bimodal Distribution of 0.5” to 1” Dia. Concentricity / Superimposed Curve

Appendix N: **CMM Sample Data**

ZEISS Calypso

ZEISS

Measurement Plan Winston-3D print	Date August 8, 2014		
Measurement Duration 00:03:00.0	Time 12:10:42 pm	Order	
	CMM C32Bit	Incremental Part Number 1	

Overall Result

- All Characteristics: 15
- Out of tolerance: 0
- Over Warning Limit: 0
- Not Calculated: 0

Characteristic	Actual	Nominal	Upper Tol.	Lower Tol.	Deviation
Small Diameter-Top (Minimum Circumscribed Element)	0.50335	0.50000			0.00335
Small Diameter-Middle (Minimum Circumscribed Element)	0.50400	0.50000			0.00400
Small Diameter-Bottom (Minimum Circumscribed Element)	0.50360	0.50000			0.00360
Thickness Top	0.12252	0.09000			0.03252
Thickness Middle	0.12296	0.09000			0.03296
Thickness Bottom	0.12258	0.09000			0.03258
Cylindricity-Small Ø	0.00549	0.00000	0.10000		0.00549
Radius .30 (LSQ Evaluation)	0.28370	0.30000			-0.01630
Cylindricity-Large Ø	0.00981	0.00000	0.10000		0.00981

Plan Name	Operator	Time	Date
Winston-3D print	Master	12:10:42 pm	August 8, 2014

	Actual	Nominal	Upper Tol.	Lower Tol.	Deviation
Large Diameter Top	1.01012	1.00000			0.01012
	Minimum Circumscribed Element				
Large Diameter Middle	1.00933	1.00000			0.00933
	Minimum Circumscribed Element				
Large Diameter Bottom	1.01014	1.00000			0.01014
	Minimum Circumscribed Element				
Concentricity1	0.00629	0.00000	0.10000		|- 0.00629